NOVA SCHOOL OF SCIENCE & TECHNOLOGY

DEPARTMENT OF MATHEMATICS

ALICE NEVES CASTELHANO

Bachelor in ⟨Mathematics⟩

SEIRS REACTION-DIFFUSION MODEL

ANALYSIS AND APPLICATION

MASTER IN ⟨MATHEMATICS AND APPLICATIONS⟩

NOVA University Lisbon

⟨November⟩, ⟨2021⟩

NOVA SCHOOL OF
SCIENCE & TECHNOLOGY

DEPARTMENT
OF MATHEMATICS

SEIRS REACTION-DIFFUSION MODEL

ANALYSIS AND APPLICATION

ALICE NEVES CASTELHANO

Bachelor in ⟨Mathematics⟩

Advisers: Magda Rebelo
Assistant Professor, NOVA University Lisbon
Paula Patrício
Associate Professor, NOVA University Lisbon

MASTER IN ⟨MATHEMATICS AND APPLICATIONS⟩

NOVA University Lisbon
⟨November⟩, ⟨2021⟩

SEIRS Reaction-Diffusion Model

Dedicated to my parents who always encouraged my academic evolution.

Acknowledgements

I would like to express my thanks to a wide range of people for their support, assistance and care.

Primarily, I would like to thank my principal advisors Prof. Magda Rebelo and Prof. Paula Patrício. Thank you for your guidance, support and time during the course of my master thesis at the NOVA School of Science and Technology, FCT NOVA. The knowledge acquired during our numerous meetings exceeded expectations as the work itself here presented.

In addition, I would like to acknowledge my appreciation for my bachelor professor, Prof. Elvira Coimbra, who played a central role in my evolution in mathematics and for all my master's degree professors within the Mathematics Department at FCT NOVA.

Finally, I wish to thank my parents, Gilberto and Paula, and my brother, Afonso, for their constant love, companionship and support throughout my academic years. From the choice of pursuing mathematics as my academic journey to the unlimited support and guidance through the most difficult challenges that I faced. To my boyfriend, Miguel, for all the love and support through this time, and for always lifting me up when I doubted myself. I dedicate this thesis to them.

I would also like to thank my friends for always being there and guiding me.

"Only put off until tomorrow what you are willing to die having undone." (Pablo Picasso)

Abstract

This thesis seeks to understand the effect of the inclusion of spacial heterogeneity in a SEIRS transmission model by considering a reaction-diffusion SEIRS model. Heterogeneity may correspond to different factors such as the different age classes, contact or spatial matrices, stage of the disease or behaviour. The model in study is suitable for a non-homogeneous population in which the epidemiological parameters depend on the spatial position of each individual.

A spatial SEIRS reaction-diffusion model is developed and we focus our theoretical study in the existence of solutions for the equilibrium problem of the epidemic model and their respective steady states. First a global solution of the model is shown to exist. The disease free equilibrium (DFE) is established and its asymptotic profiles determined depending on the basic reproduction number, $\mathscr{R}_0$, is defined for two distinguished problems - one with all diffusion coefficients set as positive constants and the other with some diffusion coefficients equal to zero. It is shown for both epidemic problems that if $\mathscr{R}_0 < 1$ then the DFE is locally asymptotically stable, else it is unstable.

A numerical method based on finite difference schemes is considered to approximate the solution of the reaction-diffusion system of equations and using the proposed method we present simulations that illustrate the theoretical results stated in the previous chapters.

Lastly, the model is parameterized according to studies for COVID-19 transmission dynamics in Portugal. Here, we illustrate the model predictions for the non-spatial and spatial case. Furthermore, different scenarios for the implementation of non-pharmacological interventions are illustrated from February 2020 to June 2020. Simulations suggest that the lockdown imposed in Portugal on the 18^{th} of March 2020 reduced the number of infected individuals in approximately 254490 daily cases.

Keywords: Spatial heterogeneity, Δ-SEIRS model, Basic reproduction number, Disease-free equilibrium, Endemic equilibrium, SARS-Cov-2

Resumo

A presente tese de mestrado tem como objetivo compreender o efeito da inclusão da heterogeneidade espacial em modelos epidémicos usando um modelo SEIRS de reação-difusão. A heterogeneidade pode corresponder a diferentes fatores, tais como as diferentes classes etárias, matrizes de contacto ou espaciais, fase da doença ou comportamento. O modelo em estudo está adaptado a uma população não homogénea em que os parâmetros epidemiológicos dependem da posição espacial de cada indivíduo.

Inicialmente desenvolvemos o nosso estudo teórico do modelo espacial SEIRS de reação-difusão. Demonstramos a existência de uma solução global do modelo. Para o problema de equilíbrio associado prova-se a existência de um equilíbrio sem doença (DFE) e é feito o estudo dos perfis assimptóticos da DFE. O número básico de reprodução, $\mathscr{R}_0$, é definido para dois problemas distintos - um com todos os coeficientes de difusão definidos como constantes positivas e o segundo com alguns dos coeficientes de difusão definidos iguais a zero. É demonstrado para ambos os problemas epidémicos que se $\mathscr{R}_0 < 1$, então a DFE é localmente assimptoticamente estável, caso contrário é instável.

Um método numérico baseado em esquemas de diferenças finitas é considerado para aproximar a solução do sistema reação-difusão e utilizando o método proposto apresentamos simulações que ilustram os resultados teóricos declarados nos capítulos anteriores.

Por último, o modelo é parametrizado de acordo com a literatura disponível sobre a dinâmica de transmissão de COVID-19 em Portugal. Aqui, ilustramos as simulações do modelo para o caso não-espacial e espacial. Além disso, são ilustrados diferentes cenários para a implementação de intervenções não-farmacológicas entre fevereiro de 2020 e junho de 2020. As simulações apresentadas sugerem que o confinamento imposto em Portugal a 18 de Março de 2020 reduziu o número de indivíduos infetados em aproximadamente 254490 casos diários.

Palavras-chave: Heterogeneidade espacial, Modelo Δ-SEIRS, Número básico de reprodução, Equilibrío sem doença, Equilíbrio endémico, SARS-Cov-2

Contents

List of Figures

List of Tables

Acronyms

COVID-19 Coronavirus disease 2019 4, 61, 62, 64, 69, 71, 72

DFE disease-free equilibrium 9, 13, 22, 23, 24, 25, 26, 27, 29, 33, 36, 37, 51, 55, 58, 71, 72

EE endemic equilibrium 22, 52, 58, 71

NPI non-pharmaceutical interventions 61, 63, 64, 65, 69

SEIRS susceptible-exposed-infected-recovered-susceptible 2, 3, 4, 19, 64, 66, 69, 71

SIS susceptible-infected-susceptible 2, 17

SI-type susceptible-infected-type 1

WHO World Health Organization 61

1

Introduction

In the mathematical theory of epidemics it is fundamental to understand how individual organisms being modeled interact with each other and the environment, and how these interactions determine the distribution of populations and structure of communities.

The classical epidemic model susceptible-infected-type (SI-type) was first developed by *Kermack and Mckendrick* (1927). *Kermack and Mckendrick* published a leading contribution to theoretical epidemics, in which a single infection was modeled with the contact rates estimated according to a mass-action law. The authors were concerned with understanding how a contagious disease can spread in a population where one infected person is introduced to a community of individuals totally susceptible to the disease in question. The purpose of their research was to obtain more insight regarding the effects of the various factors which govern the spread of contagious epidemics. Since then, different SI-type models have been developed. These have varied from discrete to continuous-time and non-spatial to spatial epidemic models.

The effect of the inclusion of space in these models has been subject of discussion in epidemiology and would not be of any great interest if there were no empirical reasons to suspect that space has an influence in population dynamics. In fact, there is extensive evidence (Huffaker, 1958; MacArthur, 1972; Yodzis, 1989) that suggest that space can affect the dynamics of populations and structure of communities.

Different frameworks have been proposed to include space heterogeneity, from patch models, where space is discrete, to continuous models, which are described by partial differential equations (PDE) such as reaction-diffusion models. Reaction-diffusion models provide a proper way to express movement of individuals and study the effects that migration has in the spread of diseases. Thus, they bring a good framework to understand the disease persistence or extinction. This type of model is spatially explicit and typically incorporate quantities such as diffusion or local growth rates.

Over the past few years, several SI-type epidemic reaction-diffusion models have been developed. In mathematics applied to epidemiology we have focused on the works of *Allen et.al* [2, 3], *Deng and Wu* [6], *Diekmann et.al* [7], *Van den Driessche and Watmough* [8]

and *Wang and Zhao*[21].

In [2] the authors study a susceptible-infected-susceptible (SIS) epidemic model where space is treated as a discrete collection of patches. *Allen et.al* show that when susceptible and infected individuals can move between patches, then an endemic equilibrium is reached in every patch, but that if only infected individuals are allowed to move then the disease does not persist in any patch in equilibrium.

Later, *Allen* and colleagues expand their findings to a space-continuous SIS model in [3]. Results on asymptotic profiles of the equilibrium are established, which have important implications for disease control. Furthermore, a similar model is established in [6] with the small difference that while in [3] a frequency-dependent interaction is taken, *Deng* and colleagues focus their study on a SIS reaction-diffusion model with mass-action type non-linearity. Consequently, the arguments for proving the global existence equilibrium of the model, the existence of an endemic equilibrium and the global attractivity of the endemic equilibrium require different approaches.

In [7], one of the most important concepts in mathematical theory of epidemics is introduced. The basic reproduction number, $\mathscr{R}_0$, is a threshold parameter, derived from a disease-free equilibrium solution, that allows us to study conditions in which the infectious disease is able to invade and prevail in a population. *Diekmann et.al* define $\mathscr{R}_0$ as the spectral radius of the next generation matrix. The authors in [8] apply in detail this definition to a general compartmental model suited to heterogeneous populations that can be modelled via a system of ordinary differential equations.

Wang and Zhao [21] expand the notion of the basic-reproduction number to a general reaction-diffusion space and time-continuous model, taking use of an associate elliptic eigenvalue problem for the study of the threshold dynamics.

First, we will study a continuous time transmission model. To build the mathematical model, we followed the standard strategy developed in the literature concerning the SIS model [3].

Suppose that the transmission dynamics of the disease is governed by the following system of differential equations, which we shall denote susceptible-exposed-infected-recovered-susceptible (SEIRS) model:

$$S^{'}(t) = -\beta I(t)S(t) + \alpha R(t), \qquad t > 0, \tag{1.1a}$$

$$E^{'}(t) = \beta I(t)S(t) - \varepsilon E(t), \qquad t > 0, \tag{1.1b}$$

$$I^{'}(t) = \varepsilon E(t) - \gamma I(t), \qquad t > 0, \tag{1.1c}$$

$$R^{'}(t) = \gamma I(t) - \alpha R(t), \qquad t > 0, \tag{1.1d}$$

that is represented schematically in *Figure 1.1*.

Here, $S(t)$, $E(t)$, $I(t)$ and $R(t)$ denote the fraction of susceptible, exposed, infectious and recovered (or removed) individuals at time $t \geq 0$, respectively, and the parameters β, ε, γ and α define the transmission intensity, the rate of progression to the infectious state, the recovery rate and the loss of immunity rate, respectively. We assume non-negative

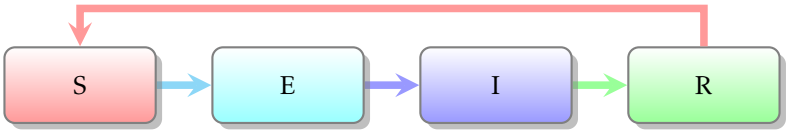

Figure 1.1: Schematic diagram of the SEIRS model.

normalized initial conditions, i.e., $S(0), E(0), I(0)$ and $R(0)$ non-negative and

$$S(0) + E(0) + I(0) + R(0) = N, \tag{1.2}$$

for some constant N.

We suppose that the disease does not have vertical transmission. In addition, for the sake of simplicity, we do not consider population dynamics, meaning that birth rate and natural death or death induced by the disease are here disregarded.

This system of differential equations does not take into account spatial dynamics, assuming that the population experiences the same homogeneous environment. Our main objective of this work is to expand (1.1) to a continuous-space reaction-diffusion model where spatial effects are taken into account.

We now consider a SEIRS reaction-diffusion model of the disease transmission for a population where individuals in each class move according to a diffusion process with non-negative constant diffusion coefficients d_S, d_E, d_I and d_R, respectively, with at least one positive diffusion coefficient. Moreover, $S(x,t)$, $E(x,t)$, $I(x,t)$ and $R(x,t)$ are set as the density of susceptible, exposed, infected and recovered individuals at location x and time t, respectively.

To incorporate the spatial heterogeneity in the parameters, we set the disease transmission intensity, $\beta(x)$, rate of progression to the infectious state, $\varepsilon(x)$, recovery rate, $\gamma(x)$, and the lost of immunity rate, $\alpha(x)$, as positive Hölder-continuous functions dependent of x in Ω.

We get the following reaction-diffusion system, which we will refer to as the Δ-SEIRS model:

$$\frac{\partial S(x,t)}{\partial t} = d_S \Delta S(x,t) - \beta(x) I(x,t) S(x,t) + \alpha(x) R(x,t), \qquad x \in \Omega, t > 0, \tag{1.3a}$$

$$\frac{\partial E(x,t)}{\partial t} = d_E \Delta E(x,t) + \beta(x) I(x,t) S(x,t) - \varepsilon(x) E(x,t), \qquad x \in \Omega, t > 0, \tag{1.3b}$$

$$\frac{\partial I(x,t)}{\partial t} = d_I \Delta I(x,t) + \varepsilon(x) E(x,t) - \gamma(x) I(x,t), \qquad x \in \Omega, t > 0, \tag{1.3c}$$

$$\frac{\partial R(x,t)}{\partial t} = d_R \Delta R(x,t) + \gamma(x) I(x,t) - \alpha(x) R(x,t), \qquad x \in \Omega, t > 0, \tag{1.3d}$$

where $\Omega \subset \mathbb{R}^l$ $(l \geq 1)$ is a bounded domain with smooth boundary $\partial\Omega$ (when $l > 1$) and $\Delta(\cdot)$ denotes the Laplacian operator.

Furthermore, we assume that there is no flux across the boundary $\partial\Omega$, *i.e.*,

$$\frac{\partial S}{\partial n} = \frac{\partial E}{\partial n} = \frac{\partial I}{\partial n} = \frac{\partial R}{\partial n} = 0, \quad x \in \partial\Omega, \tag{1.4}$$

where n denotes the outward unit normal vector to $\partial\Omega$.

We will first study the global solution of the system and the related equilibrium problem for which we establish the disease free equilibrium and study its stability depending on the basic reproduction number. Moreover, we apply this model to a current infectious disease. We take Coronavirus disease 2019 (COVID-19) as our case study and focus on the spread of the disease in Portugal, where good quality data for model parameterization is available. In this framework we refer the reader to the work of *Caetano et.al* [5], *Mammeri* [14] and *Viana et.al* [20].

The following chapters are organized as follows. In *Chapter 2*, we introduce the concept of the basic reproduction number. We define $\mathscr{R}_0$ as the spectral bound of the next generation operator and describe the computation of $\mathscr{R}_0$ for a general reaction-diffusion epidemic model. In addition the computation of $\mathscr{R}_0$ is exemplified for two simple epidemic models.

In *Chapter 3*, we study in more detail the Δ-SEIRS model (1.3). Global existence and boundedness results are proved, the equilibrium problem is introduced and the disease-free equilibrium is shown to exist. Moreover, the study of the disease-free equilibrium is distinguished in two cases: the first case focus on the model with all diffusion coefficients set as positive constants and the second with only the exposed individuals diffusion coefficient set as non-zero. Lastly, the basic reproduction number is defined for both problems.

In *Chapter 4*, a numerical method is presented in order to approximate the solution of the epidemic model (1.3) and illustrations of the theoretical results stated in *Chapter 3* are given. We use a centered finite difference scheme for the Laplacian and a backward finite difference formula to approximate the derivative in time.

In *Chapter 5* we introduce COVID-19 and detail the parameters choice for model (1.3) in relation to those observed in Portugal from February 2020 to June 2020. Illustrations of the model simulations for this period are showed for the non-spatial case and for a heterogeneous population distributed between two big cities. Moreover, for the spatially heterogeneous population, we present the model predictions for the effect that non-pharmaceutical interventions implemented in Portugal had on the disease transmission and create scenarios to evaluate the effect of different lockdown and unlockdown measures.

Lastly, in *Chapter 6* we discuss the results presented from *Chapter 3* to *5* and express our proposal for future work.

In addiction, for further reference, we included an Appendix with auxiliary definitions and results to complement the work here presented.

2

Basic Reproduction Number

One of the most important concerns about any infectious disease is its capability to invade a population.

The basic reproduction number, $\mathscr{R}_0$, is a crucial concept in epidemiology. Firstly developed for the study of demographics (Böckh, 1886; Sharp and Lotka, 1911; Dublin and Lotka, 1925; Kuczynski, 1928), it was latterly singly studied for vector-borne disease, such as malaria (Ross, 1911; MacDonald, 1952), and directly transmitted human diseases (Kermack and McKendrick, 1927; Dietz, 1975; Hethcote, 1975). It is now extensively used in the study of infectious diseases.

For modelling purposes, in a population which can be broken into homogeneous subpopulations, or compartments, such that individuals in a given compartment are indistinguishable from one another, $\mathscr{R}_0$ defines the expected number of secondary individuals produced by an infected individual in its life span. In epidemiology, $\mathscr{R}_0$ is taken as the number of new infectious cases caused by a single infected individual during its infectious period, in a population which is completely susceptible. $\mathscr{R}_0$ can characterize the infection threat of a disease, having an important implication for disease control.

Here, we study the concept of the basic reproduction number and the theory associated with it. Firstly, a definition for $\mathscr{R}_0$ is given following *Diekmann*'s formulation. A general reaction-diffusion epidemic model is considered in *Section 2.2*. It is shown in *Theorem 2.2.6* that for epidemic models with positive diffusion coefficients, the respective reproduction number agrees with the spectral radius of an operator associated with the model and in *Theorem 2.2.7* a similar result is taken for models with at least one diffusion coefficient equal to zero. Lastly, the definition of the basic reproduction number is illustrated by some preliminary examples in *Section 2.3*.

For the definitions of spectral radius, spectral bound, quasi-positive matrix and principal eigenvalue, we redirect the reader to *Appendix* in page 73.

2.1 The Next Generation Operator

Suppose that we wish to study if an infectious disease will invade or not a population, which is in its steady demographic state with all individuals susceptible. In the analysis of the simplest models, to answer this question, it was defined the basic reproduction number R_0 as the expected number of secondary cases produced, in a completely susceptible population, by a typical infected individual during its infective period and developed the *Threshold Criterion*:

$$\text{The disease can invade the population if } R_0 > 1, \text{ whereas it cannot if } R_0 < 1. \tag{2.1}$$

Diekmann et al. [7] expanded this notion to less simple models involving heterogeneity in the population.

Following [7], let ξ denote the individuals in h-state (h for heterogeneity), $S = S(\xi)$ the density function of susceptibles describing the steady demographic state in the absence of disease, and $A(t, \xi, \eta)$ be the expected infectivity of an individual which was infected t time units ago, while having h-state η, towards a susceptible which has h-state ξ. *Diekmann et al.* [7] defined the **next generation factor** of η as the quantity given by

$$\int_\Omega S(\xi) \int_0^\infty A(t, \xi, \eta) dt d\xi, \tag{2.2}$$

where Ω denotes the domain of ξ. This quantity describes the expected number of infections produced by an individual during its entire infectious period, which was also infected while having h-state η.

However, (2.2) does not give an exact representation of what happens in the subsequent generations since the new cases arise with h-states different from η. Hence, we consider a density ϕ that represents a "distributed" individual.

From [7], the **next generation operator** $K(S)$ is defined as

$$\Big(K(S)\phi\Big)(\xi) = S(\xi) \int_\Omega \int_0^\infty A(t, \xi, \eta) dt \phi(\eta) d\eta. \tag{2.3}$$

After m generations the magnitude of the infected population is (in the linear approximation) $K(S)^m \phi$ and consequently the per-generation growth factor is $\|K(S)^m\|^{\frac{1}{m}}$. Here $\|\cdot\|$ denotes the operator norm given by

$$\|K\| = \sup_{\|S\|=1} \|K(S)\|.$$

Taking m to ∞ in order to study the further generations, we have

$$\lim_{m\to\infty} \|K(S)^m\|^{\frac{1}{m}} = \inf_{m\geq 1} \|K(S)^m\|^{\frac{1}{m}} = \rho(K(S)), \tag{2.4}$$

where ρ denotes the spectral radius of an operator. One can specify conditions on K (for example compactness) that guarantee that $\rho(K(S))$ is an eigenvalue, which we shall call the dominant eigenvalue and denote by ρ_d.

Note that, starting from the *zero*th generation ϕ, the mth generation $K(S)^m\phi$ converges to zero for $m \to \infty$ if $\rho(K(S)) < 1$, whereas it can be made arbitrarily large by a suitable choice of ϕ and m when $\rho(K(S)) > 1$. In addition, we have

$$K(S)^m\phi \sim C(\phi)\rho_d^m\phi_d, \quad \text{as} \quad m \to \infty, \tag{2.5}$$

where ϕ_d is the corresponding eigenvector (which is positive) and $C(\phi)$ a scalar which is positive whenever ϕ is non-negative and not identically zero. Therefore after M generations, for $M > m$ chosen big enough, each generation is ρ_d times bigger than the preceding one.

We are now in conditions to define the expected number of secondary individuals produced by an individual in its infective life span. The next result establishes the basic reproduction number, $\mathscr{R}_0$.

Definition 2.1.1 [7]
The basic reproduction number is defined as

$$\mathscr{R}_0 = \rho(K(S)) = \rho_d, \tag{2.6}$$

where K is the next generation operator defined by (2.3).

As we will further verify, with this definition the *threshold criterion* (2.1) still can be established.

2.2 $\mathscr{R}_0$ of a Reaction-Diffusion Epidemic Model

To explore the basic reproduction number of a general reaction-diffusion epidemic model, we first proceed to study the formulation developed by *Wang and Zhao* [21].

Consider a heterogeneous population whose individuals can be grouped into n homogeneous compartments. Let ∇ denote the Delta operator. Consider the reaction-diffusion epidemic model described by

$$\frac{\partial u_i}{\partial t} = \nabla \cdot (d_i(x)\nabla u_i) + f_i(x,u), \qquad 1 \le i \le n, \quad t > 0, \quad x \in \Omega, \tag{2.7a}$$

$$\frac{\partial u_i}{\partial n} = 0, \qquad \forall 1 \le i \le n \text{ with } d_i(x) > 0, \quad t > 0, \quad x \in \partial\Omega, \tag{2.7b}$$

where u_i is the density of a population in compartment i, $d_i(x)$ the diffusion coefficient of population u_i, f_i the reaction term in compartment i under the influence of demographic processes and epidemic interactions, Ω is the spatial habitat in $\mathbb{R}^l$ with smooth boundary $\partial\Omega$ and n denotes the unit normal vector on $\partial\Omega$.

Following the settings of [21], let $u = (u_1, \ldots, u_n)^T$, with each $u_i \ge 0$, be the number of individuals in each compartment. We assume that u is sorted into two types: infected compartments, labeled by $i = 1, \ldots, m$, and uninfected compartments, labeled by $i = m+1, \ldots, n$.

In order to compute $\mathscr{R}_0$, it is important do distinguish new infections from other changes. Note that, as highlighted in [8], this decomposition is biologically driven, meaning that it is dependent of the biological interpretation of the model. Thus, we first set $\mathscr{F}_i(x,u)$ as the input rate of newly infected individuals in the ith compartment, $1 \leq i \leq n$, $\mathscr{V}_i^+(x,u)$ the rate of transfer of individuals into compartment i by other means and $\mathscr{V}_i^-(x,u)$ the rate of transfer of individuals out of compartment i. Hence, the disease transmission model can be written as the following system of equations

$$\frac{\partial u_i}{\partial t} = \nabla \cdot (d_i(x)\nabla u_i) + \mathscr{F}_i(x,u) - \mathscr{V}_i(x,u), \qquad 1 \leq i \leq n, \quad t > 0, \quad x \in \Omega, \tag{2.8a}$$

$$\frac{\partial u_i}{\partial n} = 0, \qquad \forall 1 \leq i \leq n \text{ with } d_i(x) > 0, \quad t > 0, \quad x \in \partial\Omega, \tag{2.8b}$$

together with the assumption that initial conditions are non-negative, where $\mathscr{V}_i = \mathscr{V}_i^- - \mathscr{V}_i^+$, $1 \leq i \leq n$.

For our purposes, we define a *disease free-equilibrium* (DFE) of (2.8) to be a locally asymptotically stable equilibrium solution of the disease free model.

Suppose that system (2.8) admits a disease free steady state

$$u^0(x) = \Big(0, \ldots, 0, u_{m+1}^0(x), \ldots, u_n^0(x)\Big), \tag{2.9}$$

where $u_i^0(x) \geq 0$, $m+1 \leq i \leq n$, for all $x \in \Omega$, with at least one $u_i^0(x) > 0$.

In view of the results in [**Section 3**, 21], we impose the following assumptions:

(A1) For each $1 \leq i \leq n$, functions $\mathscr{F}_i(x,u)$, $\mathscr{V}_i^+(x,u)$, $\mathscr{V}_i^-(x,u)$ and $d_i(x)$ are non-negative, continuous on $\Omega \times \mathbb{R}_+^l$ and continuously differential with respect to u;

(A2) If $u_i \equiv 0$ then $\mathscr{V}_i^- \equiv 0$. In particular, if u is a DFE then $\mathscr{V}_i^- \equiv 0$ for $i = 1, \ldots, m$;

(A3) $\mathscr{F}_i \equiv 0$ for $1 \leq i < m$;

(A4) If u is a DFE, then $\mathscr{F}_i \equiv \mathscr{V}_i^+ \equiv 0$ for $1 \leq i \leq m$.

Note that since each function describes a direct transfer of individuals, they are all non-negative. Biologically, $(A2)$ means that there is no transfer of individuals out of a compartment if the compartment is empty, $(A3)$ indicates that there is no infection for uninfected compartments and $(A4)$ implies that the population will remain free of disease if it is free of disease at the beginning.

From assumptions $(A1)$-$(A4)$, we can set

$$D_u\mathscr{F}(x,u^0) = \begin{bmatrix} F(x) & 0 \\ 0 & 0 \end{bmatrix}, \quad D_u\mathscr{V}(x,u^0) = \begin{bmatrix} V(x) & 0 \\ J(x) & -M^0(x) \end{bmatrix},$$

where $F(x)$ and $V(x)$ are $m \times m$ matrices defined by

$$F(x) = \left\{ \frac{\partial \mathscr{F}_i(x,u^0)}{\partial u_j} \right\}_{1 \leq i,j \leq m}, \quad V(x) = \left\{ \frac{\partial \mathscr{V}_i(x,u^0)}{\partial u_j} \right\}_{1 \leq i,j \leq m}, \tag{2.10}$$

$J(x)$ is a $(n-m)\times n$ matrix and

$$M^0(x) = \left\{ \frac{\partial f_i(x,u^0)}{\partial u_j} \right\}_{m+1\le i,j\le n}. \tag{2.11}$$

Observe that, from assumptions $(A1)$ and $(A4)$, $F(x)$ is a non-negative matrix, *i.e.*, it has non-negative entries for all $x \in \Omega$.

Set $X_1 := \mathscr{C}(\overline{\Omega}, \mathbb{R}^m)$, $X_1^+ := \mathscr{C}(\overline{\Omega}, \mathbb{R}^m_+)$ and

$$u_I = \Big(u_1(x,t),\dots,u_m(x,t)\Big)^T, \qquad d_I(x) = \Big(d_1(x),\dots,d_m(x)\Big)^T,$$
$$u_S = \Big(u_{m+1}(x,t),\dots,u_n(x,t)\Big)^T, \qquad d_S(x) = \Big(d_{m+1}(x),\dots,d_n(x)\Big)^T.$$

Linearizing system (2.8) around the disease-free equilibrium (DFE), u^0, the parabolic problem becomes

$$\frac{\partial u_I}{\partial t} = \nabla\cdot(d_I(x)\nabla u_I) + F(x)u_I - V(x)u_I, \qquad t>0, \quad x\in\Omega, \tag{2.12a}$$
$$\frac{\partial u_S}{\partial t} = \nabla\cdot(d_S(x)\nabla u_S) - J(x)u_I + M^0(x)u_S, \qquad t>0, \quad x\in\Omega, \tag{2.12b}$$
$$\frac{\partial u_i}{\partial n} = 0, \qquad \forall 1\le i\le n \text{ with } d_i>0, \quad t>0, \quad x\in\partial\Omega. \tag{2.12c}$$

We now divide this system into two separate problems, one regarding only the infectious compartments and the other regarding the non-infectious compartments.

Let $T(t)$ be the solution semigroup on X_1 associated with the following linear reaction-diffusion system

$$\frac{\partial u_I}{\partial t} = \nabla\cdot(d_I(x)\nabla u_I) - V(x)u_I, \qquad t>0, \quad x\in\Omega, \tag{2.13a}$$
$$\frac{\partial u_i}{\partial n} = 0, \qquad \forall 1\le i\le m \text{ with } d_i>0, \quad t>0, \quad x\in\partial\Omega. \tag{2.13b}$$

We take the following assumption

(A5) $-V(x)$ is quasi-positive for all $x\in\overline{\Omega}$ and

$$\lambda^0(-V) := s\Big(\nabla\cdot(d_I(x)\nabla) - V\Big) < 0,$$

where $s(B)$ is the spectral bound of the operator B (see Appendix A). Resulting from the previous decomposition, consider the linear reaction-diffusion system

$$\frac{\partial u_S}{\partial t} = \nabla\cdot(d_S(x)\nabla u_S) + M^0(x)u_S, \qquad t>0, \quad x\in\Omega, \tag{2.14a}$$
$$\frac{\partial u_i}{\partial n} = 0, \qquad \forall m+1\le i\le n \text{ with } d_i>0, \quad t>0, \quad x\in\partial\Omega, \tag{2.14b}$$

where $M^0(x)$ is given by (2.11). Following [21], in order to ensure that the *disease-free equilibrium* is linearly stable in the disease-free space we impose a condition on $M^0(x)$:

(A6) $M^0(x)$ is quasi-positive for all $x\in\overline{\Omega}$ and

$$\lambda^0(M^0) := s\Big(\nabla\cdot(d_S(x)\nabla) + M^0\Big) < 0.$$

2.2.1 An Eigenvalue Problem

In this Section, we give a characterization of the $\mathscr{R}_0$ of (2.7) from the spectral bound of the eigenvalue problem associated with system (2.12). For that purpose, we first introduce two results characterizing the eigenvalues of two general eigenvalue problems, the first with all diffusion coefficients set as positive constants and the last with at least one diffusion coefficient identically zero.

Let $M(x)$ be a continuous $k \times k$ matrix-valued function of $x \in \overline{\Omega}$. Following [21], we take the eigenvalue problem:

$$\nabla \cdot \Big(d_K(x)\nabla u_K\Big) + M(x)u_K = \lambda u_K, \qquad x \in \Omega, \tag{2.15a}$$

$$\frac{\partial u_i}{\partial n} = 0, \qquad \forall 1 \le i \le k \text{ such that } d_i > 0, \quad x \in \partial\Omega, \tag{2.15b}$$

where $u_K = (u_1(x),\dots,u_k(x))^T$, $d_K(x) = (d_1(x),\dots,d_k(x))^T$ and Mu_K denotes the multiplication operator defined by $M(\phi)(x) = M(x)\phi(x)$. We assume the following

(D1) there exists a $d_0 > 0$ such that $d_i(x) \ge d_0$, for all $x \in \overline{\Omega}$ and $1 \le i \le k$.

The next result characterizes the spectral bound of the operator $L+M$, with $L(\phi)(x) = \nabla \cdot \Big(d_K(x)\nabla\phi(x)\Big)$, associated to the eigenvalue problem (2.15).

Theorem 2.2.1 [21]
Let (D1) hold.
If $M(x)$ is quasi-positive for all $x \in \overline{\Omega}$ and there exists an $x_0 \in \Omega$ such that $M(x_0)$ is irreducible, then $\lambda^* := s(L+M)$ is an algebraically simple eigenvalue of (2.15) with a strongly positive eigenvector, and $Re(\lambda) < \lambda^*$ for all $\lambda \in \sigma(L+M) \setminus \{\lambda^*\}$.

When some diffusion coefficients in (2.15) are zero, we cannot obtain the existence of the principal eigenvalue by the same arguments as in the last result. Without loss of generality, we assume

(D2) There exists a positive constant, d_0, and an integer $1 \le j_1 < k$ such that $d_i(x) \ge d_0$ for all $x \in \overline{\Omega}$, $1 \le i \le j_1$, and $d_{j_1+i}(x) = 0$ for all $x \in \overline{\Omega}$, $1 \le i \le j_2 := k - j_1$.

Let $Y_1 = \mathscr{C}(\overline{\Omega}, \mathbb{R}^{j_1})$ and $Y_2 = \mathscr{C}(\overline{\Omega}, \mathbb{R}^{j_2})$. We split matrix $M(x)$ into the following form

$$M(x) = \begin{bmatrix} M_{11}(x) & M_{12}(x) \\ M_{21}(x) & M_{22}(x) \end{bmatrix}, \tag{2.16}$$

where $M_{11}(x)$ and $M_{22}(x)$ are $j_1 \times j_1$ and $j_2 \times j_2$ matrices, respectively.

Let $Q(t)$ be the solution semigroup on X associated with the linear parabolic system

$$\frac{\partial \mathbf{u}_{j_1}}{\partial t} = \nabla \cdot \left(\mathbf{d}_{j_1}(x)\nabla \mathbf{u}_{j_1}\right) + M_{11}(x)\mathbf{u}_{j_1} + M_{12}(x)\mathbf{u}_{j_2}, \qquad t > 0, \quad x \in \Omega, \tag{2.17a}$$

$$\frac{\partial \mathbf{u}_{j_2}}{\partial t} = M_{21}(x)\mathbf{u}_{j_1} + M_{22}(x)\mathbf{u}_{j_2}, \qquad t > 0, \quad x \in \Omega, \tag{2.17b}$$

$$\frac{\partial \mathbf{u}_{j_1}}{\partial n} = 0, \qquad x \in \partial\Omega, \tag{2.17c}$$

where $\mathbf{u}_{j_1} = \left(u_1(x), \ldots, u_{j_1}(x)\right)^T$, $\mathbf{u}_{j_2} = \left(u_{j_1+1}(x), \ldots, u_k(x)\right)^T$ and $\mathbf{d}_{j_1} = \left(d_1(x), \ldots, d_{j_1}(x)\right)^T$.

$Q(t)$ is a positive semigroup on X and its generator B is a closed and resolvent-positive operator, which can be written as

$$B = \begin{bmatrix} L_1 + M_{11} & M_{12} \\ M_{21} & M_{22} \end{bmatrix},$$

where $L_1(\mathbf{u}_{j_1})(x) := \nabla \cdot \left(\mathbf{d}_{j_1}(x)\nabla \mathbf{u}_{j_1}\right)$.

Let $T_2(t)\phi_2(x) = e^{M_{22}(x)t}\phi_2(x)$. Then $T_2(t)$ is a positive $\mathscr{C}_0$-semigroup on Y_2 with its generator M_{22} being resolvent-positive. Following *Theorem A.0.8*, in *Auxiliary Definitions and Results*, we have

$$\left(\lambda I - M_{22}\right)^{-1}\phi_2 = \int_0^\infty e^{-\lambda t} T_2(t)\phi_2 dt, \quad \forall \lambda > s(M_{22}), \quad \phi_2 \in Y_2. \tag{2.18}$$

Thus, we can define a one-parameter family of linear operators

$$\mathscr{L}_\lambda = L_1 + M_{11} + M_{12}(\lambda I - M_{22})^{-1}M_{21}, \qquad \forall \lambda > s(M_{22}). \tag{2.19}$$

We now establish a similar result to *Theorem 2.2.1* for eigenvalue problems with some diffusion coefficients identically zero.

Theorem 2.2.2 [21]

Let (D2) hold. Suppose that $M(x)$ is quasi-positive for all $x \in \overline{\Omega}$, and that for any $\lambda > s(M_{22})$, there exists some $x_\lambda \in \Omega$ such that $M_{11}(x_\lambda) + M_{12}(\lambda I - M_{22})^{-1}M_{21}(x_\lambda)$ is irreducible. If there exists $\lambda_0 > s(M_{22})$ and $\phi_0 > 0$ such that

$$\mathscr{L}_{\lambda_0}\phi_0 \geq \lambda_0\phi_0,$$

then the following statements are valid:

(i) $s(B)$ is a geometrically simple eigenvalue of (2.17) with a positive eigenvector;

(ii) $s(B)$ is the unique $\lambda \in \left(s(M_{22}), \infty\right)$ with $s(\mathscr{L}_\lambda) = \lambda$;

(iii) $s(B)$ has the same sign a $s(\mathscr{L}_0)$ provided that $s(M_{22}) < 0$.

Suppose now that system (2.7) has an equilibrium solution, *i.e.*, a solution u of problem

$$\nabla(d_i(x)\nabla u_i(x)) + f_i(x,u) = 0, \qquad 1 \le i \le n, \quad t > 0, \quad x \in \Omega, \tag{2.20a}$$

$$\frac{\partial u_i}{\partial n} = 0, \qquad \forall 1 \le i \le n \text{ with } d_i(x) > 0, \quad t > 0, \quad x \in \partial\Omega. \tag{2.20b}$$

An important question usually raised in relation with the equilibrium solution is whether this solution is **stable**, *i.e.*, whether it remains unchanged on the infinite time interval under small changes in the initial data.

Let $\phi(t,p)$ denote the solution of system (2.20) that takes the value p when $t = 0$. The next definition explains the different characterizations for the stability of equilibrium solutions.

Definition 2.2.3 Equilibrium Solution [9]

Consider the problem

$$\frac{dx}{dt} + Ax = f(t,x), \quad t > t_0, \tag{2.21}$$

where A be a linear operator in a Banach space X and $f : U \to X$. Let x_0 be an equilibrium point of (2.21), *i.e.*, $x_0 \in D(A) = \{x(t)|\ x(t)$ solution of (2.21) and $x(t_0) = x_0\}$ and

$$Ax_0 = f(t,x_0), \quad t > t_0.$$

An equilibrium point, x_0, is **stable** if, for any $\epsilon > 0$, there exists $\delta > 0$ such that any solution x of (2.21) with $\|x(t_0) - x_0\|_\alpha < \delta$ exists on $[t_0, \infty)$ and satisfies

$$\|x(t) - x_0\|_\alpha < \epsilon,$$

for all $t \ge t_0$.

The equilibrium point, x_0, is **asymptotically stable** if it is stable and for $x(t)$ solution of (2.21) where $x(t_1) = x_1$, with $t_1 > t_0$, $x(t) \to x_0$ as $t \to \infty$ and

$$\|x - x_0\|_\alpha < \delta,$$

for some constant δ.

We now characterize the stability of a solution from the eigenvalues of the equilibrium problem (2.20).

Theorem 2.2.4

The DFE is asymptotically stable for problem (2.21) if the real part of every eigenvalue of the operator A is negative. It is unstable if any eigenvalue has a positive real part.

Returning to the study of problem (2.7) and in view of (2.3), we now introduce the distribution of initial infections, described by $\phi(x)$, and the distribution of those infective

members as times evolves, given by $T(t)\phi(x)$. Thus, the next generation operator $K(\phi)$ for system (2.8) is given by

$$K(\phi)(x) := \int_0^\infty F(x)T(t)\phi dt = F(x)\int_0^\infty T(t)\phi dt. \tag{2.22}$$

Therefore the basic reproduction number for model (2.8) is defined as the spectral radius of K, *i.e.*,

$$\mathscr{R}_0 := \rho(K). \tag{2.23}$$

Recalling system (2.13), let

$$B := \nabla\cdot(d_I\nabla) - V. \tag{2.24}$$

The following result characterizes the basic reproduction number computed for system (2.8), using the eigenvalues of the eigenvalue problem associated with (2.12) and the local stability of the equilibrium solution. In addition, it states that if $\mathscr{R}_0 < 1$ the DFE is locally asymptotically stable which implies that the disease is eliminated and the population does not become endemic.

Theorem 2.2.5 [21]
Let (A1)-(A5) hold. The following statements are valid:

(i) $\mathscr{R}_0 - 1$ has the same sign as $\lambda^* := s(B+F)$, where F and V are given by (2.10) and (2.24), respectively;

(ii) If in addition (A6) holds and $\mathscr{R}_0 < 1$, then u^0 is asymptotically stable for system (2.8).

Proof. *In view of the results presented in Chapter 3, we are primarily interested in the proof of condition (i). For the proof of (ii) we redirect the reader to [***Theorem 3.1***, 21].*

Without loss of generality, suppose that all diffusion coefficients are positive constants.

Set $X_1 := \mathscr{C}(\overline{\Omega},\mathbb{R}^l)$ and $X_1^+ := \mathscr{C}(\overline{\Omega},\mathbb{R}^l_+)$. Let $T(t)$ be the solution semigroup on X_1 associated with system (2.13). Observe that $T(t)$ is a positive semigroup in the sense that $T(t)X_1^+ \subseteq X_1^+$ for all $t \geq 0$.

Following the settings of Diekmann et al. [7] for the basic reproduction number, we have that the distribution of new infections at time t is $F(x)T(t)\phi(x)$, where $\phi(x)$ sets the distribution of initial infection. Thus, from (2.2), we define the next generation operator of problem (2.8) as

$$K(\phi)(x) := F(x)\int_0^\infty T(t)\phi(x)dt. \tag{2.25}$$

Hence, following (2.6), we have that the basic reproduction number for model (2.8) is defined as

$$\mathscr{R}_0 := \rho(K).$$

Let B denote the operator defined in (2.24). Clearly B is the generator semigroup of $T(t)$ on X_1.

From Theorem A.0.8, in Auxiliary Definitions and Results, it then follows that B is resolvent positive and

$$(\lambda I - B)^{-1}\phi = \int_0^\infty e^{-\lambda t} T(t)\phi(x)dt, \quad \forall \lambda > s(B), \quad \forall \phi(x) \in X_1. \tag{2.26}$$

Since $V(x)$ verifies assumption (A5), we have $s(B) < 0$. Letting $\lambda = 0$, (2.26) becomes

$$-B^{-1}\phi = \int_0^\infty T(t)\phi(x)dt, \quad \forall \phi(x) \in X_1.$$

Thus, following (2.25), we have

$$K(\phi)(x) = -FB^{-1}.$$

Let A denote the linear operator $A := B + F$. Then A generates a positive $\mathscr{C}_0$-semigroup. Following Theorem A.0.8, A is a resolvent-positive operator and thus it follows from Theorem A.0.9 that $s(A)$ has the same sign as $\rho(-FB^{-1}) - 1 = \mathscr{R}_0 - 1$.

From Theorem 2.2.1, we have that the eigenvalue problem associated with (2.13) has a principal eigenvalue λ^*, which is defined as

$$\lambda^* := s(B + F) = s(A).$$

Hence, $\mathscr{R}_0 - 1$ has the same sign as the principal eigenvalue λ^* of the eigenvalue problem associated with (2.13).

■

2.2.2 Characterization of $\mathscr{R}_0$

We now state the two main results of [21], that characterize the basic reproduction number, $\mathscr{R}_0$, in terms of the principal eigenvalue of an elliptic eigenvalue problem.

Theorem 2.2.6 [21]

Let (A1)–(A4) hold. Assume that there exists $d_0 > 0$ such that $d_i(x) \geq d_0$, for all $1 \leq i \leq m$. If the elliptic eigenvalue problem

$$\begin{aligned} -\nabla \cdot (d_I(x)\nabla\phi) + V(x)\phi(x) &= \mu F(x)\phi, && x \in \Omega, \\ \frac{\partial \phi}{\partial n} &= 0, && x \in \partial\Omega, \end{aligned}$$

admits a unique positive eigenvalue μ_0 with a positive eigenfunction, then

$$\mathscr{R}_0 = \rho(-FB^{-1}) = \rho(-B^{-1}F) = \frac{1}{\mu_0}, \tag{2.27}$$

where F and B are given by (2.10) and (2.24), respectively.

In the case where some $d_i(x)$ are identically zero, we can reduce the computation of $\mathscr{R}_0$ to that of the principal eigenvalue of a lower dimensional elliptic eigenvalue problem under additional conditions.

Theorem 2.2.7 [21]

Let (A1)-(A4) hold, and assume that $s(-V_{22}) < 0$. Let $B_1 := \nabla \cdot (d_{i_1} \nabla) - V_1$, where $V_1 := V_{11} - V_{12} V_{22}^{-1} V_{21}$. Then the following statements are valid:

(i) If $F_{12} = 0$ and $F_{22} = 0$, then $\mathscr{R}_0 = \rho(-B^{-1}F) = \rho(-B_1^{-1}F_1)$, where $F_1 = F_{11} - V_{12}V_{22}^{-1}F_{21}$;

(ii) If $F_{21} = 0$ and $F_{22} = 0$, then $\mathscr{R}_0 = \rho(-B^{-1}F) = \rho(-B_1^{-1}F_2)$, where $F_2 = F_{11} - F_{12}V_{22}^{-1}V_{21}$.

2.3 Illustration of the Computation of $\mathscr{R}_0$

The decomposition of $f(x)$ into components $\mathscr{F}$ and $\mathscr{V}$ and the computation of the basic reproduction number is here illustrated using two simple disease models.

The first describes a disease transmission model without space and the latter a discrete in space disease transmission model, and so we may take a simpler theory to compute their respective $\mathscr{R}_0$. Hence, we adopt the settings of *van den Driessche et al*, [8], to characterize the basic reproduction number of the following models via the matrices $\mathscr{F}$, $\mathscr{V}$, F and V for discrete type models.

2.3.1 SEIRS Model

Let $S(t), E(t), I(t), R(t)$ be the fraction of susceptible, exposed, infectious and recovered individuals at time $t \geq 0$.

Consider the simple model described by the following differential equations together with non-negative initial conditions

$$\frac{dE}{dt} = \beta I(t)S(t) - \varepsilon E(t), \qquad t > 0, \tag{2.28a}$$

$$\frac{dI}{dt} = \varepsilon E(t) - \gamma I(t), \qquad t > 0, \tag{2.28b}$$

$$\frac{dS}{dt} = -\beta I(t)S(t) + \alpha R(t), \qquad t > 0, \tag{2.28c}$$

$$\frac{dR}{dt} = \gamma I(t) - \alpha R(t), \qquad t > 0, \tag{2.28d}$$

where β, ε, γ, α are non-negative constants that define the transmission intensity, the rate of progression to the infectious state, the recovery rate and the lost of immunity rate, respectively. We assume non-negative normalized initial conditions, i.e., $S(0), E(0), I(0)$ and $R(0)$ non-negative and

$$S(0) + E(0) + I(0) + R(0) = N,$$

for some constant N.

Note that progression from compartment E to I is not considered to be new infections, since it only describes the progression of an infected individual through different infected compartments. Hence

$$\mathscr{F}(u) = \begin{Bmatrix} \beta S_0 I(t) \\ 0 \\ 0 \\ 0 \end{Bmatrix} \quad \text{and} \quad \mathscr{V}(u) = \begin{Bmatrix} \varepsilon E(t) \\ \gamma I(t) - \varepsilon E(t) \\ \beta I(t) S(t) - \alpha R(t) \\ \alpha R(t) - \gamma I(t) \end{Bmatrix}.$$

Following from (2.9), an equilibrium solution with $E = I = 0$ has the form

$$u^0 = \Big(0, 0, S_0, 0\Big)^T = \Big(0, 0, N, 0\Big)^T.$$

Then

$$F = \begin{bmatrix} 0 & \beta N \\ 0 & 0 \end{bmatrix}, \quad V = \begin{bmatrix} \varepsilon & 0 \\ -\varepsilon & \gamma \end{bmatrix},$$

giving

$$V^{-1} = \begin{bmatrix} \frac{1}{\varepsilon} & 0 \\ \frac{1}{\gamma} & \frac{1}{\gamma} \end{bmatrix}.$$

Hence

$$FV^{-1} = \begin{bmatrix} \frac{\beta}{\gamma} N & \frac{\beta}{\gamma} N \\ 0 & 0 \end{bmatrix},$$

and

$$\mathscr{R}_0 = \rho(FV^{-1}) = \frac{\beta}{\gamma} N.$$

Following *Diekmann et al.* [7], we define FV^{-1} to be the next generation matrix for (2.28). To interpret its entries, consider the rate of an infected individual introduced into compartment k of a disease free population. The (j,k) entry of V^{-1} describes the average length of time this individual spends in compartment j, assuming that the population remains near the DFE. The (i,j) entry of F is the rate at which infected individuals in compartment j produce new infections in compartment i. Therefore, the (i,k) entry of the matrix product FV^{-1} is the expected number of new infections in compartment i produced by the infected individual originally introduced in compartment k.

Note that since γ defines the recovery rate of the infectious state, $\frac{1}{\gamma}$ translates the number of days that an individual stays in the infectious compartment. Therefore $\mathscr{R}_0$ is simply the product of the infection rate and the mean duration of the infection times the total population N.

Thus, we have that $\mathscr{R}_0 < 1$ if, and only if, the recovery rate is bigger than the infection rate, meaning that the infection cannot persist. Conversely, $\mathscr{R}_0 > 1$ if, and only if, the recovery rate is smaller than the infection rate. Hence the disease can invade the population when $\mathscr{R}_0 > 1$.

2.3.2 SIS Patch Model

Now, to consider the spacial contribution to the definition of $\mathscr{R}_0$ but in a simpler context, we consider a SIS patch model as in [2]. Let $n \geq 2$ be the number of patches, $\Omega = \{1, 2, \ldots, n\}$ and $S_j(t)$ and $I_j(t)$ denote the number of susceptible and infected individuals in patch j at time $t \geq 0$.

Consider the following system of differential equations

$$\frac{dS_j}{dt} = d_S \sum_{k\in\Omega} \left(L_{jk}S_k - L_{kj}S_j\right) - \frac{\beta_j S_j I_j}{S_j + I_j} + \gamma I_j, \qquad j \in \Omega, \quad t > 0, \tag{2.29a}$$

$$\frac{dI_j}{dt} = d_I \sum_{k\in\Omega} \left(L_{jk}I_k - L_{kj}I_j\right) + \frac{\beta_j S_j I_j}{S_j + I_j} - \gamma I_j, \qquad j \in \Omega, \quad t > 0, \tag{2.29b}$$

where d_S and d_I are positive diffusion coefficients for the susceptible and infected subpopulations, L_{jk} represents the degree of movement from patch k into patch j, and β_j and γ_j are nonnegative constants that express the rate of disease transmission and recovery in patch j.

The respective equilibrium solution $(\overline{S}, \overline{I})$ satisfies

$$d_S \sum_{k\in\Omega} \left(L_{jk}\overline{S}_k - L_{kj}\overline{S}_j\right) - \frac{\beta_j \overline{S}_j \overline{I}_j}{\overline{S}_j + \overline{I}_j} + \gamma \overline{I}_j = 0, \qquad j \in \Omega, \quad t > 0, \tag{2.30a}$$

$$d_I \sum_{k\in\Omega} \left(L_{jk}\overline{I}_k - L_{kj}\overline{I}_j\right) + \frac{\beta_j \overline{S}_j \overline{I}_j}{\overline{S}_j + \overline{I}_j} - \gamma \overline{I}_j = 0, \qquad j \in \Omega, \quad t > 0, \tag{2.30b}$$

Following the previous theory, we can write (2.29b) as

$$\frac{d\overline{I}}{dt} = \mathscr{F} - \mathscr{V},$$

where $\mathscr{F}$ denotes the vector of new infections and $\mathscr{V}$ the vector of transitions in the n infected states. Thus, the basic reproduction number for (2.29) is the spectral radius of the next generation matrix, $\rho(FV^{-1})$, with

$$F = diag(\beta_j), \quad V = diag(\gamma_j + d_I L_j) - d_I L,$$

where V depends on the rate of recovery and the connection matrix between the different patches, L, which determine the average time of stay in each infectious compartment.

3

The Model

In this Chapter we consider an epidemic problem modeled using a non-linear reaction-diffusion system. *Chapter 3* is organized as follows. In *Section 3.1* the epidemic model is presented, the initial conditions and assumptions are stated and the global existence and uniform boundedness of solution of the model is established. In *Section 3.2* the equilibrium problem is formulated and the different equilibrium solutions are defined. Lastly, in *Section 3.3* the existence of a *disease-free equilibrium* is proved and we investigate the threshold dynamics in terms of the basic reproduction number for two different problems: we consider the case where all the diffusion coefficients are positive and the case where only the diffusion coefficient of the exposed individuals is positive and the others are set to zero.

3.1 The Δ-SEIRS Model

We now consider a SEIRS reaction-diffusion model of the disease transmission for a population where individuals in each class move according to a diffusion process with non-negative constant diffusion coefficients d_S, d_E, d_I and d_R, respectively, with at least one positive diffusion coefficient. Moreover, $S(x,t)$, $E(x,t)$, $I(x,t)$ and $R(x,t)$ are set as the density of susceptible, exposed, infected and recovered individuals at location x and time t, respectively.

To incorporate the spatial heterogeneity, we set the disease transmission intensity, $\beta(x)$, rate of progression to the infectious state, $\varepsilon(x)$, recovery rate, $\gamma(x)$, and the lost of immunity rate, $\alpha(x)$, as positive Hölder-continuous functions dependent of x in Ω. *Table 3.1* describes the model's parameters.

The SEIRS reaction-diffusion model, which we will refer to as the Δ-SEIRS model, corresponds to the following partial differential equation system:

$$\frac{\partial S(x,t)}{\partial t} = d_S \Delta S(x,t) - \beta(x) I(x,t) S(x,t) + \alpha(x) R(x,t), \qquad x \in \Omega, \quad t > 0, \tag{3.1a}$$

$$\frac{\partial E(x,t)}{\partial t} = d_E \Delta E(x,t) + \beta(x) I(x,t) S(x,t) - \varepsilon(x) E(x,t), \qquad x \in \Omega, \quad t > 0, \tag{3.1b}$$

$$\frac{\partial I(x,t)}{\partial t} = d_I \Delta I(x,t) + \varepsilon(x) E(x,t) - \gamma(x) I(x,t), \qquad x \in \Omega, \quad t > 0, \tag{3.1c}$$

$$\frac{\partial R(x,t)}{\partial t} = d_R \Delta R(x,t) + \gamma(x) I(x,t) - \alpha(x) R(x,t), \qquad x \in \Omega, \quad t > 0, \tag{3.1d}$$

where $\Omega \subset \mathbb{R}^l$ ($l \geq 1$) is a bounded domain with smooth boundary $\partial\Omega$ (when $l > 1$).

Furthermore, we assume that there is no flux across the boundary $\partial\Omega$, *i.e.*,

$$\frac{\partial S}{\partial n} = \frac{\partial E}{\partial n} = \frac{\partial I}{\partial n} = \frac{\partial R}{\partial n} = 0, \quad x \in \partial\Omega, \quad t > 0, \tag{3.2}$$

where n denotes the outward unit normal vector to $\partial\Omega$. This means that no individuals cross the boundary.

Parameter	Description
$S(x,t)$, $E(x,t)$, $I(x,t)$, $R(x,t)$	Density of individuals at location x and time t
d_S, d_E, d_I, d_R	Diffusion coefficients
$\beta(x)$	Disease transmission intensity
$\beta(x)S(x,t)I(x,t)$	Density-dependent transmission
$\varepsilon(x)$	Progression to the infectious state rate
$\gamma(x)$	Recovery rate
$\alpha(x)$	Lost of immunity rate

Table 3.1: Description of the parameters used in the model.

We will also assume that the initial values $S(x,0)$, $E(x,0)$, $I(x,0)$ and $R(x,0)$ are non-negative continuous functions in $\overline{\Omega}$. Moreover, assume that there are initially positive number of exposed or infected individuals, *i.e.*,

$$\int_\Omega E(x,0)dx > 0 \quad \text{or} \quad \int_\Omega I(x,0)dx > 0, \tag{3.3}$$

and that the total number of individuals in Ω at time $t = 0$ is equal to some positive constant $N_0 > 0$, *i.e.*,

$$\int_\Omega \Big(S(x,0) + E(x,0) + I(x,0) + R(x,0)\Big)dx = N_0. \tag{3.4}$$

Note that, from adding equations (3.1a)-(3.1d), we have

$$\begin{aligned}
& \frac{\partial S}{\partial t} + \frac{\partial E}{\partial t} + \frac{\partial I}{\partial t} + \frac{\partial R}{\partial t} = d_S \Delta S + d_E \Delta E + d_I \Delta I + d_R \Delta R \\
\Leftrightarrow \quad & \frac{\partial}{\partial t}\Big(S + E + I + R\Big) = \Delta(d_S S + d_E E + d_I I + d_R R) \\
\Rightarrow \quad & \int_\Omega \frac{\partial}{\partial t}\Big(S + E + I + R\Big)dx = \int_\Omega \Delta\Big(d_S S + d_E E + d_I I + d_R R\Big)dx.
\end{aligned}$$

From Green's formula, we know

$$\int_U \Big(\nabla u \cdot \nabla v\Big) dy = -\int_U u \Delta v dy + \int_{\partial U} u \frac{\partial v}{\partial n} dS_y, \tag{3.5}$$

which implies

$$\begin{aligned} & \int_\Omega \frac{\partial}{\partial t}\Big(S+E+I+R\Big)dx = \int_\Omega \Delta\Big(d_S S + d_E E + d_I I + d_R R\Big)dx \\ \Leftrightarrow \quad & \frac{\partial}{\partial t}\int_\Omega \Big(S+E+I+R\Big)dx = -\int_\Omega \nabla 1 \cdot \nabla\Big(d_S S + d_E E + d_I I + d_R R\Big)dx + \\ & \qquad + \int_{\partial\Omega} \frac{\partial}{\partial n}\Big(d_S S + d_E E + d_I I + d_R R\Big) dS_y \end{aligned}$$

Hence, from (3.2), we have

$$\frac{\partial}{\partial t}\Big[\int_\Omega \Big(S(x,t)+E(x,t)+I(x,t)+R(x,t)\Big)dx\Big] = 0, \tag{3.6}$$

which, in addition to (3.4), implies that the total population size over time is a constant given by

$$\int_\Omega \Big(S(x,t)+E(x,t)+I(x,t)+R(x,t)\Big)dx = N_0, \quad t \geq 0. \tag{3.7}$$

The next result establishes the global existence for the solution of problem (3.1)-(3.4).

Theorem 3.1.1

Suppose that $S(x,0)$, $E(x,0)$, $I(x,0)$ and $R(x,0)$ are non-negative continuous functions in $\overline{\Omega}$, and that assumptions (3.3) and (3.4) hold. Then problem (3.1)-(3.2) has a unique solution globally, such that

$$S(x,t), E(x,t), I(x,t), R(x,t) \geq 0, \quad x \in \overline{\Omega}, \quad t > 0. \tag{3.8}$$

Proof. *The proof is similar to that of [***Theorem 2.1***, 6].*

■

3.2 The Equilibrium Problem

Throughout this section we will be interest primarily in the equilibrium solutions of system (3.1) with (3.2), *i.e.*, solutions (S,E,I,R) such that there exists a $t_0 > 0$ such that

$$\frac{\partial S(x,t)}{\partial t} = \frac{\partial E(x,t)}{\partial t} = \frac{\partial I(x,t)}{\partial t} = \frac{\partial R(x,t)}{\partial t} = 0, \quad \forall x \in \Omega, \quad t > t_0.$$

Thus the equilibrium solution $(\overline{S}, \overline{E}, \overline{I}, \overline{R})$ satisfies

$$d_S \Delta \overline{S}(x) - \beta(x)\overline{I}(x)\overline{S}(x) + \alpha(x)\overline{R}(x) = 0, \qquad x \in \Omega, \tag{3.9a}$$

$$d_E \Delta \overline{E}(x) + \beta(x)\overline{I}(x)\overline{S}(x) - \varepsilon(x)\overline{E}(x) = 0, \qquad x \in \Omega, \tag{3.9b}$$

$$d_I \Delta \overline{I}(x) + \varepsilon(x)\overline{E}(x) - \gamma(x)\overline{I}(x) = 0, \qquad x \in \Omega, \tag{3.9c}$$

$$d_R \Delta \overline{R}(x) + \gamma(x)\overline{I}(x) - \alpha(x)\overline{R}(x) = 0, \qquad x \in \Omega, \tag{3.9d}$$

$$\frac{\partial \overline{S}(x)}{\partial n} = \frac{\partial \overline{E}(x)}{\partial n} = \frac{\partial \overline{I}(x)}{\partial n} = \frac{\partial \overline{R}(x)}{\partial n} = 0, \qquad x \in \partial\Omega. \tag{3.9e}$$

Here, $\overline{S}(x)$, $\overline{E}(x)$, $\overline{I}(x)$ and $\overline{R}(x)$ denote the densities of susceptible, exposed, infected and recovered individuals, respectively, at equilibrium for $x \in \Omega$. From (3.7) follows

$$\int_\Omega \Big(\overline{S}(x) + \overline{E}(x) + \overline{I}(x) + \overline{R}(x)\Big)dx = N_0. \tag{3.10}$$

For the purpose of our study, we are only interested in non-negative solutions $(\overline{S}, \overline{E}, \overline{I}, \overline{R})$ of system (3.9).

Since the infected subgroups are linked in such a way that one infected subgroup cannot go to zero unless all of the infected subgroups go to zero, we define a ***DFE*** as a solution of problem (3.9)-(3.10) in which $\overline{E}(x)$ and $\overline{I}(x)$ are identically zero for every $x \in \Omega$. Biologically, this means that a DFE is a solution of system (3.9)-(3.10) where all infectious compartments become extinct. By close inspection of system (3.9), we see that by replacing $\overline{E} \equiv \overline{I} \equiv 0$ on equation (3.9d) and integrating both parts of the equation in Ω, we have

$$\underbrace{\int_\Omega d_R \Delta \overline{R}(x)dx}_{=0} - \int_\Omega \alpha(x)\overline{R}(x)dx = 0 \Leftrightarrow \int_\Omega \alpha(x)\overline{R}(x)dx = 0.$$

Since $\alpha(x)$ is positive and continuous in Ω and $\overline{R}(x)$ is non-negative and continuous in Ω, we conclude that $\overline{R}(x) \equiv 0$ for all $x \in \Omega$ when $\overline{E} \equiv \overline{I} \equiv 0$. Thus, the *disease-free equilibrium* is of the form $\Big(\overline{S}(x), 0, 0, 0\Big)$.

On the other hand, an ***endemic equilibrium (EE)*** is a solution of system (3.9) on which $\overline{E}(x)$ or $\overline{I}(x)$ are positive functions for some $x \in \Omega$, *i.e.*, the disease still prevails.

For notational purposes, we will denote the DFE by $(\widetilde{S}, 0, 0, 0)$ and the EE by $(\widehat{S}, \widehat{E}, \widehat{I}, \widehat{R})$.

3.3 The Disease-Free Equilibrium

Suppose that assumptions taken on *Theorem 3.1.1* hold and N_0 in (3.7) is fixed. Consider the reaction-diffusion epidemic model described by (3.1)-(3.4). We distinguish two different reaction-diffusion epidemic problems.

First we focus our study in the problem with all diffusion coefficients set as positive constants where we establish the existence and uniqueness of a DFE for this problem. Following the settings of *Wang and Zhao* studied in *Chapter 2*, the respective basic reproduction number is defined and the threshold criterion is shown to hold.

Next, a reaction-diffusion problem with some diffusion coefficients equal to zero is studied. Similar results to those of the first problem are proved. Lastly, an explicit characterization of the basic reproduction number is given and the respective threshold dynamics are studied.

3.3.1 Reaction-diffusion epidemic problem with all diffusion coefficients positive

Suppose that all diffusion coefficients d_S, d_E, d_I and d_R are positive.

First we study the existence and uniqueness of a disease-free equilibrium of problem (3.1)-(3.4).

Proposition 3.3.1

Problem (3.1)-(3.4) has a unique DFE on Ω, which is given by

$$\left(\widetilde{S}, \widetilde{E}, \widetilde{I}, \widetilde{R}\right) = \left(\frac{N_0}{|\Omega|}, 0, 0, 0\right), \tag{3.11}$$

where $|\Omega|$ denotes the measure of Ω.

Proof. *Observe first, by replacing $\left(\frac{N_0}{|\Omega|}, 0, 0, 0\right)$ in (3.1), that this is a solution of the equilibrium problem. Thus, existence of a DFE comes directly from noting that $\left(\frac{N_0}{|\Omega|}, 0, 0, 0\right)$ is by definition a DFE since it is a non-negative solution of (3.1)-(3.4) and*

$$\widetilde{E} = \widetilde{I} = 0.$$

Now, let $(\widetilde{S}, 0, 0, 0)$ be any DFE. From (3.9), we have

$$d_S \Delta \widetilde{S}(x) = 0.$$

Therefore, since by hypothesis $d_S > 0$, $\widetilde{S}(x)$ satisfies

$$\Delta \widetilde{S}(x) = 0, \quad x \in \Omega \quad \text{and} \quad \frac{\partial \widetilde{S}(x)}{\partial n} = 0, \quad x \in \partial\Omega.$$

Hence, by the maximum principle, we have that $\widetilde{S}$ is constant in Ω. In view of (3.10), we then obtain

$$\widetilde{S}(x) = \frac{N_0}{|\Omega|}, \quad \forall x \in \Omega,$$

which establishes the uniqueness of the DFE solution.

■

Following the settings in *Chapter 2*, we now define matrices $F(x)$ and $V(x)$, with $x \in \Omega$, for model (3.1)-(3.4). Here we point out that, as $\mathscr{F}$ is defined by the infection process and this process only occurs from susceptibles to exposed individuals, we have $\mathscr{F}_I(x,u) = 0$ given that new individuals in this compartment are only transfers from the previous one.

Hence, we have

$$\mathscr{F}(x,u) = \begin{Bmatrix} \mathscr{F}_E(x,u) \\ \mathscr{F}_I(x,u) \\ \mathscr{F}_S(x,u) \\ \mathscr{F}_R(x,u) \end{Bmatrix} = \begin{Bmatrix} \beta(x)I(x,t)S(x,t) \\ 0 \\ 0 \\ 0 \end{Bmatrix}$$

and

$$\mathscr{V}(x,u) = \begin{Bmatrix} \mathscr{V}_E(x,u) \\ \mathscr{V}_I(x,u) \\ \mathscr{V}_S(x,u) \\ \mathscr{V}_R(x,u) \end{Bmatrix} = \begin{Bmatrix} \mathscr{V}_E^-(x,u) - \mathscr{V}_E^+(x,u) \\ \mathscr{V}_I^-(x,u) - \mathscr{V}_I^+(x,u) \\ \mathscr{V}_S^-(x,u) - \mathscr{V}_S^+(x,u) \\ \mathscr{V}_R^-(x,u) - \mathscr{V}_R^+(x,u) \end{Bmatrix} = \begin{Bmatrix} \varepsilon(x)E(x,t) \\ \gamma(x)I(x,t) - \varepsilon(x)E(x,t) \\ \beta(x)I(x,t)S(x,t) - \alpha(x)R(x,t) \\ \alpha(x)R(x,t) - \gamma(x)I(x,t) \end{Bmatrix}.$$

Note that, for all compartments, functions $\mathscr{F}(x,u)$ and $\mathscr{V}(x,u)$ satisfy assumptions $(A1)$ – $(A4)$.

We then can set

$$D_u\mathscr{F}(x,DFE) = \begin{bmatrix} 0 & \frac{N_0}{|\Omega|}\beta(x) & 0 & 0 \\ 0 & 0 & 0 & 0 \\ 0 & 0 & 0 & 0 \\ 0 & 0 & 0 & 0 \end{bmatrix}, \quad D_u\mathscr{V}(x,DFE) = \begin{bmatrix} \varepsilon(x) & 0 & 0 & 0 \\ -\varepsilon(x) & \gamma(x) & 0 & 0 \\ 0 & \frac{N_0}{|\Omega|}\beta(x) & 0 & -\alpha(x) \\ 0 & -\gamma(x) & 0 & \alpha(x). \end{bmatrix}$$

Hence matrices $F(x)$ and $V(x)$, only related to the infectious compartments, are defined by

$$F(x) = \begin{bmatrix} 0 & \frac{N_0}{|\Omega|}\beta(x) \\ 0 & 0 \end{bmatrix}, \quad V(x) = \begin{bmatrix} \varepsilon(x) & 0 \\ -\varepsilon(x) & \gamma(x) \end{bmatrix}. \tag{3.12}$$

Since $\varepsilon(x)$ and $\gamma(x)$ are positive, then $-V(x)$ is a quasi-positive matrix, for $x \in \Omega$. Let C be the operator defined by

$$C := \nabla \cdot (d_{inf}(x)\nabla) - V(x) = \begin{bmatrix} d_E\Delta - \varepsilon(x) & 0 \\ \varepsilon(x) & d_I\Delta - \gamma(x) \end{bmatrix},$$

with $d_{inf}(x) = diag\Big(d_E, d_I\Big)^T$. Operator C is resolvent-positive with $s(C) < 0$ [13].

Our goal now is to study the stability of the DFE. First we establish an eigenvalue value problem associated to system (3.1).

Let $\eta(x,t) = S(x,t) - \widetilde{S}(x)$, $\xi(x,t) = E(x,t)$, $\mu(x,t) = I(x,t)$ and $\nu(x,t) = R(x,t)$. For the susceptibles, since $\frac{\partial \widetilde{S}}{\partial t} = 0$, we have

$$\begin{aligned} & \frac{\partial \eta}{\partial t} = d_S\Delta S(x,t) - \beta(x)I(x,t)S(x,t) + \alpha(x)R(x,t) \\ \Leftrightarrow \quad & \frac{\partial \eta}{\partial t} = d_S\Delta\eta(x,t) - \beta(x)\mu(x,t)\Big[\eta(x,t) - \widetilde{S}(x)\Big] + \alpha(x)\nu(x,t). \end{aligned}$$

Hence, disregarding the non-linear factor $\beta(x)\mu(x,t)\eta(x,t)$, equation (3.1a) linearized around the DFE becomes

$$\frac{\partial \eta}{\partial t} = d_S \Delta \eta(x,t) - \frac{N_0}{|\Omega|}\beta(x)\mu(x,t) + \alpha(x)\nu(x,t).$$

Following the same arguments, we get similar equations for the exposed, infected and recovered variables. Therefore, linearizing (3.1) around the DFE, we obtain

$$\frac{\partial \eta}{\partial t} = d_S \Delta \eta(x,t) - \frac{N_0}{|\Omega|}\beta(x)\mu(x,t) + \alpha(x)\nu(x,t), \qquad x \in \Omega, \quad t > 0, \tag{3.13a}$$

$$\frac{\partial \xi}{\partial t} = d_E \Delta \xi(x,t) + \frac{N_0}{|\Omega|}\beta(x)\mu(x,t) - \varepsilon(x)\xi(x,t), \qquad x \in \Omega, \quad t > 0, \tag{3.13b}$$

$$\frac{\partial \mu}{\partial t} = d_I \Delta \mu(x,t) + \varepsilon(x)\xi(x,t) - \gamma(x)\mu(x,t), \qquad x \in \Omega, \quad t > 0, \tag{3.13c}$$

$$\frac{\partial \nu}{\partial t} = d_R \Delta \nu(x,t) + \gamma(x)\mu(x,t) - \alpha(x)\nu(x,t), \qquad x \in \Omega, \quad t > 0. \tag{3.13d}$$

Suppose that

$$\Big(\eta(x,t), \xi(x,t), \mu(x,t), \nu(x,t)\Big) = \Big(e^{\lambda t}\phi_S(x), e^{\lambda t}\phi_E(x), e^{\lambda t}\phi_I(x), e^{\lambda t}\phi_R(x)\Big), \tag{3.14}$$

is a solution of the linear system (3.13), with $\lambda \in \mathbb{R}$. Replacing (3.14) into (3.13) and dividing the resulting by $e^{\lambda t}$, we get the following linear eigenvalue problem

$$d_S \Delta \phi_S(x) - \frac{N_0}{|\Omega|}\beta(x)\phi_I(x) + \alpha(x)\phi_R(x) - \lambda\phi_S(x) = 0, \qquad x \in \Omega, \tag{3.15a}$$

$$d_E \Delta \phi_E(x) + \frac{N_0}{|\Omega|}\beta(x)\phi_I(x) - \varepsilon(x)\phi_E(x) - \lambda\phi_E(x) = 0, \qquad x \in \Omega, \tag{3.15b}$$

$$d_I \Delta \phi_I(x) + \varepsilon(x)\phi_E(x) - \gamma(x)\phi_I(x) - \lambda\phi_I(x) = 0, \qquad x \in \Omega, \tag{3.15c}$$

$$d_R \Delta \phi_R(x) + \gamma(x)\phi_I(x) - \alpha(x)\phi_R(x) - \lambda\phi_R(x) = 0, \qquad x \in \Omega. \tag{3.15d}$$

From (3.2), we must impose

$$\frac{\partial \phi_S(x)}{\partial n} = \frac{\partial \phi_E(x)}{\partial n} = \frac{\partial \phi_I(x)}{\partial n} = \frac{\partial \phi_R(x)}{\partial n} = 0, \quad x \in \partial\Omega. \tag{3.16}$$

On the other hand, from (3.10) and *Proposition 3.3.1*, we have

$$\int_\Omega [\eta(x,t)+\xi(x,t)+\mu(x,t)+\nu(x,t)]dx = \int_\Omega [S(x,t)+E(x,t)+I(x,t)+R(x,t)]dx - \int_\Omega \widetilde{S}(x)dx = 0,$$

and thus

$$\begin{aligned} & e^{\lambda t}\int_\Omega \Big[\phi_S(x)+\phi_E(x)+\phi_I(x)+\phi_R(x)\Big]dx = 0 \\ \Leftrightarrow \quad & \int_\Omega \Big[\phi_S(x)+\phi_E(x)+\phi_I(x)+\phi_R(x)\Big]dx = 0. \end{aligned} \tag{3.17}$$

We now wish to focus our study in the system associated only with the equations regarding the infectious compartments in system (3.15)-(3.16), which is given by

$$d_E \Delta \phi_E(x) + \frac{N_0}{|\Omega|}\beta(x)\phi_I(x) - \varepsilon(x)\phi_E(x) - \lambda\phi_E(x) = 0, \qquad x \in \Omega, \tag{3.18a}$$

$$d_I \Delta \phi_I(x) + \varepsilon(x)\phi_E(x) - \gamma(x)\phi_I(x) - \lambda\phi_I(x) = 0, \qquad x \in \Omega, \tag{3.18b}$$

$$\frac{\partial \phi_E}{\partial n} = \frac{\partial \phi_I}{\partial n} = 0, \qquad x \in \partial\Omega. \tag{3.18c}$$

We are now in conditions to study system (3.13) and the stability of the *disease-free equilibrium*.

In view of the elliptic eigenvalue problem (3.18), the next result establishes the existence of a principal simple eigenvalue with a positive eigenfunction.

Lemma 3.3.2
The elliptic eigenvalue problem (3.18) has a principal simple eigenvalue λ^*.

Proof. *Our goal is to apply Theorem 2.2.1.*

Let $d_0 := \min\{d_S, d_E, d_I, d_R\}$. Then condition $(D1)$ in Theorem 2.2.1 is satisfied.

Set

$$M(x) = \begin{bmatrix} -\varepsilon(x) & \frac{N_0}{|\Omega|}\beta(x) \\ \varepsilon(x) & -\gamma(x) \end{bmatrix},$$

and

$$L = diag\Big(d_E\Delta, d_I\Delta\Big).$$

Since $\varepsilon(x)$ and $\beta(x)$ are positive functions, $M(x)$ is a quasi-positive matrix for all $x \in \Omega$. Thus, it is enough to show that there exists an $x_0 \in \Omega$ such that $M(x_0)$ is irreducible.

We have

$$(I + |M(x)|) = \begin{bmatrix} 1 + \varepsilon(x) & \frac{N_0}{|\Omega|}\beta(x) \\ \varepsilon(x) & 1 + \gamma(x) \end{bmatrix},$$

with $|M(x)|$ denoting the matrix given by $M(x)$ entries in module.

Functions $\varepsilon(x)$, $\beta(x)$ and $\gamma(x)$ are positive, then all entries of matrix $(I + |M(x)|)$ are bigger than zero. Hence $(I + |M(x)|)$ is a positive matrix for all $x \in \Omega$. Following Theorem A.0.6, in Auxiliary Definitions and Results, we conclude that $M(x)$ is an irreducible matrix for all $x \in \Omega$.

Therefore, from Theorem 2.2.1, system (3.18) has an algebraically simple eigenvalue with a strongly positive eigenvector.

■

Following the settings of *Wang and Zhao* studied in *Chapter 2*, let $\mathscr{R}_0$ represent the basic reproduction number of system (3.1)-(3.4).

To prove the DFE local stability we cannot apply directly *Theorem 2.2.5 (ii)*, since, as we will see more in detail, condition (A6) is not verified for our system. Hence we divide our analysis into two steps. First, we establish an important relation between the sign of $\mathscr{R}_0 - 1$ and the principal eigenvalue of system (3.18). The proof is similar to the proof of *Theorem 2.2.5 (i)*.

Theorem 3.3.3 [21]
$\mathscr{R}_0 - 1$ has the same sign as λ^*, where λ^* is the principal eigenvalue of (3.18) with a positive eigenfunction.

Proof. *The proof is similar to that of Theorem 2.2.5 (i).*

■

Let $M^0(x)$ denote matrix (2.11) defined in *Chapter 2.* For our epidemic model, we have

$$M^0(x) = \begin{bmatrix} 0 & \alpha(x) \\ 0 & -\alpha(x) \end{bmatrix}. \tag{3.19}$$

Although $M^0(x)$ is a quasi-positive matrix, from close inspection one can see that it does not verify assumption (A6) since we do not have

$$s\Big(diag(d_S\Delta, d_R\Delta) + M^0(x)\Big) < 0.$$

Hence, the next result is a reformulation of the proof of statement in *Theorem 2.2.5 (ii)*, following *Theorem 2.2.4*.

Theorem 3.3.4
If $\mathscr{R}_0 < 1$ then the DFE is asymptotically stable for problem (3.1).

Proof. *Suppose that $\mathscr{R}_0 < 1$.*

Our goal is to show that the disease-free equilibrium is asymptotically stable. Following Theorem 2.2.4, we then want to show that if $(\lambda, \vec{\phi})$ is a solution of problem (3.15)-(3.17), where $\vec{\phi} = \Big(\phi_S, \phi_E, \phi_I, \phi_R\Big)^T$ with at least one entry not identically zero, then

$$Re(\lambda) < 0.$$

For this purpose, we argue by contradiction. Suppose that $(\lambda, \vec{\phi})$ is a solution of system (3.15)-(3.17), with $\vec{\phi}$ not identically zero and

$$Re(\lambda) \geq 0. \tag{3.20}$$

Assume that $\phi_E \equiv 0$. Then, following (3.15), we have

$$\begin{aligned} &d_I\Delta\phi_I(x) - \gamma(x)\phi_I(x) = \lambda\phi_I(x), && x \in \Omega, \\ &\frac{\partial\phi_I(x)}{\partial n} = 0, && x \in \partial\Omega. \end{aligned}$$

Since $\gamma(x)$ is positive in Ω, from [21], we have

$$s\Big(d_I\Delta - \gamma(x)\Big) < 0 \quad \textit{and} \quad Re(\lambda) < s\Big(d_I\Delta - \gamma(x)\Big).$$

Then $\lambda < 0$ which is a contradiction. Hence $\phi_I \equiv 0$.

Note that, if ϕ_E and ϕ_I are identically zero, from (3.15d) we have

$$\begin{aligned} &d_R\Delta\phi_R - \alpha(x)\phi_R(x) - \lambda\phi_R(x) = 0, && x \in \Omega, \\ &\frac{\partial\phi_R(x)}{\partial n} = 0, && x \in \partial\Omega. \end{aligned}$$

Since $\alpha(x)$ is positive in Ω, we can argue in the same way as before. Hence, we have $Re(\lambda) < 0$ and so we come to a contradiction. Thus $\phi_R \equiv 0$.

If ϕ_E, ϕ_I and ϕ_R are identically zero, following equation (3.15a) we have

$$d_S \Delta \phi_S(x) - \lambda \phi_S(x) = 0, \qquad x \in \Omega \tag{3.21}$$

$$\frac{\partial \phi_S(x)}{\partial n} = 0, \qquad x \in \partial\Omega. \tag{3.22}$$

Since the laplacian is a self-adjoint operator, then λ is real. Following (3.21), we have

$$d_S \Delta \phi_S - \lambda \phi_S(x) = 0 \Leftrightarrow d_S \phi_S(x) \Delta \phi_S(x) - \lambda \phi_S^2(x) = 0.$$

Then

$$\int_\Omega d_S \phi_S(x) \Delta \phi_S(x) dx = \lambda \int_\Omega \phi_S^2(x) dx,$$

and using Green's Formula, (3.5), we get

$$\begin{aligned} & -\int_\Omega d_S |\nabla \phi_S(x)|^2 dx = \lambda \int_\Omega \phi_S^2(x) dx \\ \Leftrightarrow \quad & \lambda = \frac{-d_S \int_\Omega |\nabla \phi_S(x)|^2 dx}{\int_\Omega \phi_S^2(x) dx} < 0. \end{aligned}$$

Thus, from (3.20), we come to a contradiction. Therefore, $\phi_S \equiv 0$ which implies that $\vec{\phi} \equiv 0$, which is a contradiction and so we conclude that $\phi_E \not\equiv 0$.

Now suppose that $\phi_S \equiv 0$. Then, from equation (3.15b), we have

$$\begin{aligned} & d_E \Delta \phi_E(x) - \epsilon(x) \phi_E(x) - \lambda \phi_E(x) = 0, && x \in \Omega, \\ & \frac{\partial \phi_E(x)}{\partial n} = 0, && x \in \partial\Omega. \end{aligned}$$

Since $\varepsilon(x)$ is a positive function on Ω, using the same arguments as before we get that $\lambda < 0$, which is a contradiction. Hence, $\phi_S \not\equiv 0$.

Now, since $\phi_E \not\equiv 0$ then we must have $\phi_I \not\equiv 0$.

Let $\vec{\phi}_{inf} = \Big(\phi_E(x), \phi_I(x)\Big)$. Since by assumption $(\lambda, \vec{\phi})$ is a solution to system (3.15)-(3.17), then $(\lambda, \vec{\phi}_{inf})$ is a solution of the following eigenvalue problem

$$B\vec{\phi}_{inf} + F\vec{\phi}_{inf} - \lambda \vec{\phi}_{inf} = 0, \qquad x \in \Omega, \tag{3.23}$$

$$\frac{\partial \phi_E}{\partial n} = \frac{\partial \phi_I}{\partial n} = 0, \qquad x \in \partial\Omega, \tag{3.24}$$

where F is defined as in (3.12) and $B = diag\Big(d_E \Delta, d_I \Delta\Big) - V$.

Let $\lambda^* := s(B + F)$. From Theorem 2.2.1 and (3.20), we have

$$\lambda^* > Re(\lambda) \geq 0.$$

However, Theorem 3.3.3 implies that λ^* has the same sign as $\mathscr{R}_0 - 1$, i.e.,

$$\lambda^* < 0,$$

hence we come to a contradiction.

We conclude that if $(\lambda, \vec{\phi})$ is a solution to (3.15)-(3.17), with at least one of ϕ_S, ϕ_E, ϕ_I or ϕ_R not identically zero on Ω, then

$$Re(\lambda) < 0.$$

This proves that the DFE is asymptotically stable.

■

It is only left to study the conditions where the DFE is not a stable solution of system (3.9). We have the following result:

Theorem 3.3.5

If $\mathscr{R}_0 > 1$ then there exists $\epsilon_0 > 0$ such that any positive solution of (3.1) satisfies

$$\limsup_{t\to\infty} \|\Big(S(\cdot,t), E(\cdot,t), I(\cdot,t), R(\cdot,t)\Big) - \Big(\frac{N_0}{|\Omega|}, 0, 0, 0\Big)\|_{L^\infty(\Omega)} \geq \epsilon_0.$$

Proof. *Suppose that $\mathscr{R}_0 > 1$. Theorem 3.3.3 states that $\mathscr{R}_0 - 1$ has the same sign as λ^*, where λ^* is the principal eigenvalue of the elliptic eigenvalue problem (3.18) with a positive eigenfunction. Hence*

$$\lambda^* > 0.$$

For $\epsilon \in \Big(0, \frac{N_0}{|\Omega|}\Big)$, we consider the following eigenvalue problem

$$d_E \Delta E(x) + \beta(x) I(x)\Big(\frac{N_0}{|\Omega|} - \epsilon\Big) - \varepsilon(x) E(x) = \lambda E(x), \qquad x \in \Omega, \tag{3.25a}$$

$$d_I \Delta I(x) + \varepsilon(x) E(x) - \gamma(x) I(x) = \lambda I(x), \quad x \in \Omega, \qquad x \in \Omega, \tag{3.25b}$$

$$\frac{\partial E}{\partial n} = \frac{\partial I}{\partial n} = 0, \qquad x \in \partial\Omega. \tag{3.25c}$$

One can show, by the same arguments as in Lemma 3.3.2, that problem (3.25) has a principal eigenvalue λ_ϵ^* with a positive eigenfunction $\phi_\epsilon^*(x)$. We set $\phi_\epsilon^*(x) = \Big(\phi_{\epsilon_0}^{*E}(x), \phi_{\epsilon_0}^{*I}(x)\Big)^T$.

Taking $\epsilon \to 0$, problem (3.25) becomes problem (3.18) and we conclude

$$\lim_{\epsilon\to 0} \lambda_\epsilon^* = \lambda^* > 0.$$

Then we can fix a small $\epsilon_0 \in \Big(0, \frac{N_0}{|\Omega|}\Big)$ so that $\lambda_{\epsilon_0}^* > 0$.

For the sake of contradiction, assume that there exists a positive solution $\Big(S(x,t), E(x,t), I(x,t), R(x,t)\Big)$ of problem (3.1) such that

$$\limsup_{t\to\infty} \Big\|(S(x,t), E(x,t), I(x,t), R(x,t)) - \Big(\frac{N_0}{|\Omega|}, 0, 0, 0\Big)\Big\|_{L^\infty(\Omega)} < \epsilon_0. \tag{3.26}$$

Then there exists a large enough $t_0 > 0$ such that

$$\frac{\partial E(x,t)}{\partial t} \geq d_E \Delta E(x) + \beta(x) I(x)\Big(\frac{N_0}{|\Omega|} - \epsilon_0\Big) - \varepsilon(x) E(x), \tag{3.27}$$

$$\frac{\partial I(x,t)}{\partial t} \geq d_I \Delta I(x) + \varepsilon(x) E(x) - \gamma(x) I(x), \tag{3.28}$$

for all $t \geq t_0$. Since $E(\cdot, t_0)$ and $I(\cdot, t_0)$ are non-negative in $\mathscr{C}(\Omega)$, we can choose a sufficiently small number $\eta > 0$ such that

$$E(\cdot, t_0) \geq \eta \phi^{*E}_{\epsilon_0}(x) \quad \text{and} \quad I(\cdot, t_0) \geq \eta \phi^{*I}_{\epsilon_0}(x).$$

Set $u(x,t) = \eta e^{\lambda^*_{\epsilon_0}(t-t_0)} \phi^*_{\epsilon_0}(x)$. Note that $u(x,t)$ is a solution of the following linear system

$$\frac{\partial E}{\partial t} = d_E \Delta E(x,t) + \beta(x) I(x,t)\left(\frac{N_0}{|\Omega|} - \epsilon_0\right) - \varepsilon(x) E(x,t), \qquad x \in \Omega, \tag{3.29a}$$

$$\frac{\partial I}{\partial t} = d_I \Delta I(x,t) + \varepsilon(x) E(x,t) - \gamma(x) I(x,t), \qquad x \in \Omega, \tag{3.29b}$$

$$\frac{\partial E}{\partial n} = \frac{\partial I}{\partial n} = 0, \qquad x \in \partial\Omega, \tag{3.29c}$$

for all $t \geq t_0$. It then follows from inequalities (3.27) and (3.28) that $\Big(E(x,t), I(x,t)\Big)$ and $u(x,t)$ are, respectively, a super-solution and sub-solution of the linear system (3.29). From the Comparison Principle, we get

$$E(\cdot, t_0) \geq \eta e^{\lambda^*_{\epsilon_0}(t-t_0)} \phi^{*E}_{\epsilon_0}(x) \quad \text{and} \quad I(\cdot, t_0) \geq \eta e^{\lambda^*_{\epsilon_0}(t-t_0)} \phi^{*I}_{\epsilon_0}(x),$$

for all $x \in \Omega$ and $t \geq t_0$. Hence $E(x,t)$ and $I(x,t)$ approach ∞ as $t \to \infty$, which is a contradiction in view of (3.26).

We conclude that

$$\limsup_{t\to\infty} \| \Big(S(\cdot,t), E(\cdot,t), I(\cdot,t), R(\cdot,t)\Big) - \left(\frac{N_0}{|\Omega|}, 0, 0, 0\right) \|_{L^\infty(\Omega)} \geq \epsilon_0.$$

■

3.3.1.1 Characterization of the $\mathscr{R}_0$

The subsequent result characterizes the basic reproduction number, $\mathscr{R}_0$, of system (3.1)-(3.4) in terms of the principal eigenvalue of the following elliptic eigenvalue problem.

Theorem 3.3.6

Let μ_0 be the unique positive eigenvalue with a positive eigenfunction of the eigenvalue problem

$$-d_E \Delta \phi_E(x) + \varepsilon(x)\phi_E(x) = \mu \frac{N_0}{|\Omega|} \beta(x) \phi_I(x), \qquad x \in \Omega, \tag{3.30a}$$

$$-d_I \Delta \phi_I(x) - \varepsilon(x)\phi_E(x) + \gamma(x)\phi_I(x) = 0, \qquad x \in \Omega, \tag{3.30b}$$

$$\frac{\partial \phi_E}{\partial n} = \frac{\partial \phi_I}{\partial n} = 0, \qquad x \in \partial\Omega. \tag{3.30c}$$

Then

$$\mathscr{R}_0 = \frac{1}{\mu_0}.$$

Proof. *From (3.12), we have*

$$F(x) = \begin{bmatrix} 0 & \beta(x)\frac{N_0}{|\Omega|} \\ 0 & 0 \end{bmatrix}, \quad V(x) = \begin{bmatrix} \varepsilon(x) & 0 \\ -\varepsilon(x) & \gamma(x) \end{bmatrix}.$$

Let

$$B := diag\Big(d_E\Delta, d_I\Delta\Big) - V. \tag{3.31}$$

Following the same arguments as [10], it follows that the eigenvalue problem

$$-B\phi(x) = \mu F\phi(x), \quad x \in \Omega \tag{3.32a}$$

$$\frac{\partial\phi}{\partial n} = 0, \quad x \in \partial\Omega, \tag{3.32b}$$

has a unique positive eigenvalue with a positive eigenfunction, μ_0.

Applying Theorem 2.2.6 to the triple (F, V, B), it then follows

$$\mathscr{R}_0 = \rho(B^{-1}F) = \frac{1}{\mu_0}.$$

■

Even with the characterization obtained in the previous model, it is difficult to numerical compute $\mathscr{R}_0$. The next result gives an estimate for the basic reproduction number.

Lemma 3.3.7 [18]

For any $d_E > 0$ and $d_I > 0$ the following inequalities hold:

$$\min\left\{\frac{N_0}{|\Omega|}\frac{\beta(x)}{\gamma(x)}, x \in \overline{\Omega}\right\} \leq \mathscr{R}_0 \leq \max\left\{\frac{N_0}{|\Omega|}\frac{\beta(x)}{\gamma(x)}, x \in \overline{\Omega}\right\}. \tag{3.33}$$

Proof. *Following Theorem 3.3.6, we have that $\mathscr{R}_0 = \frac{1}{\mu_0}$, where μ_0 denotes the unique positive eigenvalue with a positive eigenfunction, $\phi(x) = \Big(\phi_E(x), \phi_I(x)\Big)^T$, of the eigenvalue problem (3.30). Hence, from adding (3.30a) together with (3.30b), we get*

$$\begin{aligned} &-d_E\Delta\phi_E(x) + \varepsilon(x)\phi_E(x) - d_I\Delta\phi_I(x) - \varepsilon(x)\phi_E(x) + \gamma(x)\phi_I(x) = \frac{1}{\mathscr{R}_0}\frac{N_0}{|\Omega|}\beta(x)\phi_I(x) \\ \Leftrightarrow\ &-d_E\Delta\phi_E(x) - d_I\Delta\phi_I(x) + \gamma(x)\phi_I(x) = \frac{1}{\mathscr{R}_0}\frac{N_0}{|\Omega|}\beta(x)\phi_I(x), \quad x \in \Omega. \end{aligned}$$

Integrating by parts on Ω and using Green's Formula, (3.5), we have

$$\begin{aligned} &\underbrace{\int_\Omega (-d_E\Delta\phi_E(x) - d_I\Delta\phi_I(x))dx}_{=0} + \int_\Omega \gamma(x)\phi_I(x) = \int_\Omega \frac{1}{\mathscr{R}_0}\frac{N_0}{|\Omega|}\beta(x)\phi_I(x)dx \\ \Leftrightarrow\ &\int_\Omega \gamma(x)\phi_I(x)\Big[\mathscr{R}_0 - \frac{N_0}{|\Omega|}\frac{\beta(x)}{\gamma(x)}\Big]dx = 0. \end{aligned} \tag{3.34}$$

Let $f(x) = \frac{N_0}{|\Omega|}\frac{\beta(x)}{\gamma(x)}$ *be a positive and continuous function on* Ω*. Then, following (3.34), we get that there exists a* $c \in \Omega$ *such that*

$$\int_\Omega \gamma(x)\phi_I(x)\Big[\mathscr{R}_0 - f(x)\Big]dx = 0 \Leftrightarrow \Big[\mathscr{R}_0 - f(c)\Big]\int_\Omega \gamma(x)\phi_I(x)dx = 0.$$

Thus, since $\gamma(x)$ *and* $\phi_I(x)$ *are positive on* Ω*, we have that*

$$\mathscr{R}_0 = f(c), \tag{3.35}$$

which implies that

$$\min_{x\in\overline{\Omega}} f(x) \leq \mathscr{R}_0 \leq \max_{x\in\overline{\Omega}} f(x).$$

■

3.3.2 Reaction-diffusion epidemic problem with $d_S = d_I = d_R = 0$

Our main goal in this subsection is to understand how the interactions of individuals between each other and the environment affect the spatial distribution of the disease.

In the previous subsection a reaction-diffusion model was studied where all diffusion coefficients were set as positive constants, describing in this way a random dispersal of individuals. However, for longer periods of time this may lead to a spatial uniform dispersal of individuals due to natural migration. Thus, for larger time periods, a more realistic model of biological diffusion may come from setting only the diffusion coefficient of the exposed non zero, to capture only infection dispersal and not the total population dispersal. In this case, we can reduce the computation of $\mathscr{R}_0$ to that of the principal eigenvalue of a lower dimensional elliptic eigenvalue problem under additional conditions.

Here we focus our study in the case where only the diffusion coefficient of the exposed individuals, d_E, is positive. Thus, throughout this subsection we set

$$d_S = d_I = d_R = 0.$$

Hence, system (3.1) for this case is given by

$$\frac{\partial S(x,t)}{\partial t} = -\beta(x)I(x,t)S(x,t) + \alpha(x)R(x,t), \qquad x \in \Omega, t > 0, \tag{3.36a}$$

$$\frac{\partial E(x,t)}{\partial t} = d_E\Delta E(x,t) + \beta(x)I(x,t)S(x,t) - \varepsilon(x)E(x,t), \qquad x \in \Omega, t > 0, \tag{3.36b}$$

$$\frac{\partial I(x,t)}{\partial t} = \varepsilon(x)E(x,t) - \gamma(x)I(x,t), \qquad x \in \Omega, t > 0, \tag{3.36c}$$

$$\frac{\partial R(x,t)}{\partial t} = \gamma(x)I(x,t) - \alpha(x)R(x,t), \qquad x \in \Omega, t > 0, \tag{3.36d}$$

$$\frac{\partial E}{\partial n} = 0, \qquad x \in \partial\Omega, \quad t > 0, \tag{3.36e}$$

with

$$\int_\Omega \Big(S(x,t) + E(x,t) + I(x,t) + R(x,t)\Big)dx = N_0, \quad t \geq 0. \tag{3.37}$$

and so the equilibrium problem becomes

$$-\beta(x)\overline{I}(x)\overline{S}(x)+\alpha(x)\overline{R}(x)=0, \qquad x\in\Omega, \tag{3.38a}$$
$$d_E\Delta\overline{E}(x)+\beta(x)\overline{I}(x)\overline{S}(x)-\varepsilon(x)\overline{E}(x)=0, \qquad x\in\Omega, \tag{3.38b}$$
$$\varepsilon(x)\overline{E}(x)-\gamma(x)\overline{I}(x)=0, \qquad x\in\Omega, \tag{3.38c}$$
$$\gamma(x)\overline{I}(x)-\alpha(x)\overline{R}(x)=0, \qquad x\in\Omega, \tag{3.38d}$$
$$\frac{\partial\overline{E}(x)}{\partial n}=0, \qquad x\in\partial\Omega, \tag{3.38e}$$

with

$$\int_\Omega\Big(\overline{S}(x)+\overline{E}(x)+\overline{I}(x)+\overline{R}(x)\Big)dx=N_0. \tag{3.39}$$

We first show that the *disease-free solution* exists.

Proposition 3.3.8

Problem (3.38)-(3.39) has a disease-free equilibrium on Ω.

Proof. *Let* $(\widetilde{S}(x),0,0,0)$ *be any DFE. By replacing* $(\widetilde{S}(x),0,0,0)$ *in (3.38)-(3.39), one can see that this is a solution of the equilibrium problem. Thus, existence of a DFE comes directly from observing that* $(\widetilde{S}(x),0,0,0)$ *is by definition a DFE since it is a non-negative solution to (3.38)-(3.39) and*

$$\widetilde{E}(x)=\widetilde{I}(x)=0, \quad x\in\Omega.$$

■

Note that $\left(\frac{N_0}{|\Omega|},0,0,0\right)$ is also a solution to the equilibrium problem (3.38)-(3.39). However, for the case where only the diffusion coefficient of exposed individuals is non-zero we cannot obtain uniqueness of the disease-free equilibrium solution. Moreover, the DFE can be non-homogeneous in space.

For notation purposes, let $u=(\widetilde{S}(x),0,0,0)$ denote a disease-free equilibrium for system (3.38)-(3.39).

As we did for the preceding section, linearizing (3.36) around the DFE, we obtain

$$\frac{\partial\eta}{\partial t}=-\widetilde{S}(x)\beta(x)\mu(x,t)+\alpha(x)\nu(x,t), \qquad x\in\Omega, \tag{3.40a}$$
$$\frac{\partial\xi}{\partial t}=d_E\Delta\xi(x,t)+\widetilde{S}(x)\beta(x)\mu(x,t)-\varepsilon(x)\xi(x,t), \qquad x\in\Omega, \tag{3.40b}$$
$$\frac{\partial\mu}{\partial t}=\varepsilon(x)\xi(x,t)-\gamma(x)\mu(x,t), \qquad x\in\Omega, \tag{3.40c}$$
$$\frac{\partial\nu}{\partial t}=\gamma(x)\mu(x,t)-\alpha(x)\nu(x,t), \qquad x\in\Omega, \tag{3.40d}$$

where $\eta(x,t)=S(x,t)-\widetilde{S}(x)$, $\xi(x,t)=E(x,t)$, $\mu(x,t)=I(x,t)$ and $\nu(x,t)=R(x,t)$.

Observe now that, knowing the solution of (3.40b)-(3.40d) then (3.40a) together with the initial conditions is only a differential problem, *i.e.*, if $\left(\xi^*(x,t), \mu^*(x,t), \nu(x,t)^*\right)$ is a solution of problem (3.40b)-(3.40d) then

$$\begin{aligned} &\frac{\partial \eta}{\partial t} = g(x,t) = -\widetilde{S}(x)\beta(x)\mu^*(x,t) + \alpha(x)\nu^*(x,t), && x \in \Omega, \\ &\eta(x,0) = \eta_0, && x \in \Omega, \end{aligned}$$

is a differential equation whose solution is given by

$$\eta(x,t) = \int_0^t g(x,t)dt + \eta_0.$$

Thus, we can focus the study of the linearized system only in (3.40b)-(3.40d), decreasing in this way the number of equations for our problem.

Suppose that

$$\left(\xi(x,t), \mu(x,t), \nu(x,t)\right) = \left(e^{\lambda t}\phi_E(x), e^{\lambda t}\phi_I(x), e^{\lambda t}\phi_R(x)\right), \tag{3.41}$$

is a solution of the linear system (3.40b)-(3.40d), with $\lambda \in \mathbb{R}$. Replacing (3.41) into (3.40b)-(3.40d) and dividing the resulting by $e^{\lambda t}$, we get the following linear eigenvalue problem

$$\begin{aligned} d_E\Delta\phi_E(x) + \widetilde{S}(x)\beta(x)\phi_I(x) - \varepsilon(x)\phi_E(x) - \lambda\phi_E(x) = 0, && x \in \Omega, && \text{(3.42a)} \\ \varepsilon(x)\phi_E(x) - \gamma(x)\phi_I(x) - \lambda\phi_I(x) = 0, && x \in \Omega, && \text{(3.42b)} \\ \gamma(x)\phi_I(x) - \alpha(x)\phi_R(x) - \lambda\phi_R(x) = 0, && x \in \Omega. && \text{(3.42c)} \end{aligned}$$

In view of (3.36e) we must impose the additional condition

$$\frac{\partial \phi_E}{\partial n} = 0, \quad x \in \partial\Omega. \tag{3.43}$$

In this case, the eigenvalue problem associated to the system of equations (3.18) regarding the infectious compartments, is given by

$$\begin{aligned} d_E\Delta\phi_E(x) + \beta(x)\widetilde{S}(x)\phi_I(x) - \varepsilon(x)\phi_E(x) - \lambda\phi_E(x) = 0, && x \in \Omega, && \text{(3.44a)} \\ \varepsilon(x)\phi_E(x) - \gamma(x)\phi_I(x) - \lambda\phi_I(x) = 0, && x \in \Omega, && \text{(3.44b)} \\ \frac{\partial \phi_E}{\partial n} = 0, && x \in \partial\Omega. && \text{(3.44c)} \end{aligned}$$

The next result establishes the existence of a principal simple eigenvalue to system (3.44).

Lemma 3.3.9

The elliptic eigenvalue problem (3.44) has a principal simple eigenvalue λ^* with a positive eigenfunction.

Proof. *Our goal is to apply Theorem 2.2.2. Consider the one parameter family of the linear operators $\mathscr{L}_\lambda$ given by*

$$\mathscr{L}_\lambda = L_1 + M_{11} + M_{12}(\lambda I - M_{22})^{-1} M_{21} \quad \forall \lambda > s(M_{22}),$$

where $L_1 = d_E \Delta$ and

$$M(x) = \begin{bmatrix} -\varepsilon(x) & \beta(x)\widetilde{S}(x) \\ \varepsilon(x) & -\gamma(x) \end{bmatrix}.$$

Note that $\varepsilon(x)$ and $\beta(x)$ are positive functions of x and $M(x)$ is a quasi-positive matrix. Hence, it follows

$$\mathscr{L}_\lambda \phi(x) = d_E \Delta\phi(x) - \varepsilon(x)\phi(x) + \widetilde{S}(x)\frac{\beta(x)\varepsilon(x)}{\lambda + \gamma(x)}\phi(x) \quad \forall \lambda > -\inf_{x\in\Omega} \gamma(x).$$

Let

$$A := \min_{x\in\Omega} \beta(x)\varepsilon(x)\widetilde{S}(x),$$

and λ_1 denote the principal eigenvalue of the elliptic eigenvalue problem

$$\begin{aligned} d_E \Delta\phi(x) - \varepsilon(x)\phi(x) &= \lambda\phi(x), && x \in \Omega, \\ \frac{\partial \phi}{\partial n} &= 0, && x \in \partial\Omega. \end{aligned}$$

Set

$$\gamma_m = \max_{x\in\Omega} \gamma(x),$$

and

$$\lambda_0 := \frac{\lambda_1 - \gamma_m + \sqrt{(\lambda_1 + \gamma_m)^2 + 4A}}{2}. \tag{3.45}$$

Observe now that, given that by definition $A > 0$, we have

$$\lambda_0 > -\gamma_m \Leftrightarrow \lambda_0 + \gamma_m > 0.$$

Since $\gamma_m \geq \gamma(x)$, we have

$$\begin{aligned} &\lambda_0 + \gamma_m \geq \lambda_0 + \gamma(x) \\ \Leftrightarrow &\frac{1}{\lambda_0 + \gamma_m} \leq \frac{1}{\lambda_0 + \gamma(x)}, \quad \forall x \in \Omega, \end{aligned}$$

and so it follows

$$\begin{aligned} \mathscr{L}_{\lambda_0}\phi^*(x) &\geq d_E \Delta\phi^*(x) - \varepsilon(x)\phi^*(x) + \frac{A}{\lambda_0 + \gamma_m}\phi^*(x) \\ &= \lambda_1 \phi^*(x) + \frac{A}{\lambda_0 + \gamma_m}\phi^*(x). \end{aligned}$$

Note that, from (3.45), we have the following equivalences

$$\begin{aligned}
&\lambda_1 + \frac{A}{\lambda_0 + \gamma_m} = \lambda_0 \\
\Leftrightarrow &\lambda_1(\lambda_0 + \gamma_m) + A = \lambda_0(\lambda_0 + \gamma_m) \\
\Leftrightarrow &\lambda_0^2 + \lambda_0(\gamma_m - \lambda_1) - (\lambda_1\gamma_m + A) = 0 \\
\Leftrightarrow &\lambda_0 = \frac{\lambda_1 - \gamma_m \pm \sqrt{(\lambda_1 - \gamma_m)^2 + 4(\lambda_1\gamma_m + A)}}{2} \\
\Leftrightarrow &\lambda_0 = \frac{\lambda_1 - \gamma_m \pm \sqrt{\lambda_1^2 + \gamma_m^2 + 2\lambda_1\gamma_m + 4A}}{2} \\
\Leftrightarrow &\lambda_0 = \frac{\lambda_1 - \gamma_m \pm \sqrt{(\lambda_1 + \gamma_m)^2 + 4A}}{2}.
\end{aligned}$$

Thus

$$\mathscr{L}_{\lambda_0}\phi^*(x) \geq \lambda_0\phi^*(x). \tag{3.46}$$

Following Theorem 2.2.2, problem (3.44) has an eigenvalue with geometric multiplicity one and a non-negative eigenfunction.

Using (3.44) and its associated system, we easily see that this eigenfunction is positive.

■

Let $\mathscr{R}_0$ represent the basic reproduction number of system (3.36). To explore more properties of $\mathscr{R}_0$, the next result states an important condition for the sign of $\mathscr{R}_0 - 1$.

Theorem 3.3.10 [21]

$\mathscr{R}_0 - 1$ has the same sign as λ^*, where λ^* is the principal eigenvalue of (3.44) with a positive eigenfunction.

Proof. *The proof is similar to that of Theorem 3.3.3.*

■

The following theorem shows that the stability of the DFE relies on the magnitude of $\mathscr{R}_0$.

Theorem 3.3.11

If $\mathscr{R}_0 < 1$ then the DFE is asymptotically stable for problem (3.38).

Proof. *Suppose that $\mathscr{R}_0 < 1$. Following the same arguments as in Theorem 3.3.4, we wish to demonstrate that if $(\lambda, \vec{\phi})$ is a solution of problem (3.42)-(3.43), where $\vec{\phi}(x) = \left(\phi_E(x), \phi_I(x), \phi_R(x)\right)$ with at least one entry not identically zero, then*

$$Re(\lambda) < 0. \tag{3.47}$$

To this end, we argue by contradiction. Suppose that $(\lambda, \vec{\phi})$ *is a solution of problem (3.42)-(3.43) with* $\vec{\phi}(x)$ *not identically zero and*

$$Re(\lambda) \geq 0. \tag{3.48}$$

First suppose that $\phi_E(x) \equiv 0$*. Then, following (3.42b),*

$$-\gamma(x)\phi_I(x) = \lambda\phi_I(x).$$

Since $\gamma(x)$ *is a positive function on* Ω*, we have*

$$\begin{aligned} & -\gamma(x)\phi_I(x) = \lambda\phi_I(x) \\ \Leftrightarrow \quad & \phi_I(x)\Big(-\gamma(x) - \lambda\Big) = 0 \\ \Rightarrow \quad & \phi_I(x) = 0 \quad \vee \quad -\gamma(x) - \lambda = 0. \end{aligned}$$

Observe that the second condition implies that $\gamma(x)$ *is constant in* Ω *and that* $\gamma(x) = -\lambda < 0$*. Since* $\gamma(x)$ *is positive on* Ω *and from (3.48), we conclude that*

$$\phi_I \equiv 0.$$

Therefore, if $\phi_E(x) \equiv 0$ *we also have* $\phi_I(x) \equiv 0$*. Hence,* $\phi_R(x) \not\equiv 0$*.*

Note that, from (3.42c) together with ϕ_E *and* ϕ_I *identically zero, we have*

$$-\alpha(x)\phi_R(x) = \lambda\phi_R(x).$$

Since $\alpha(x)$ *is a positive function on* Ω*, following the previous arguments, we get that* $\phi_R \equiv 0$ *which helds a contradiction. Thus, we have that* $\phi_E(x) \not\equiv 0$*.*

Suppose now that $\phi_I(x) \equiv 0$*. Then, from (3.42a) we get*

$$\begin{aligned} & d_E\Delta\phi_E(x) - \epsilon(x)\phi_E(x) - \lambda\phi_E(x) = 0, && x \in \Omega, \\ & \frac{\partial\Omega}{\partial n} = 0, && x \in \partial\Omega. \end{aligned}$$

Following the same arguments as in Theorem's 3.3.4 proof, we come to a contradiction. Therefore, we have $\phi_E(x) \not\equiv 0$ *and* $\phi_I(x) \not\equiv 0$*.*

From equations (3.42a)-(3.42a) and (3.43) we get problem (3.44). Thus, by Theorem 3.3.10, the principal eigenvalue problem (3.44) has the same sign as $\mathscr{R}_0 - 1$*.*

Since $\mathscr{R}_0 - 1 < 0$ *by assumption, we have* $\lambda^* < 0$*. Thus, following Theorem 2.2.2, we have*

$$Re(\lambda) < \lambda^* < 0,$$

which contradicts (3.48).

Thus, the DFE is asymptotically stable solution of (3.42)-(3.43).

■

We now state a result which is similar to *Theorem 3.3.7*.

Theorem 3.3.12

If $\mathscr{R}_0 > 1$ then there exists $\epsilon_0 > 0$ such that any positive solution of (3.36) satisfies

$$\limsup_{t\to\infty} \|\Big(S(\cdot,t), E(\cdot,t), I(\cdot,t), R(\cdot,t)\Big) - \Big(\widetilde{S}(x), 0, 0, 0\Big)\|_{L^\infty(\Omega)} \geq \epsilon_0.$$

Proof. *The proof follows the same arguments as the proof of Theorem 3.3.7.*

■

3.3.2.1 Characterization of the $\mathscr{R}_0$

In a similar way to *Theorem 3.3.6*, the following result characterizes the basic reproduction number of problem (3.36)-(3.37) using a reduced eigenvalue problem associated with system (3.44).

Theorem 3.3.13

Let μ_1 be the unique positive eigenvalue of the eigenvalue problem

$$-d_E\Delta\phi(x) + \varepsilon(x)\phi(x) = \mu\widetilde{S}(x)\frac{\varepsilon(x)\beta(x)}{\gamma(x)}\phi(x), \qquad x\in\Omega, \tag{3.49a}$$

$$\frac{\partial\phi}{\partial n} = 0, \qquad x\in\partial\Omega, \tag{3.49b}$$

with a positive eigenfunction. Then

$$\mathscr{R}_0 = \frac{1}{\mu_1}.$$

Proof. *By the same arguments as in Theorem 3.3.6 proof, we first set*

$$\hat{F}(x) = \begin{bmatrix} 0 & \beta(x)\widetilde{S}(x) \\ 0 & 0 \end{bmatrix} \quad , \quad \hat{V}(x) = \begin{bmatrix} \varepsilon(x) & 0 \\ -\varepsilon(x) & \gamma(x) \end{bmatrix},$$

and

$$\hat{B} := diag\Big(d_E\Delta, 0\Big) - \hat{V}.$$

*Given that we have $\hat{F}_{21} = 0$ and $\hat{F}_{22} = 0$, it then follows, from [***Theorem 3.3 (ii)***, 21], that*

$$\mathscr{R}_0 = \rho(-\hat{B}^{-1}\hat{F}) = \rho(-\hat{B}_1^{-1}\hat{F}_2),$$

where

$$\begin{aligned} \hat{B}_1\phi_1(x) &:= d_E\Delta\phi_1(x) - \hat{V}_1\phi_1(x), \\ \hat{V}_1\phi_1(x) &:= \varepsilon(x)\phi_1(x), \\ \hat{F}_2\phi_1(x) &:= \widetilde{S}(x)\frac{\varepsilon(x)\beta(x)}{\gamma(x)}. \end{aligned}$$

From Theorem 2.2.7, as applied to the triple $(\hat{B}_1, \hat{V}_1, \hat{F}_2)$*, it follows*

$$\rho(-\hat{B}_1^{-1}\hat{F}_2) = \frac{1}{\mu_1},$$

where μ_1 *is the unique positive eigenvalue of* $-\hat{B}_1\phi_1(x) = \mu\hat{F}_2\phi_1(x)$*, i.e.,*

$$-d_E\frac{d^2\phi}{dx^2} + \varepsilon(x)\phi = \mu\widetilde{S}(x)\frac{\varepsilon(x)\beta(x)}{\gamma(x)}\phi, \quad x \in \Omega$$

with a positive eigenfunction. Therefore we have

$$\mathscr{R}_0 = \frac{1}{\mu_1}.$$

■

We now wish to study the asymptotic properties of the basic reproduction number. In view of the eigenvalue problem (3.49), we first give an estimate for $\mathscr{R}_0$.

Lemma 3.3.14 [18]
For any $d_E > 0$ *the following inequalities hold:*

$$\min\left\{\widetilde{S}(x)\frac{\beta(x)}{\gamma(x)}, x \in \overline{\Omega}\right\} \leq \mathscr{R}_0 \leq \max\left\{\widetilde{S}(x)\frac{\beta(x)}{\gamma(x)}, x \in \overline{\Omega}\right\}. \tag{3.50}$$

Proof. *The proof is identical to that of Lemma 3.3.7.*

■

From *Theorem 3.3.13* we can define the basic reproduction number, $\mathscr{R}_0$, for system (3.36) using the next generation approach for heterogeneous populations. To this end, consider the eigenvalue problem

$$-d_E\Delta\phi(x) + \varepsilon(x)\phi(x) = \mu\widetilde{S}(x)\frac{\varepsilon(x)\beta(x)}{\gamma(x)}\phi(x), \qquad x \in \Omega, \tag{3.51a}$$

$$\frac{\partial\phi}{\partial n} = 0, \qquad x \in \partial\Omega. \tag{3.51b}$$

Let $\frac{1}{\lambda}$ be an eigenvalue of (3.51) and $\phi(x)$ it's associated eigenfunction. We have

$$\begin{aligned} &-d_E\Delta\phi(x) + \varepsilon(x)\phi(x) = \frac{1}{\lambda}\widetilde{S}(x)\frac{\varepsilon(x)\beta(x)}{\gamma(x)}\phi(x) \\ \Rightarrow \quad &-d_E\phi(x)\Delta\phi(x) + \varepsilon(x)\phi^2(x) = \frac{1}{\lambda}\widetilde{S}(x)\frac{\varepsilon(x)\beta(x)}{\gamma(x)}\phi^2(x). \end{aligned}$$

Thus, from Green's Formula (3.5),

$$\begin{aligned} &\int_\Omega \Big(-d_E\phi(x)\Delta\phi(x) + \varepsilon(x)\phi^2(x)\Big)dx = \frac{1}{\lambda}\int_\Omega \widetilde{S}(x)\frac{\varepsilon(x)\beta(x)}{\gamma(x)}\phi^2(x)dx \\ \Leftrightarrow \quad &\int_\Omega \Big(d_E|\nabla\phi(x)|^2 + \varepsilon(x)\phi^2(x)\Big)dx = \frac{1}{\lambda}\int_\Omega \widetilde{S}(x)\frac{\varepsilon(x)\beta(x)}{\gamma(x)}\phi^2(x)dx. \end{aligned}$$

Let

$$\varphi \in W^{1,2}(\Omega) \equiv H^1(\Omega) := \Big\{\varphi^2(\Omega) : f(x) \in L^2(x)\Big\}.$$

Following [3], the value of $\mu = \frac{1}{\lambda}$ is given by the following variational characterization:

$$\mu_1 = \inf\left\{\frac{\int_\Omega \Big(d_E|\nabla\varphi(x)|^2 + \varepsilon(x)\varphi^2(x)\Big)dx}{\int_\Omega \widetilde{S}(x)\frac{\varepsilon(x)\beta(x)}{\gamma(x)}\varphi^2(x)dx} : \quad \varphi \in H^1(\Omega) \text{ and } \varphi \neq 0\right\}. \tag{3.52}$$

Therefore, noting that $\frac{1}{\inf_{x\in D} h(x)} = \sup_{x\in D}\left(\frac{1}{h(x)}\right)$, from *Theorem 3.3.13* and (3.52) we have

$$\mathscr{R}_0 = \sup\left\{\frac{\int_\Omega \widetilde{S}(x)\frac{\varepsilon(x)\beta(x)}{\gamma(x)}\varphi^2(x)dx}{\int_\Omega \Big(d_E|\nabla\varphi(x)|^2 + \varepsilon(x)\varphi^2(x)\Big)dx} : \quad \varphi \in H^1(\Omega) \text{ and } \varphi \neq 0\right\}. \tag{3.53}$$

Using (3.53), the next result relates the behaviour of $\mathscr{R}_0$ with d_E.

Theorem 3.3.15
The following statements are valid for the basic reproduction number:

1. *$\mathscr{R}_0$ is a positive and monotone decreasing function of $d_E > 0$;*
2. *$\mathscr{R}_0 \to \max\left\{\frac{\beta(x)\widetilde{S}(x)}{\gamma(x)} : x \in \overline{\Omega}\right\}$ as $d_E \to 0$;*
3. *$\mathscr{R}_0 \to \frac{\int_\Omega \beta(x)\varepsilon(x)\gamma(x)^{-1}\widetilde{S}(x)dx}{\int_\Omega \varepsilon(x)dx}$ as $d_E \to \infty$.*

Proof. *First we show statement (i). Since functions $\beta(x)$, $\varepsilon(x)$ and $\gamma(x)$ are by definition positive functions on $\overline{\Omega}$, the right hand side of (3.53) exists and is positive.*

Let $\varphi^*(x) \in H^1(\Omega)$ with $\varphi^*(x) \neq 0$ such that

$$\mathscr{R}_0 = \frac{\int_\Omega \widetilde{S}(x)\varepsilon(x)\beta(x)\gamma(x)^{-1}\varphi^{*2}(x)dx}{\int_\Omega (d_E|\nabla\varphi^*(x)|^2 + \varepsilon(x)\varphi^{*2}(x))dx}.$$

Set $g(x) = \varepsilon(x)\beta(x)\gamma(x)^{-1}\varphi^{*2}(x)$. Since $g(x)$ and $\widetilde{S}(x)$ are continuous and positive on Ω, we have that there exists a constant $c \in \Omega$ such that

$$\int_\Omega \widetilde{S}(x)g(x)dx = g(c)\int_\Omega \widetilde{S}(x)dx = g(c)N_0.$$

Thus

$$\mathscr{R}_0 = \frac{g(c)N_0}{\int_\Omega (d_E|\nabla\varphi^*(x)|^2 + \varepsilon(x)\varphi^{*2}(x))dx}.$$

Observe that, for $d_E > 0$, $\int_\Omega (d_E|\nabla\varphi^*(x)|^2 + \varepsilon(x)\varphi^{*2}(x))dx$ is an increasing function of d_E since $\varepsilon(x)$ is positive. It's only left to show that this dependence is strict.

We have

$$\frac{\partial}{\partial d_E}\Big[\int_\Omega (d_E|\nabla\varphi^*(x)|^2 + \varepsilon(x)\varphi^{*2}(x))dx\Big] = \int_\Omega |\nabla\varphi^*(x)|^2 dx > 0, \quad \forall x \in \Omega,$$

which is a positive function on Ω. *Therefore* $\int_\Omega (d_E|\nabla\varphi^*(x)|^2 + \varepsilon(x)\varphi^{*2}(x))dx$ *is a monotone increasing function for all* $x \in \Omega$.

Hence, from (3.53), we conclude that $\mathscr{R}_0$ *is a monotone decreasing function of* d_E.

*The proof of (ii) is similar to that of [***Lemma 3.1***, 12].*

It remains to establish (iii). From (3.53) with $\varphi^2(x) \equiv 1$ *for all* $x \in \Omega$, *we have*

$$\mathscr{R}_0 \geq \frac{\int_\Omega \beta(x)\varepsilon(x)\gamma(x)^{-1}\widetilde{S}(x)dx}{\int_\Omega \varepsilon(x)dx}.$$

By part (i), $\mathscr{R}_0$ *is uniformly bounded for* $d_E \geq 1$. *Thus, it has a finite limit* $\mathscr{R}_0$ *as* $d_E \to \infty$. *From Theorem 3.3.13, we know that* $\mathscr{R}_0$ *satisfies*

$$-d_E\Delta\phi(x) + \varepsilon(x)\phi(x) = \frac{1}{\mathscr{R}_0}\widetilde{S(x)}\frac{\varepsilon(x)\beta(x)}{\gamma(x)}\phi(x), \tag{3.54}$$

where $\phi(x)$ *is a positive eigenfunction with*

$$\frac{\partial\phi}{\partial n} = 0, \quad x \in \partial\Omega.$$

Dividing (3.54) by d_E, *we have*

$$-\Delta\phi(x) + \frac{\varepsilon(x) - \mathscr{R}_0^{-1}\varepsilon(x)\beta(x)\widetilde{S}(x)\gamma^{-1}(x)}{d_E}\phi(x) = 0. \tag{3.55}$$

Since $\varepsilon(x) - \mathscr{R}_0^{-1}\varepsilon(x)\beta(x)\widetilde{S}(x)\gamma^{-1}(x)$ *is positive and continuous, taking* $d_E \to \infty$ *then equation (3.55) becomes*

$$\Delta\phi = 0, \quad x \in \Omega,$$

together with

$$\frac{\partial\phi}{\partial n} = 0, \quad x \in \partial\Omega.$$

Hence $\phi(x) \to \overline{\phi}$ *in* $\mathscr{C}(\Omega)$ *as* $d_E \to \infty$, *where* $\overline{\phi}$ *denotes a constant.*

Integrating (3.54) on Ω *by parts and using Green's Formula (3.5), we get*

$$\underbrace{\int_\Omega \Big(-d_E\Delta\phi(x)\Big)dx}_{=0} + \int_\Omega \varepsilon(x)\phi(x)dx = \frac{1}{\mathscr{R}_0}\int_\Omega \beta(x)\varepsilon(x)\gamma(x)^{-1}\widetilde{S}(x)\phi(x)dx.$$

Thus

$$\mathscr{R}_0 = \frac{\int_\Omega \beta(x)\varepsilon(x)\gamma(x)^{-1}\widetilde{S}(x)\phi(x)dx}{\int_\Omega \varepsilon(x)\phi(x)dx}.$$

Therefore, letting $d_E \to \infty$ *produces the desired relation*

$$\hat{\mathscr{R}}_0 = \frac{\int_\Omega \beta(x)\varepsilon(x)\gamma(x)^{-1}\widetilde{S}(x)\overline{\phi}dx}{\int_\Omega \varepsilon(x)\overline{\phi}dx} = \frac{\int_\Omega \beta(x)\varepsilon(x)\gamma(x)^{-1}\widetilde{S}(x)dx}{\int_\Omega \varepsilon(x)dx}.$$

■

4

Numerical Approximation of the Model in Two-dimensional Case

In this Chapter we present a numerical method based on a finite difference schemes for the non-linear reaction-diffusion system (3.1)-(3.4), defined on a circular domain in $\mathbb{R}^2$.

This chapter is organized as follows. In *Section 4.1*, we describe a finite difference numerical method in order to approximate the solution of the epidemic model (3.1)-(3.4). In *Section 4.2*, simulations of the Δ-SEIRS model, using the proposed numerical method, are computed to illustrate the theoretical results presented in *Chapter 3*.

4.1 Numerical Method

In this section, following [1], we proposed a numerical method based on a finite difference scheme to approximate the solutions of the non-linear reaction-diffusion system studied in the previous chapter. By using this method, we performed several numerical simulations.

Recall that the system that we intend to obtain an approximate solution is given by

$$\frac{\partial S}{\partial t} = d_S \Delta S(x,y,t) - \beta(x,y) I(x,y,t) S(x,y,t) + \alpha(x,y) R(x,y,t), \qquad (x,y) \in \Omega, t > 0, \quad (4.1a)$$

$$\frac{\partial E}{\partial t} = d_E \Delta E(x,y,t) + \beta(x,y) I(x,y,t) S(x,y,t) - \varepsilon(x,y) E(x,y,t), \qquad (x,y) \in \Omega, t > 0, \quad (4.1b)$$

$$\frac{\partial I}{\partial t} = d_I \Delta I(x,y,t) + \varepsilon(x,y) E(x,y,t) - \gamma(x,y) I(x,y,t), \qquad (x,y) \in \Omega, t > 0, \quad (4.1c)$$

$$\frac{\partial R}{\partial t} = d_R \Delta R(x,y,t) + \gamma(x,y) I(x,y,t) - \alpha(x,y) R(x,y,t), \qquad (x,y) \in \Omega, t > 0, \quad (4.1d)$$

$$\frac{\partial S(x,y,t)}{\partial n} = \frac{\partial E(x,y,t)}{\partial n} = \frac{\partial I(x,y,t)}{\partial n} = \frac{\partial R(x,y,t)}{\partial n} = 0, \qquad (x,y) \in \partial\Omega, t > 0. \quad (4.1e)$$

where Ω is a bounded domain with smooth boundary $\partial\Omega$. Thus, for the sake of simplicity, we consider a disk domain, hence regular, *i.e.*,

$$\Omega = \{(x,y) \in \mathbb{R}^2 | \quad x^2 + y^2 < r^2\}, \qquad (4.2)$$

as our numerical domain for the following method.

Following [1], for $(x,y) \in \Omega$ we consider the following change of variables:

$$x = r\cos\theta \quad , \quad y = r\sin\theta,$$

where

$$r = \sqrt{x^2+y^2} \quad , \quad \theta = \tan^{-1}\left(\frac{y}{x}\right).$$

The motivation behind this change of coordinates comes from the limitations of numerically approximating the points in our circular domain with a grid in cartesian coordinates.

Without loss of generality, we denote $S(x,y,t) = S(r\cos\theta, r\sin\theta, t)$, $E(x,y,t) = E(r\cos\theta, r\sin\theta, t)$, $I(x,y,t) = I(r\cos\theta, r\sin\theta, t)$ and $R(x,y,t) = R(r\cos\theta, r\sin\theta, t)$ by $S(r,\theta,t)$, $E(r,\theta,t)$, $I(r,\theta,t)$ and $R(r,\theta,t)$, respectively.

Taking into account the new set of variables, we have

$$\frac{\partial S}{\partial r} = \frac{\partial S}{\partial x}\frac{\partial x}{\partial r} + \frac{\partial S}{\partial y}\frac{\partial y}{\partial r} = \cos\theta\frac{\partial S}{\partial x} + \sin\theta\frac{\partial S}{\partial y}.$$

Hence

$$\frac{\partial^2 S}{\partial r^2} = \frac{\partial}{\partial r}\left(\cos\theta\frac{\partial S}{\partial x} + \sin\theta\frac{\partial S}{\partial y}\right) = \cos^2\theta\frac{\partial^2 S}{\partial x^2} + \sin^2\theta\frac{\partial^2 S}{\partial y^2}. \tag{4.3}$$

In a similar way, we also have

$$\frac{\partial S}{\partial \theta} = -r\sin\theta\frac{\partial S}{\partial x} + r\cos\theta\frac{\partial S}{\partial y},$$

which gives

$$\begin{aligned}\frac{\partial^2 S}{\partial \theta^2} &= -r\cos\theta\frac{\partial S}{\partial x} - r\sin\theta\frac{\partial S}{\partial y} - r\sin\theta\left(-r\sin\theta\frac{\partial^2 S}{\partial x^2} + r\cos\theta\frac{\partial^2 S}{\partial x\partial y}\right) + \\ &\qquad + r\cos\theta\left(-r\sin\theta\frac{\partial^2 S}{\partial x\partial y} + r\cos\theta\frac{\partial^2 S}{\partial y^2}\right) \\ &= -r\left(\cos\theta\frac{\partial S}{\partial x} + \sin\theta\frac{\partial S}{\partial y}\right) + r^2\left(\sin^2\theta\frac{\partial^2 S}{\partial x^2} - 2\cos\theta\sin\theta\frac{\partial^2 S}{\partial x\partial y} + \cos^2\theta\frac{\partial^2 S}{\partial y^2}\right).\end{aligned}$$

Therefore, since

$$\cos\theta\frac{\partial S}{\partial x} + \sin\theta\frac{\partial S}{\partial y} = \frac{\partial S}{\partial r},$$

we have

$$\frac{1}{r^2}\frac{\partial^2 S}{\partial \theta^2} = \frac{-1}{r}\frac{\partial S}{\partial r} + \sin^2\theta\frac{\partial^2 S}{\partial x^2} - 2\cos\theta\sin\theta\frac{\partial^2 S}{\partial x\partial y} + \cos^2\theta\frac{\partial^2 S}{\partial y^2}. \tag{4.4}$$

Finally, adding (4.3) with (4.4), comes

$$\frac{1}{r}\frac{\partial S}{\partial r} + \frac{\partial^2 S}{\partial r^2} + \frac{1}{r^2}\frac{\partial^2 S}{\partial \theta^2} = \frac{\partial^2 S}{\partial x^2} + \frac{\partial^2 S}{\partial y^2}.$$

We then conclude that the Laplacian operator in polar coordinates is given by

$$\Delta S = \frac{\partial^2 S}{\partial r^2} + \frac{1}{r}\frac{\partial S}{\partial r} + \frac{1}{r^2}\frac{\partial^2 S}{\partial \theta^2}. \tag{4.5}$$

Similarly we have identical expressions for ΔE,ΔI and ΔR.

On the other hand, the Neumann boundary conditions (4.1e) in polar coordinates become

$$\left.\frac{\partial S(x,y,t)}{\partial n}\right|_{\partial\Omega} = \left.\frac{\partial S(r,\theta,t)}{\partial r}\right|_{r=\mathbf{r}} = 0, \qquad t>0, \tag{4.6a}$$

$$\left.\frac{\partial E(x,y,t)}{\partial n}\right|_{\partial\Omega} = \left.\frac{\partial E(r,\theta,t)}{\partial r}\right|_{r=\mathbf{r}} = 0, \qquad t>0, \tag{4.6b}$$

$$\left.\frac{\partial I(x,y,t)}{\partial n}\right|_{\partial\Omega} = \left.\frac{\partial I(r,\theta,t)}{\partial r}\right|_{r=\mathbf{r}} = 0, \qquad t>0, \tag{4.6c}$$

$$\left.\frac{\partial R(x,y,t)}{\partial n}\right|_{\partial\Omega} = \left.\frac{\partial R(r,\theta,t)}{\partial r}\right|_{r=\mathbf{r}} = 0, \qquad t>0, \tag{4.6d}$$

where $\mathbf{r}$ denotes the radius of the circular domain. Thus, system (4.1) becomes

$$\begin{aligned}
\frac{\partial S(r,\theta,t)}{\partial t} &= d_S\Big(\frac{\partial^2 S}{\partial r^2}+\frac{1}{r}\frac{\partial S}{\partial r}+\frac{1}{r^2}\frac{\partial^2 S}{\partial \theta^2}\Big)-\beta(r\cos\theta,r\sin\theta)I(r,\theta,t)S(r,\theta,t)+\\
&\quad+\alpha(r\cos\theta,r\sin\theta)R(r,\theta,t), \quad t>0,\\
\frac{\partial E(r,\theta,t)}{\partial t} &= d_E\Big(\frac{\partial^2 E}{\partial r^2}+\frac{1}{r}\frac{\partial E}{\partial r}+\frac{1}{r^2}\frac{\partial^2 E}{\partial \theta^2}\Big)+\beta(r\cos\theta,r\sin\theta)I(r,\theta,t)S(r,\theta,t)-\\
&\quad-\varepsilon(r\cos\theta,r\sin\theta)E(r,\theta,t), \quad t>0,\\
\frac{\partial I(r,\theta,t)}{\partial t} &= d_I\Big(\frac{\partial^2 I}{\partial r^2}+\frac{1}{r}\frac{\partial I}{\partial r}+\frac{1}{r^2}\frac{\partial^2 I}{\partial \theta^2}\Big)+\varepsilon(r\cos\theta,r\sin\theta)E(r,\theta,t)-\\
&\quad-\gamma(r\cos\theta,r\sin\theta)I(r,\theta,t), \quad t>0,\\
\frac{\partial R(r,\theta,t)}{\partial t} &= d_R\Big(\frac{\partial^2 R}{\partial r^2}+\frac{1}{r}\frac{\partial R}{\partial r}+\frac{1}{r^2}\frac{\partial^2 R}{\partial \theta^2}\Big)+\gamma(r\cos\theta,r\sin\theta)I(r,\theta,t)-\\
&\quad-\alpha(r\cos\theta,r\sin\theta)R(r,\theta,t), \quad t>0,\\
\frac{\partial S(r,\theta,t)}{\partial n} &= \frac{\partial E(r,\theta,t)}{\partial n} = \frac{\partial I(r,\theta,t)}{\partial n} = \frac{\partial R(r,\theta,t)}{\partial n} = 0, \qquad r=\mathbf{r}, t>0.
\end{aligned}$$

In order to obtain an approximate solution of (4.1) we must discretize the domain and approximate the operators (Laplacian and partial derivatives in order to time).

To discretize Ω we choose a grid such that the points are integers in zimuthal direction and half-integer in radial direction, *i.e.*,

$$r_i = \Big(i-\frac{1}{2}\Big)\Delta r, \quad i=1,\dots,P \quad \text{and} \quad \theta_j=(j-1)\Delta\theta, \quad j=1,\dots,M,$$

where

$$\Delta r = \frac{2}{2P+1}, \quad \Delta\theta = \frac{2\pi}{M}.$$

We consider an uniform mesh in time, $t_i=\Delta T$, $i=0,1,\dots,N$, where

$$\Delta T = \frac{T}{N}.$$

Let $S^m_{i,j}$, $E^m_{i,j}$, $I^m_{i,j}$ and $R^m_{i,j}$ denote the approximations of $S(r_i,\theta_j,t_m)$, $E(r_i,\theta_j,t_m)$, $I(r_i,\theta_j,t_m)$ and $R(r_i,\theta_j,t_m)$, respectively. Analogously, we will denote parameters $\beta(r_i\cos\theta_j,r_i\sin\theta_j)$, $\varepsilon(r_i\cos\theta_j,r_i\sin\theta_j)$, $\gamma(r_i\cos\theta_j,r_i\sin\theta_j)$ and $\alpha(r_i\cos\theta_j,r_i\sin\theta_j)$ as $\beta_{i,j}$, $\varepsilon_{i,j}$, $\gamma_{i,j}$ and $\alpha_{i,j}$, respectively.

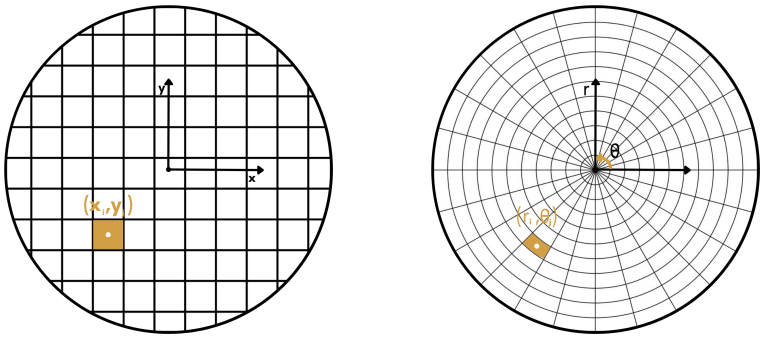

(a) Grid in cartesian coordinates (b) Grid in polar coordinates

Figure 4.1: Change on choice of grid.

For $i = 2,\dots,P$, $j = 1,\dots,M$ and using centered difference formulas to discretize the Laplacian operator (4.5), we have

$$\Delta S^m_{i,j} \simeq \frac{S^m_{i-1,j} - 2S^m_{i,j} + S^m_{i+1,j}}{(\Delta r)^2} + \frac{S^m_{i+1,j} - S^m_{i-1,j}}{2r_i \Delta r} + \frac{S^m_{i,j-1} - 2S^m_{i,j} + S^m_{i,j+1}}{r_i^2 (\Delta\theta)^2}. \tag{4.7}$$

Using a a backward difference formula, from Neumann boundary conditions we get

$$\frac{S^m_{P+1,j} - S^m_{P,j}}{\Delta r} = 0 \Leftrightarrow S^m_{P+1,j} = S^m_{P,j}. \tag{4.8}$$

Hence the numerical boundary values at $r = \mathbf{r}$, $S^m_{P+1,j}$, can be approximated by $S^m_{P,j}$. Additionally, given that S is 2π periodic in θ, we also have that the numerical boundary values at $\theta = 0$ and $\theta = M+1$, $S^m_{i,0}$ and $S^m_{i,M+1}$, can be approximated by $S^m_{i,M}$ and $S^m_{i,1}$, respectively.

In order to approximate the derivative in time of $S(r_i, \theta_j, t_m)$, we use a backward difference formula:

$$\frac{\partial S(r_i, \theta_j, t_m)}{\partial t} \simeq \frac{S^m_{i,j} - S^{m-1}_{i,j}}{\Delta T}. \tag{4.9}$$

Following the same arguments as in (4.7)-(4.9), we get similar equations for the exposed, infected and recovered variables and obtain the following numerical scheme

$$S_{i,j}^m - d_S\Delta T\left[\frac{S_{i-1,j}^m - 2S_{i,j}^m + S_{i+1,j}^m}{(\Delta r)^2} + \frac{S_{i+1,j}^m - S_{i-1,j}^m}{2r_i\Delta r} + \frac{S_{i,j-1}^m - 2S_{i,j}^m + S_{i,j+1}^m}{r_i^2(\Delta\theta)^2}\right] - \\ - \Delta T\alpha_{i,j}R_{i,j}^m + \Delta T\beta_{i,j}S_{i,j}^m I_{i,j}^m = S_{i,j}^{m-1},$$

$$E_{i,j}^m - d_E\Delta T\left[\frac{E_{i-1,j}^m - 2E_{i,j}^m + E_{i+1,j}^m}{(\Delta r)^2} + \frac{E_{i+1,j}^m - E_{i-1,j}^m}{2r_i\Delta r} + \frac{E_{i,j-1}^m - 2E_{i,j}^m + E_{i,j+1}^m}{r_i^2(\Delta\theta)^2}\right] + \\ + \Delta T\varepsilon_{i,j}E_{i,j}^m - \Delta T\beta_{i,j}S_{i,j}^m I_{i,j}^m = E_{i,j}^{m-1},$$

$$I_{i,j}^m - d_I\Delta T\left[\frac{I_{i-1,j}^m - 2I_{i,j}^m + I_{i+1,j}^m}{(\Delta r)^2} + \frac{I_{i+1,j}^m - I_{i-1,j}^m}{2r_i\Delta r} + \frac{I_{i,j-1}^m - 2I_{i,j}^m + I_{i,j+1}^m}{r_i^2(\Delta\theta)^2}\right] - \\ - \Delta T\varepsilon_{i,j}E_{i,j}^m + \Delta T\gamma_{i,j}I_{i,j}^m = I_{i,j}^{m-1},$$

$$R_{i,j}^m - d_R\Delta T\left[\frac{R_{i-1,j}^m - 2R_{i,j}^m + R_{i+1,j}^m}{(\Delta r)^2} + \frac{R_{i+1,j}^m - R_{i-1,j}^m}{2r_i\Delta r} + \frac{R_{i,j-1}^m - 2R_{i,j}^m + R_{i,j+1}^m}{r_i^2(\Delta\theta)^2}\right] - \\ - \Delta T\gamma_{i,j}I_{i,j}^m + \Delta T\alpha_{i,j}r_{i,j}^m = R_{i,j}^{m-1},$$

for $i = 1,\dots,P$, $j = 1,\dots,M$ and $m = 0,\dots,T$.

In the previous system we have a nonlinear term $S_{i,j}^m I_{i,j}^m$. In order to obtain a linear system of equations, we consider as approximations of $S_{i,j}^m$ and $I_{i,j}^m$ the values $S_{i,j}^{m-1}$ and $I_{i,j}^{m-1}$, respectively. Finally, the proposed numerical scheme to obtain an approximate solution of (4.1) is given by

$$S_{i,j}^m - d_S\Delta T\left[\frac{S_{i-1,j}^m - 2S_{i,j}^m + S_{i+1,j}^m}{(\Delta r)^2} + \frac{S_{i+1,j}^m - S_{i-1,j}^m}{2r_i\Delta r} + \frac{S_{i,j-1}^m - 2S_{i,j}^m + S_{i,j+1}^m}{r_i^2(\Delta\theta)^2}\right] - \\ - \Delta T\alpha_{i,j}R_{i,j}^m = S_{i,j}^{m-1} - \Delta T\beta_{i,j}S_{i,j}^{m-1}I_{i,j}^{m-1}, \tag{4.10a}$$

$$E_{i,j}^m - d_E\Delta T\left[\frac{E_{i-1,j}^m - 2E_{i,j}^m + E_{i+1,j}^m}{(\Delta r)^2} + \frac{E_{i+1,j}^m - E_{i-1,j}^m}{2r_i\Delta r} + \frac{E_{i,j-1}^m - 2E_{i,j}^m + E_{i,j+1}^m}{r_i^2(\Delta\theta)^2}\right] + \\ + \Delta T\varepsilon_{i,j}E_{i,j}^m = E_{i,j}^{m-1} + \Delta T\beta_{i,j}S_{i,j}^{m-1}I_{i,j}^{m-1}, \tag{4.10b}$$

$$I_{i,j}^m - d_I\Delta T\left[\frac{I_{i-1,j}^m - 2I_{i,j}^m + I_{i+1,j}^m}{(\Delta r)^2} + \frac{I_{i+1,j}^m - I_{i-1,j}^m}{2r_i\Delta r} + \frac{I_{i,j-1}^m - 2I_{i,j}^m + I_{i,j+1}^m}{r_i^2(\Delta\theta)^2}\right] - \\ - \Delta T\varepsilon_{i,j}E_{i,j}^m + \Delta T\gamma_{i,j}I_{i,j}^m = I_{i,j}^{m-1}, \tag{4.10c}$$

$$R_{i,j}^m - d_R\Delta T\left[\frac{R_{i-1,j}^m - 2R_{i,j}^m + R_{i+1,j}^m}{(\Delta r)^2} + \frac{R_{i+1,j}^m - R_{i-1,j}^m}{2r_i\Delta r} + \frac{R_{i,j-1}^m - 2R_{i,j}^m + R_{i,j+1}^m}{r_i^2(\Delta\theta)^2}\right] - \\ - \Delta T\gamma_{i,j}I_{i,j}^m + \Delta T\alpha_{i,j}r_{i,j}^m = R_{i,j}^{m-1}, \tag{4.10d}$$

for $i = 1,\dots,P$, $j = 1,\dots,M$ and $m = 0,\dots,T$.

The linear system associated to (4.1) is given by

$$AZ = B,$$

where Z denotes the unknown vector

$$\begin{pmatrix} \vec{S}^m \\ \vec{E}^m \\ \vec{I}^m \\ \vec{R}^m \end{pmatrix},$$

defined by

$$\vec{S}^m = \begin{pmatrix} S^m_{1,1} \\ \vdots \\ S^m_{P,1} \\ \vdots \\ S^m_{1,M} \\ \vdots \\ S^m_{P,M} \end{pmatrix}, \quad \vec{E}^m = \begin{pmatrix} E^m_{1,1} \\ \vdots \\ E^m_{P,1} \\ \vdots \\ E^m_{1,M} \\ \vdots \\ E^m_{P,M} \end{pmatrix}, \quad \vec{I}^m = \begin{pmatrix} I^m_{1,1} \\ \vdots \\ I^m_{P,1} \\ \vdots \\ I^m_{1,M} \\ \vdots \\ I^m_{P,M} \end{pmatrix}, \quad \vec{R}^m = \begin{pmatrix} R^m_{1,1} \\ \vdots \\ R^m_{P,1} \\ \vdots \\ R^m_{1,M} \\ \vdots \\ R^m_{P,M} \end{pmatrix}.$$

The matrix A is given by

$$A = \begin{bmatrix} A_S & 0 & 0 & 0 \\ 0 & A_E & 0 & 0 \\ 0 & 0 & A_I & 0 \\ 0 & 0 & 0 & A_R \end{bmatrix},$$

with

$$A_S = I - \frac{d_S \Delta t}{(\Delta r)^2} L, \quad A_E = I - \frac{d_E \Delta t}{(\Delta r)^2} L, \quad A_I = I - \frac{d_I \Delta t}{(\Delta r)^2} L, \quad A_R = I - \frac{d_R \Delta t}{(\Delta r)^2} L.$$

Here I denotes the identity matrix and L a $M \times M$ matrix defined as

$$L = \begin{bmatrix} Q-2S & S & 0 & \dots & 0 & S \\ S & Q-2S & \ddots & \ddots & \ddots & 0 \\ 0 & \ddots & \ddots & \ddots & \ddots & \vdots \\ \vdots & \ddots & \ddots & \ddots & \ddots & \vdots \\ 0 & \ddots & \ddots & \ddots & \ddots & S \\ S & \dots & \dots & \dots & S & Q-2S \end{bmatrix},$$

where

$$Q = \begin{bmatrix} -2 & 1+\lambda_1 & 0 & \dots & 0 & 0 \\ 1-\lambda_2 & \ddots & \ddots & \ddots & \ddots & \vdots \\ 0 & \ddots & \ddots & \ddots & \ddots & \vdots \\ \vdots & \ddots & \ddots & \ddots & \ddots & \vdots \\ \vdots & \ddots & \ddots & \ddots & -2 & 1+\lambda_{P-1} \\ 0 & \dots & \dots & \dots & 1-\lambda_P & 1+\lambda_P \end{bmatrix}, \quad S = \begin{bmatrix} \beta_1 & 0 & 0 & \dots & 0 & 0 \\ 0 & \beta_2 & \ddots & \ddots & \ddots & 0 \\ 0 & \ddots & \ddots & \ddots & \ddots & \vdots \\ \vdots & \ddots & \ddots & \ddots & \ddots & \vdots \\ \vdots & \ddots & \ddots & \ddots & \ddots & 0 \\ 0 & \dots & \dots & \dots & 0 & \beta_P \end{bmatrix},$$

with

$$\lambda_i = \frac{1}{2(i-\frac{1}{2})} \quad \text{and} \quad \beta_i = \frac{1}{(i-\frac{1}{2})^2(\Delta\theta)^2}, \quad i = 1,\dots,P. \tag{4.11}$$

The known vector B is defined as $B = \left(\vec{B}_S, \vec{B}_E, \vec{B}_I, \vec{B}_R\right)^T$, with

$$\vec{B}_S = \begin{pmatrix} S_{1,1}^{m-1} - \Delta T \beta_{1,1} S_{1,1}^{m-1} I_{1,1}^{m-1} \\ \vdots \\ S_{P,1}^{m-1} - \Delta T \beta_{P,1} S_{P,1}^{m-1} I_{P,1}^{m-1} \\ \vdots \\ S_{1,M}^{m-1} - \Delta T \beta_{1,M} S_{1,M}^{m-1} I_{1,M}^{m-1} \\ \vdots \\ S_{P,M}^{m-1} - \Delta T \beta_{P,M} S_{P,M}^{m-1} I_{P,M}^{m-1} \end{pmatrix}, \vec{B}_E = \begin{pmatrix} E_{1,1}^{m-1} + \Delta T \beta_{1,1} S_{1,1}^{m-1} I_{1,1}^{m-1} \\ \vdots \\ E_{P,1}^{m-1} + \Delta T \beta_{P,1} S_{P,1}^{m-1} I_{P,1}^{m-1} \\ \vdots \\ E_{1,M}^{m-1} + \Delta T \beta_{1,M} S_{1,M}^{m-1} I_{1,M}^{m-1} \\ \vdots \\ E_{P,M}^{m-1} + \Delta T \beta_{P,M} S_{P,M}^{m-1} I_{P,M}^{m-1} \end{pmatrix}, \vec{B}_I = \begin{pmatrix} I_{1,1}^{m-1} \\ \vdots \\ I_{P,1}^{m-1} \\ \vdots \\ I_{1,M}^{m-1} \\ \vdots \\ I_{P,M}^{m-1} \end{pmatrix}, \vec{B}_R = \begin{pmatrix} R_{1,1}^{m-1} \\ \vdots \\ R_{P,1}^{m-1} \\ \vdots \\ R_{1,M}^{m-1} \\ \vdots \\ R_{P,M}^{m-1} \end{pmatrix}.$$

Let $h = d_S \frac{\Delta T}{(\Delta r)^2}$. The *Neumann Lemma* [4] shows that the inverse of the matrix $A = I - hL$ exists whenever $h\|L\| < 1$ for some matrix norm. Therefore for $h = d_S \frac{\Delta T}{(\Delta r)^2}$ sufficiently small the linear algebraic system $AZ = B$ has a unique solution.

4.2 Illustration of the Theoretical Results

In order to illustrate the theoretical results presented in *Chapter 3* and to better understand the basic features of the Δ-SEIRS model, we performed several numerical simulations.

Suppose that we have a circular domain Ω as defined in (4.2), with radius equal to 1. Thus, $|\Omega| = \pi$.

In all illustrations below, it is assumed that the infected and recovered individuals at $t = 0$ are equal to zero, *i.e.*,

$$I(x,y,0) = R(x,y,0) = 0, \quad \forall (x,y) \in \Omega.$$

Furthermore, functions $\varepsilon(x,y)$, $\gamma(x,y)$, $\alpha(x,y)$ and all diffusion coefficients are fixed. We set

$$\varepsilon(x,y) = \frac{1}{5}, \quad \gamma(x,y) = \frac{1}{6}, \quad \alpha(x,y) = \frac{1}{30}, \quad (x,y) \in \Omega,$$

and $N_0 = 100$. The transmission intensity we define it to be of the form

$$\beta(x,y) = \beta_0 f(x,y,a,b,c), \quad (x,y) \in \Omega, \tag{4.12}$$

where β_0 denotes a positive constant and

$$f(x,y,a,b,c) = e^{-c[(x-a)^2+(y-b)^2]}, \quad (x,y) \in \Omega. \tag{4.13}$$

In view of assumption (3.4), for the double integral approximations we use the composite trapezoidal rule given by

$$\int_a^b f(x)dx \simeq \frac{1}{2}\sum_{j=1}^{n}(x_j - x_{j-1})\Big[f(x_{j-1} - f(x_j)\Big]. \tag{4.14}$$

Hence, for the numerical approximation of the double integral (3.4) we have

$$\int_\Omega \Big(S+E+I+R\Big)(x,y,t)dxdy = \int_0^{2\pi}\int_0^1 r\Big(S+E+I+R\Big)(r,\theta,t)drd\theta$$

$$\simeq \frac{\Delta r\Delta\theta}{4}\Big[\Big(S+E+I+R\Big)(1,2\pi,t_m)+\Big(S+E+I+R\Big)(1,0,t_m)\Big]+\frac{\Delta r\Delta\theta}{2}\sum_{j=1}^{M}\Big(S+E+I+R\Big)(1,\theta_j,t_m)+$$

$$+\frac{\Delta r\Delta\theta}{2}\sum_{i=1}^{P}\Big[\Big(S+E+I+R\Big)(r_i,2\pi,t_m)+\Big(S+E+I+R\Big)(r_i,2\pi,t_m)\Big]+$$

$$+\Delta r\Delta\theta\sum_{i=1}^{P}\sum_{j=1}^{M}\Big(S+E+I+R\Big)(r_i,\theta_j,t_m),$$

with $i=1,\dots,P$ and $j=1,\dots,M$.

For the numerical results presented, we chose $P=M=30$ and a step $\Delta T=0,05$.

4.2.1 Reaction-diffusion epidemic problem with positive diffusion coefficients

All of the following figures illustrate the model simulations with all diffusion coefficients set as positive constants, implemented using the numerical method (4.10). The respective diffusion coefficients are fixed as

$$d_S=0.001,\quad d_E=0.01,\quad d_I=0.01,\quad d_R=0.01. \tag{4.15}$$

This subsection is formulated as follows. First we focus our simulations for $\mathscr{R}_0<1$, for which we expect that the disease does not become endemic and $\mathscr{R}_0>1$, where it is expected to have a positive number of exposed and infected individuals in equilibrium. Since we cannot compute directly the exact value of $\mathscr{R}_0$, we guarantee that $\mathscr{R}_0$ is lower or greater then 1 by using the estimates from *Lemma 3.3.7*. Lastly, we inspect the influences that changing the transmission intensity function $\beta(x,y)$ have in our model.

4.2.1.1 $\mathscr{R}_0<1$

Figures 4.2 and *4.3* present the model simulations for the evolution of the global variables against time when

$$\beta(x,y)=\frac{2}{1000}f(x,y,0,0,1),\quad (x,y)\in\Omega. \tag{4.16}$$

It follows from *Lemma 3.3.4* that

$$\mathscr{R}_0\le\max\Big\{\frac{100}{\pi}\frac{\beta(x,y)}{\gamma(x,y)}:(x,y)\in\Omega\Big\}=0.4. \tag{4.17}$$

Hence, $\mathscr{R}_0<1$.

Whereas *Figure 4.2* illustrates a spatially homogeneous population where susceptible and exposed individuals are set as

$$S(x,y,0)=0.9\frac{100}{\pi},\quad E(x,y,0)=0.1\frac{100}{\pi},$$

in *Figure 4.3* susceptible and exposed individuals are distributed as

$$S(x,y,0) = 0.9\frac{100\cdot 2}{\pi(1-e^{-2})}f(x,y,0,0,2), \quad E(x,y,0) = 0.1\frac{100\cdot 2}{\pi(1-e^{-2})}f(x,y,0,0,2), \tag{4.18}$$

for $(x,y)\in\Omega$, corresponding to a higher concentration of the population in the center of the domain.

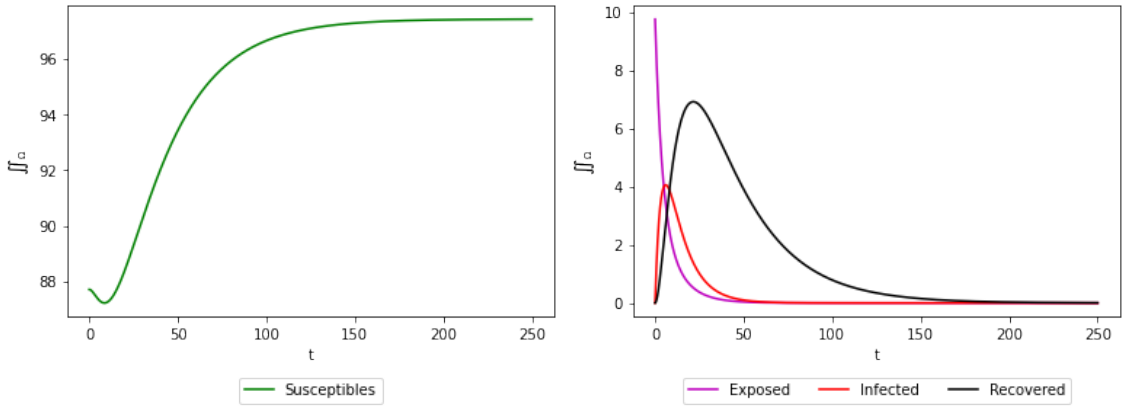

(a) (b)

Figure 4.2: **Total population in each compartment for a spatially homogeneous population for $\mathscr{R}_0 < 1$.** Approximation of the double integral over Ω for: (a) Susceptible, (b) Exposed, Infected and Recovered. Initial conditions are $S(x,y,0) = 0.9\frac{100}{\pi}$ and $E(x,y,0) = 0.1\frac{100}{\pi}$ with $\beta(x,y) = \frac{2}{1000}f(x,y,0,0,1)$.

Figures 4.2(a) and *4.3(a)* show the time evolution of the susceptible individuals, as *Figures 4.2(b)* and *4.3(b)* show the approximation of the model variables E, I and R cases. As it can be seen, as time evolves the number of exposed, infected and recovered individuals vanish, which illustrates the stability of the DFE established in *Theorem 3.3.6*.

Additionally, in *Figure 4.3* the spatial distribution of the sum of all individuals, *i.e.*, $S(x,y)+E(x,y)+I(x,y)+R(x,y)$ for $(x,y)\in\Omega$ is illustrated. Here it can be seen that, for t big enough, close to the equilibrium value, the population is uniformly distributed in space as it was expected for the equilibrium solution, following *Theorem 3.3.1*.

Note that, by taking a closer look at system (4.10), if the initial spatial conditions are set uniformly, *i.e.*, $S(x,y,0) = c_1$ and $E(x,y,0) = c_2$ for all $(x,y)\in\Omega$ with

$$\iint_\Omega (c_1+c_2)dxdy = 100,$$

then the diffusion coefficients have no weight in the following implementations. From *Figures 4.2* and 4.3, it can be seen that the number of total cases for each class in the homogeneous case shows to be similar to the non-homogeneous case. Hence, for the following simulations we disregard the case with homogeneous initial conditions.

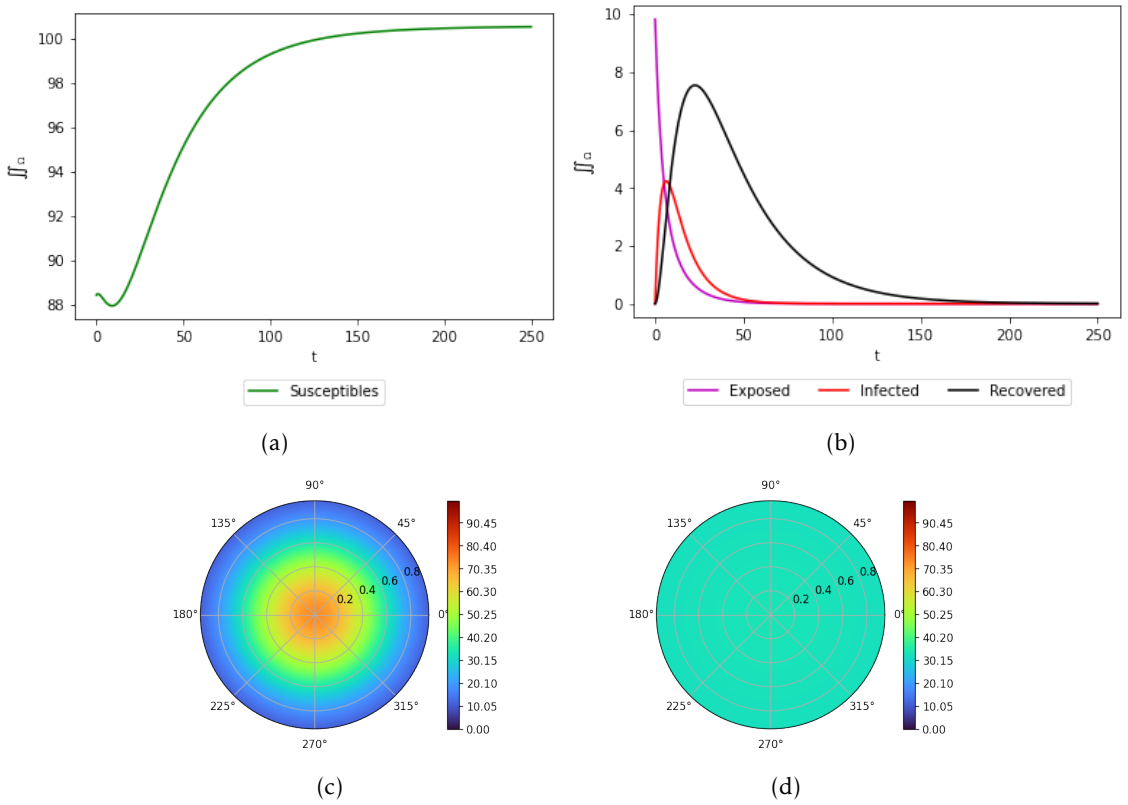

Figure 4.3: **Total population in each compartment and spatial distribution for a spatially non-homogeneous population with $\mathscr{R}_0 < 1$.** Approximation of the double integral over Ω for: (a) Susceptible, (b) Exposed, Infected and Recovered. (c) Initial spatial distribution for the total population ($t = 0$) (d) Final spatial distribution for the total population ($t = 250$). Initial conditions are $S(x,y,0) = 0.9\frac{100\cdot 2}{\pi(1-e^{-2})}f(x,y,0,0,2)$ and $E(x,y,0) = 0.1\frac{100\cdot 2}{\pi(1-e^{-2})}f(x,y,0,0,2)$ with $\beta(x,y) = \frac{2}{1000}f(x,y,0,0,1)$.

4.2.1.2 $\mathscr{R}_0 > 1$

Figure 4.4 illustrates the model predictions for the evolution of the global variables against time when

$$\beta(x,y) = \frac{1}{40}f(x,y,0,0,1), \quad (x,y) \in \Omega. \tag{4.19}$$

It follows

$$1.9 = \min\left\{\frac{100}{\pi}\frac{\beta(x,y)}{\gamma(x,y)} : (x,y) \in \Omega\right\} \leq \mathscr{R}_0, \tag{4.20}$$

which guarantees that $\mathscr{R}_0 > 1$.

Figures 4.4(a) and *4.4(b)* show the time evolution of the susceptible individuals and the model variables E, I and R cases, respectively. As time evolves, one can see that the exposed and infected cases do not converge to zero. Thus, when $\mathscr{R}_0 > 1$ and as time increases, the solution (S,E,I,R) does not converge to the DFE, as *Theorem 3.3.7* states. As it was expected but not proved in *Chapter 3*, *Figure 4.4* shows the existence of a EE solution for problem (3.9)-(3.10).

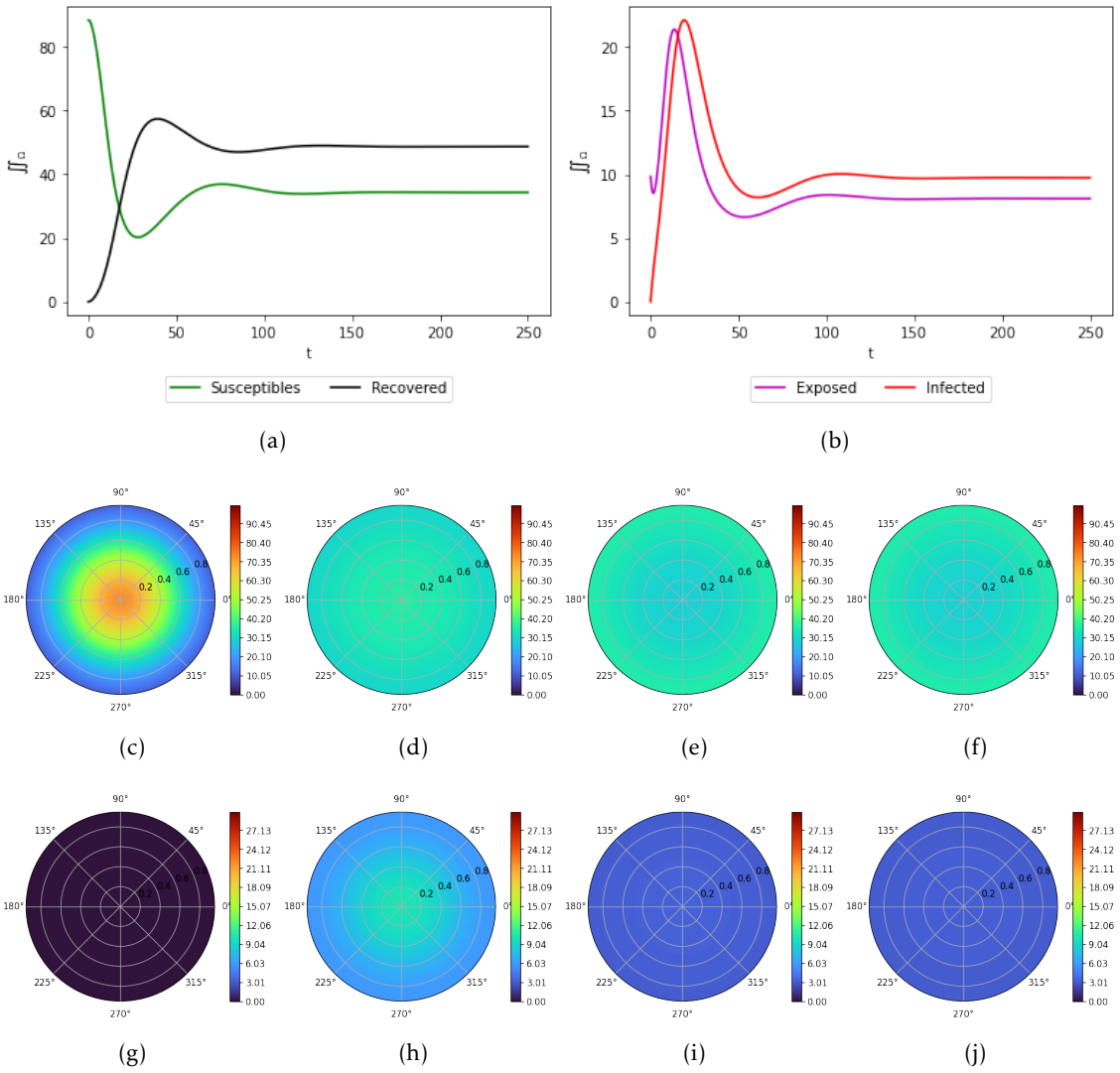

Figure 4.4: **Total population in each compartment and spatial distribution for a spatially non-homogeneous population with $\mathscr{R}_0 > 1$.** Approximation of the double integral over Ω for: (a) Susceptible and Recovered, (b) Exposed and Infected. Spatial distribution for the total population at: (c) Initial time ($t = 0$), (d) the moment of higher number of infected cases ($t = 19$), (e) at $t = 100$, (f) close to equilibrium ($t = 250$). Spatial distribution for the infectious population at: (g) Initial time ($t = 0$), (h) the moment of higher number of infected cases ($t = 19$), (i) $t = 100$, (j) close to the equilibrium ($t = 250$). Initial conditions are $S(x,y,0) = 0.9\frac{100\cdot 2}{\pi(1-e^{-2})}f(x,y,0,0,2)$ and $E(x,y,0) = 0.1\frac{100\cdot 2}{\pi(1-e^{-2})}f(x,y,0,0,2)$ with $\beta(x,y) = \frac{1}{40}f(x,y,0,0,1)$.

From *Figure 4.5(c)* to 4.5(f), the spatial spread of the total population is presented and in *Figures 4.4(g)* to 4.4(j) , the spatial spread of the infected individuals for $t = 0$, $t = 19$, $t = 100$ and $t = 250$, respectively. The results show that, as time evolves, individuals tend to scatter among space. However, in contrast to the previous case where $\mathscr{R}_0 < 1$, here near the equilibrium value the population does not become homogeneous in space.

4.2.1.3 Impact of changes in the transmission intensity function

In this subsection the goal is to better understand the spatial influences that the intensity transmission, $\beta(x, y)$, have in our epidemic model.

First we study the impact that the difference in the maximum value of the intensity transmission function has in the behaviour of the model variables. For that purpose, the following illustrations show the model simulations for two scenarios where $\beta(x, y)$ is centered in the same location (center of the domain) for both cases, only differing in the choice of the positive constant β_0.

In *Figure 4.5(a)* we present the estimate evolution of the model variables for when

$$\beta(x, y) = \frac{1}{40} f(x, y, 0, 0, 1), \quad (x, y) \in \Omega,$$

while in *Figure 4.5(b)* the disease transmission intensity function is set as

$$\beta(x, y) = \frac{1}{20} f(x, y, 0, 0, 1), \quad (x, y) \in \Omega.$$

Thus, for both scenarios $\mathscr{R}_0 > 1$ and

$$0.049 \simeq \iint_\Omega \frac{1}{40} f(x, y, 0, 0, 1) dx dy < \iint_\Omega \frac{1}{20} f(x, y, 0, 0, 1) dx dy \simeq 0.098.$$

The illustrations show that for the simulation with higher maximum value of $\beta(x, y)$, *Figure 4.5(b)*, the disease progresses through the different classes more rapidly and that the number of exposed, infected and recovered individuals is higher.

In *Figures 4.5(c)-4.5(f)* and 4.5(g)-4.5(j) the spatial distribution of infected individuals is showed for the simulations in *Figure 4.5(a)* and 4.5(b), respectively.

In *Figure 4.6* we study the effects of shifting the location where the transmission intensity function is centered. For the first scenario, *Figure 4.6(a)*, we set

$$\beta(x, y) = \frac{1}{40} f(x, y, 0, 0, 1), \quad (x, y) \in \Omega,$$

and for *Figure 4.6(b)*

$$\beta(x, y) = \frac{1}{110} + \frac{1}{70} f\left(x, y, -\frac{1}{2}, \frac{1}{2}, 1\right), \quad (x, y) \in \Omega.$$

The transmission intensities were chosen in order to correspond to similar interval for $\mathscr{R}_0$ and similar level of disease at the endemic equilibrium. The estimations for $\mathscr{R}_0$ in *Figures 4.6* and *4.6(a)* are

$$1.9 = \min\left\{\frac{100}{\pi} \frac{\beta(x, y)}{\gamma(x, y)} : (x, y) \in \Omega\right\} \leq \mathscr{R}_0 \leq \max\left\{\frac{100}{\pi} \frac{\beta(x, y)}{\gamma(x, y)} : (x, y) \in \Omega\right\} = 4.8,$$

and

$$1.9 = \min\Big\{\frac{100}{\pi}\frac{\beta(x,y)}{\gamma(x,y)} : (x,y) \in \Omega\Big\} \leq \mathscr{R}_0 \leq \max\Big\{\frac{100}{\pi}\frac{\beta(x,y)}{\gamma(x,y)} : (x,y) \in \Omega\Big\} = 4.5,$$

respectively.

In *Figures 4.6(c)-4.6(f)* and 4.6(g)-4.6(j) the spatial distribution of the total population is presented for the simulations in *Figure 4.6(a)* and 4.6(b), respectively. Confronting these results, our analysis suggests that, over time, the population migrates to the sites where the disease transmission intensity function is lower valued.

4.2.2 Reaction-diffusion epidemic problem with $d_S = d_I = d_R = 0$

To illustrate the special case where some diffusion coefficients are set as zero, we simulate the system studied in *Section 3.3.2*. Hence, for the following simulations we set

$$d_S = d_I = d_R = 0,$$

and

$$d_E = 0.01.$$

The following figures follow the same initial settings as stated above and are distributed in the following manner. First we illustrate the case where $\mathscr{R}_0 < 1$ and then proceed to the case where $\mathscr{R}_0 > 1$. From the results stated in *Chapter 3*, we expect that for the first set of simulations the equilibrium solution converges to a DFE, where susceptible individuals can be non-uniformly distributed in space, and in the second set of simulations for the number of exposed and infected individuals to be positive in equilibrium.

4.2.2.1 $\mathscr{R}_0 < 1$

As in *Section 4.2.1*, the first simulations, *Figures 4.7* and *4.8*, illustrate the evolution of global variables against time with the disease transmission intensity set as

$$\beta(x,y) = \frac{2}{1000} f(x,y,0,0,1), \quad (x,y) \in \Omega.$$

These two figures only differ from each other in how the initial spatial distribution of individuals is set up. While *Figure 4.7* depicts a spatially homogeneous population, in *Figure 4.8* the susceptible and exposed individuals are distributed as in (4.18).

From *Lemma 3.3.11*, we have

$$\min\Big\{\widehat{S}(x,y)\frac{\beta(x,y)}{\gamma(x,y)} : (x,y) \in \Omega\Big\} \leq \mathscr{R}_0 \leq \max\Big\{\widehat{S}(x,y)\frac{\beta(x,y)}{\gamma(x,y)} : (x,y) \in \Omega\Big\}, \tag{4.21}$$

where $\widehat{S}(x,y)$ denotes the susceptible individuals of the disease-free equilibrium solution. For the computation of these estimates, approximate the equilibrium solution $\widehat{S}(x,y)$ by the numerical solution of the system with $t = 250$.

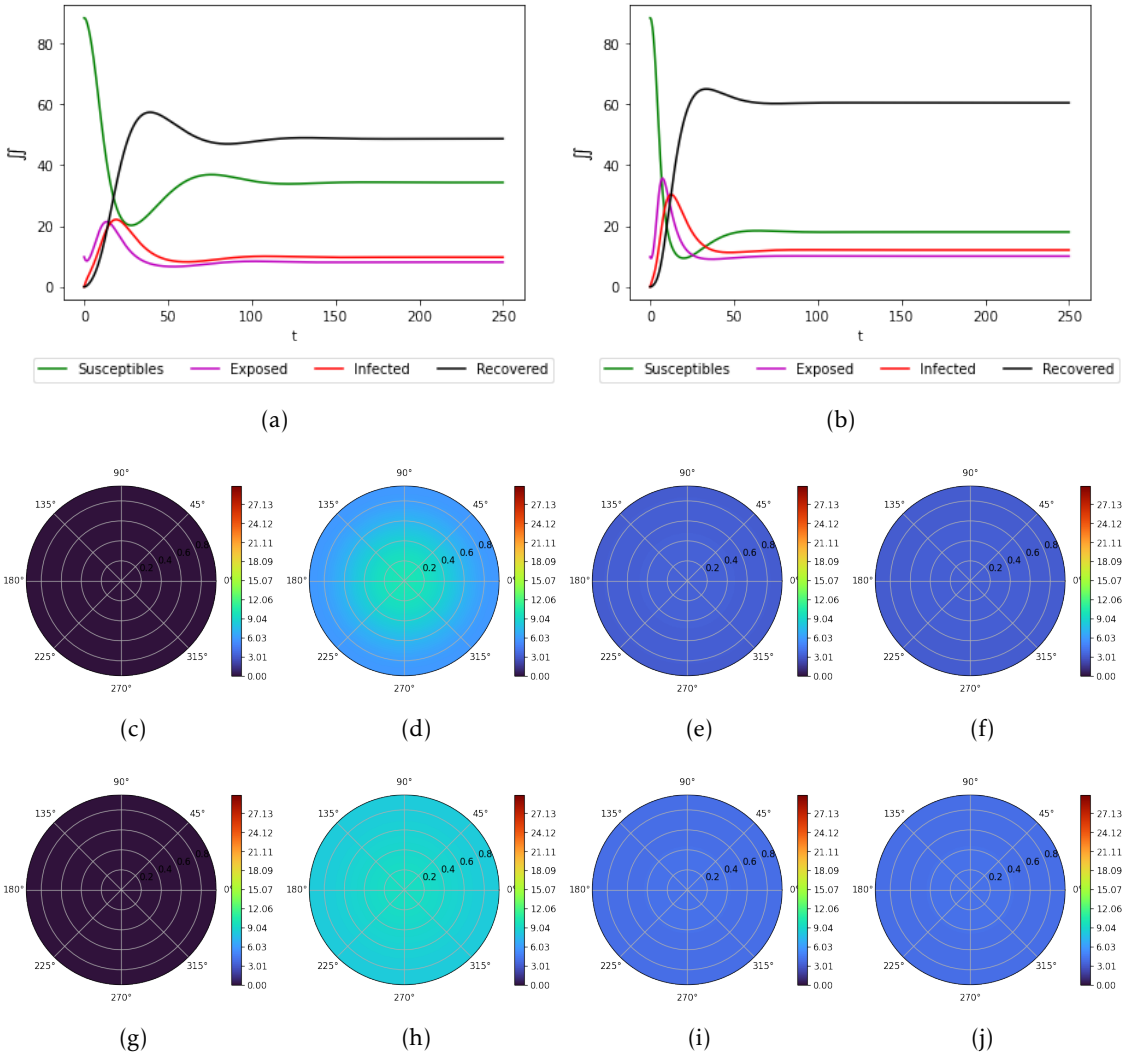

Figure 4.5: **Total population in each compartment and spatial distribution for two spatially non-homogeneous populations with $\mathscr{R}_0 > 1$.** Approximation of the double integral over Ω for: (a) Susceptible, Exposed, Infected and Recovered with $\beta(x,y) = \frac{1}{40} f(x,y,0,0,1)$. Spatial distribution for the infectious population at: (c) Initial time ($t = 0$), (d) the moment of higher number of infected cases ($t = 19$), (e) at $t = 100$, (f) close to equilibrium ($t = 250$). (b) Susceptible, Exposed, Infected and Recovered with $\beta(x,y) = \frac{1}{20} f(x,y,0,0,1)$. Spatial distribution for the infectious population at: (g) Initial time ($t = 0$), (h) the moment of higher number of infected cases ($t = 19$), (i) $t = 100$, (j) close to the equilibrium ($t = 250$). Initial conditions are $S(x,y,0) = 0.9\frac{100 \cdot 2}{\pi(1-e^{-2})} f(x,y,0,0,2)$ and $E(x,y,0) = 0.1\frac{100 \cdot 2}{\pi(1-e^{-2})} f(x,y,0,0,2)$.

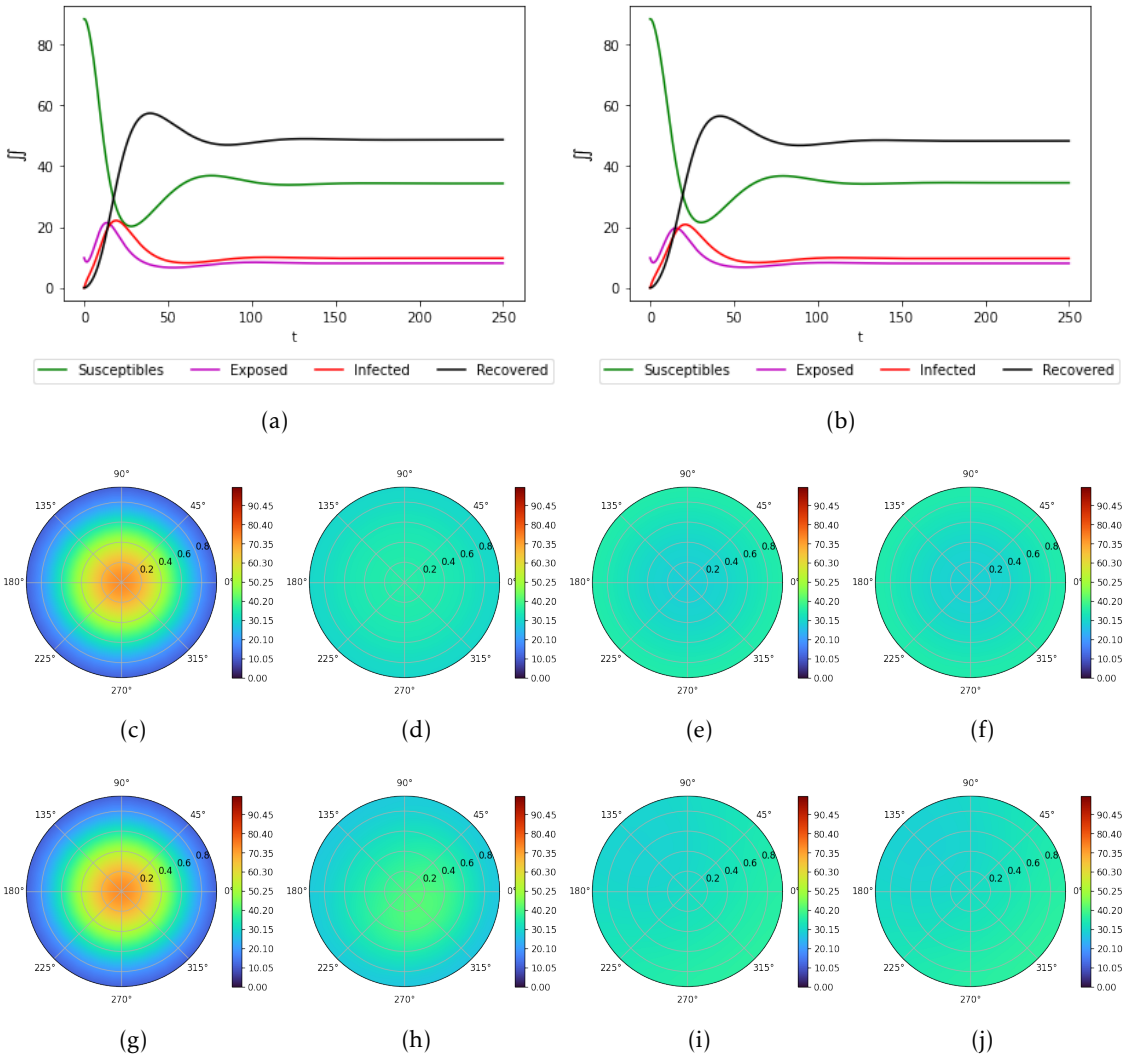

Figure 4.6: **Total population in each compartment and spatial distribution for two spatially non-homogeneous populations with $\mathscr{R}_0 > 1$.** Approximation of the double integral over Ω for: (a) Susceptible, Exposed, Infected and Recovered with $\beta(x,y) = \frac{1}{110} + \frac{1}{70} f(x,y,-1/2,1/2,1)$. Spatial distribution for the total population at: (c) Initial time ($t = 0$), (d) the moment of higher number of infected cases ($t = 19$), (e) at $t = 100$, (f) close to equilibrium ($t = 250$). (b) Susceptible, Exposed, Infected and Recovered with $\beta(x,y) = \frac{1}{20} f(x,y,0,0,1)$. Spatial distribution for the total population at: (g) Initial time ($t = 0$), (h) the moment of higher number of infected cases ($t = 19$), (i) $t = 100$, (j) close to the equilibrium ($t = 250$). Initial conditions are $S(x,y,0) = 0.9\frac{100 \cdot 2}{\pi(1-e^{-2})} f(x,y,0,0,2)$ and $E(x,y,0) = 0.1\frac{100 \cdot 2}{\pi(1-e^{-2})} f(x,y,0,0,2)$.

Thus, for the transmission intensity function of *Figures 4.7* and *4.8*, we have

$$\mathscr{R}_0 \leq \max\left\{\widehat{S}(x,y)\frac{\beta(x,y)}{\gamma(x,y)} : (x,y) \in \Omega\right\} = 0.6.$$

Hence $\mathscr{R}_0 < 1$.

Just as it was expected from *Theorem 3.3.11*, *Figures 4.7* and *4.8* show that when the basic reproduction number is less than one, the number of infected and exposed individuals goes extinct. Thus the equilibrium solutions of these are both a DFE.

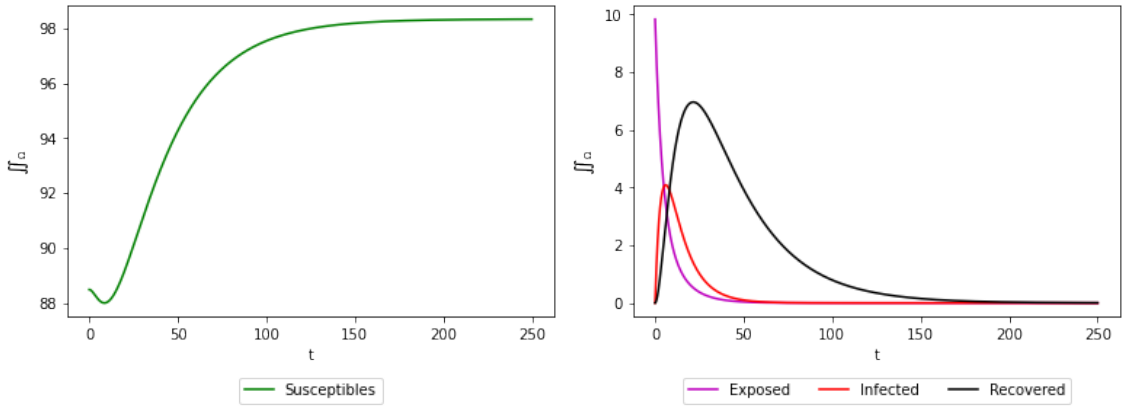

(a) (b)

Figure 4.7: **Total population in each compartment for a spatially homogeneous population for $\mathscr{R}_0 < 1$.** Approximation of the double integral over Ω for: (a) Susceptible, (b) Exposed, Infected and Recovered. Initial conditions are $S(x,y,0) = 0.9\frac{100}{\pi}$ and $E(x,y,0) = 0.1\frac{100}{\pi}$ with $\beta(x,y) = \frac{2}{1000}f(x,y,0,0,1)$.

In contrast to the results presented in *Section 4.2.1.1*, in *Figure 4.8* it can be seen that the susceptibles in the DFE are not uniformly distributed.

4.2.2.2 $\mathscr{R}_0 > 1$

The following illustrations represent the epidemic model (3.36) simulations with the transmission intensity function defined as

$$\beta(x,y) = \frac{1}{40}f(x,y,0,0,1), \quad (x,y) \in \Omega.$$

We have

$$\mathscr{R}_0 \geq \min\left\{\widehat{S}(x,y)\frac{\beta(x,y)}{\gamma(x,y)} : (x,y) \in \Omega\right\} = 1.5,$$

which guarantees that $\mathscr{R}_0 > 1$.

Although we were not able to demonstrate the existence of an endemic equilibrium for the epidemic model, from our findings illustrated in *Figure 4.9*, we observe that when the basic reproduction number is bigger than one, the number of infected and exposed individuals is positive, which corroborates our suspicions of the existence of a EE solution.

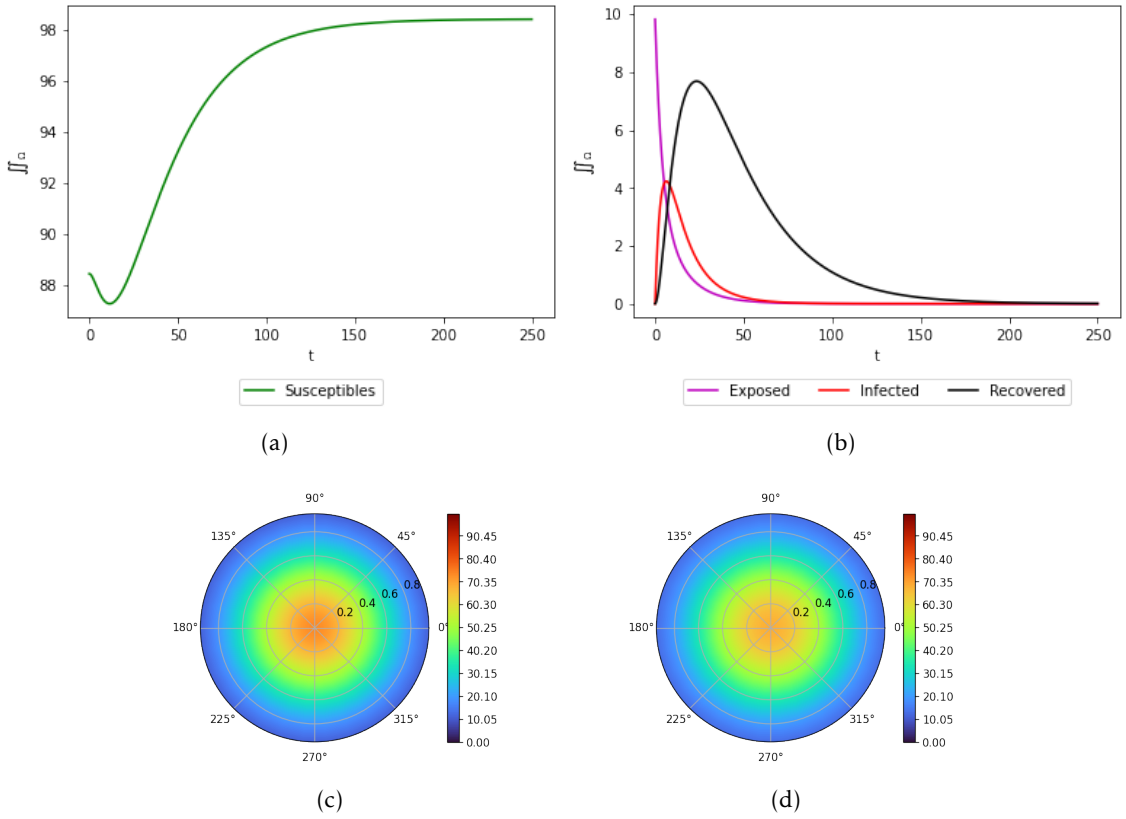

Figure 4.8: **Total population in each compartment and spatial distribution for a spatially non-homogeneous population with $\mathscr{R}_0 < 1$.** Approximation of the double integral over Ω for: (a) Susceptible, (b) Exposed, Infected and Recovered. (c) Initial spatial distribution for the total population ($t = 0$) (d) Final spatial distribution for the total population ($t = 250$). Initial conditions are $S(x,y,0) = 0.9\frac{100\cdot 2}{\pi(1-e^{-2})}f(x,y,0,0,2)$ and $E(x,y,0) = 0.1\frac{100\cdot 2}{\pi(1-e^{-2})}f(x,y,0,0,2)$ with $\beta(x,y) = \frac{2}{1000}f(x,y,0,0,1)$.

Lastly, *Figure 4.9* shows the spatial spread of the total population and infected individuals over time. Although as time evolves the sum of individuals tends to spread spatially, in contrast to *Figure 4.4*, we expect that when only d_E is set as a non-zero constant this spread happens at a lower rate than when all diffusion coefficients are set as positive constants.

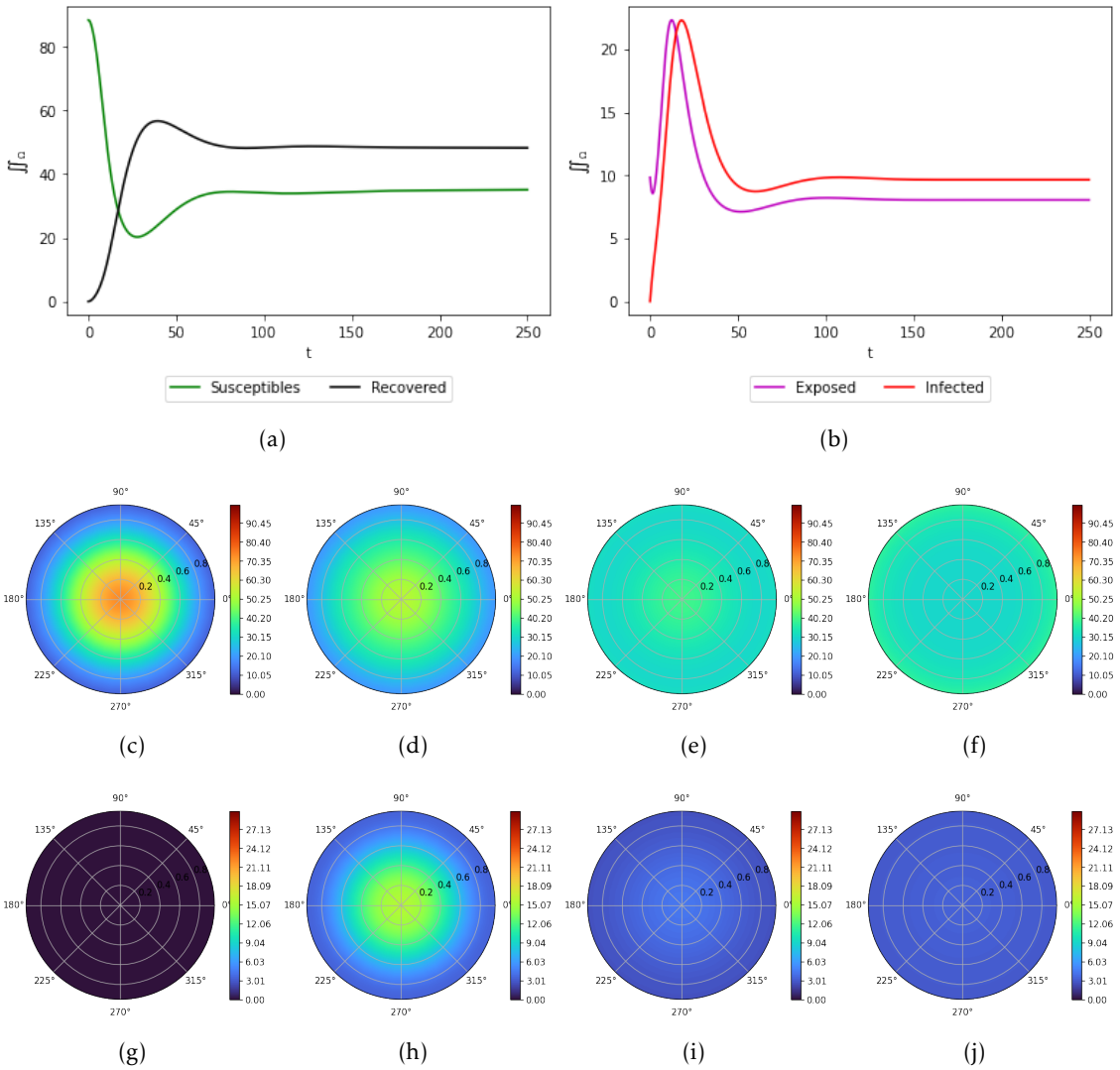

Figure 4.9: **Total population in each compartment and spatial distribution for a spatially non-homogeneous population with $\mathscr{R}_0 > 1$.** Approximation of the double integral over Ω for: (a) Susceptible and Recovered, (b) Exposed and Infected. Spatial distribution for: (c) Initial total population ($t = 0$), (d) Total population at the moment of higher number of infected cases ($t = 19$), (e) Total population ($t = 100$), (f) Final total population ($t = 250$), (g) Initial infected individuals ($t = 0$), (h) Infected individuals at the moment of higher number of infected cases ($t = 19$), (i) Infected individuals ($t = 100$), (j) Final infected individuals ($t = 250$). Initial conditions are $S(x,y,0) = 0.9\frac{100\cdot 2}{\pi(1-e^{-2})}f(x,y,0,0,2)$ and $E(x,y,0) = 0.1\frac{100\cdot 2}{\pi(1-e^{-2})}f(x,y,0,0,2)$ with $\beta(x,y) = \frac{1}{40}f(x,y,0,0,1)$.

5

Application to COVID-19

In 2019 a disease outbreak, COVID-19, emerged in the city of Wuhan, China. COVID-19 is an infectious disease caused by the SARS-COV-2 virus [15]. Later on, the World Health Organization (WHO) declared this global public health emergency a pandemic.

In response to this new public health threat, several countries implemented different non-pharmaceutical interventions (NPI) with the purpose of slowing any further spread.

The first case of COVID-19, in Portugal, was first confirmed on the 2^{nd} of March 2020 [5]. Following the first reported case, the number of infected individuals increased significantly, forcing policy makers to act. Schools were closed on the 16^{th} of March, followed by the implementation of a state of emergency on the 22^{nd}. With a mandatory stay-at-home order for the population, the movement of individuals was severely reduced, decreasing in this way the contact rate.

Through the course of COVID-19 outbreak, mathematical models have been adapted from the SEIR model to give simulations for the future course of the virus transmission. One of the main purposes of the modelling techniques is to evaluate the impact of transmission mitigation measures, giving policy makers the correct tools to impose weighted decisions. Mathematical transmission models firmly adjusted to available data are among the best tools to provide new simulations. Most mathematical models proposed for COVID-19 spread in Portugal do not take into account the spatial spread of individuals [5, 20]. However, *Mammeri et. al* implemented a SEIR epidemic flow model, where the spatial spread of individuals is taken into account, showing that the spatial epidemic model fitted to available data in France reproduced the spread of the disease correctly in this country [14].

In this chapter we present simulations for the spread of COVID-19 using the Δ-SEIRS epidemic model (3.1)-(3.4), where we consider that the population is concentrated in two regions corresponding to Portugal's most populated cities. The goal is to analyze the spatial distribution of infected cases along time with and without implementation of NPI. We use information about the impact of these interventions on transmission according to non-spacial models.

This chapter is organised as follows. First the parameters chosen for the simulations

of our model are stated and the model strategy is described. In *Section 5.2* graphics for the spatial spread of the virus in Portugal and the number of individuals in each class for each simulation are presented. Lastly, we discuss the results illustrated in *Section 5.2*.

5.1 Parameters choice and Model strategy

Whenever possible, Portuguese available data was used to fix some of the disease related parameters choice. The rate at which exposed individuals progress to the infectious state, $\varepsilon(x,y)$, and the rate of recovery, $\gamma(x,y)$, were assumed to be constant and the same as in [5]. We assumed that immunity to infection lasts for 180 days [16]. Parameters values can be found on *Table* 5.1.

Date	Description	Value
$\gamma(x,y)$	Rate of recovery	$\frac{1}{3.4} days^{-1}$
$\varepsilon(x,y)$	Rate of progression to the infectious state	$\frac{1}{3.8} days^{-1}$
$\alpha(x,y)$	Rate of loss of immunity	$\frac{1}{180} days^{-1}$
p	Proportion of asymptomatic infected individuals	$44,5\%$

Table 5.1: Description and values of parameters fixed in the epidemic model.

Following the conclusions taken on *Section 4.2*, we assume that only exposed individuals are moving and we set

$$d_E = 0,001.$$

Later on, we will vary this value since we did not have information on this parameter. Dependence of the results on the variation of this parameter will be described. Contact data was obtained from [20], where the authors estimated that, for the period prior to the pandemic, the average number of daily contacts was 12.6 and the basic reproduction number was $\mathscr{R}_0 = 2.20$.

We will consider the time period between February to June 2020. Day 0 is assumed to be 10^{th} February 2020, which was obtained from [5], where the authors estimated this date by subtracting the incubation period (approximately 5 days) from the first disease onset in Portugal.

Analogously to the simulations presented in the previous chapter, for the following illustrations we set Ω as the unit circular domain. We wish to simulate the spread of COVID-19 in Portugal by replicating it's two most populated regions, the cities of Lisbon and Oporto. Following [5], we set the infected and recovered individuals equal to zero in the initial conditions. For simplicity we assume that the population is exponentially distributed in two points $\left(\frac{1}{2}, -\frac{1}{2}\right)$ and $\left(-\frac{1}{2}, \frac{1}{2}\right)$ corresponding to the main urban centers where population density is higher: Population of Lisbon and Oporto was obtained in [17].

Initial number of exposed individuals were taken as in [5] and we assumed that these cases were also exponentially distributed with center on Oporto, as the first COVID-19 cases were notified in this region. Hence the initial conditions for exposed and susceptible are:

$$E(x,y,0) = 71\frac{100}{10286300}e^{-2000\left[(x+\frac{1}{2})^2+(y-\frac{1}{2})^2\right]},$$
$$S(x,y,0) = \left[0.001 + \frac{1}{600}\frac{2821876}{1722374}e^{-2\left[(x-\frac{1}{2})^2+(y+\frac{1}{2})^2\right]} + \frac{1}{400}e^{-2\frac{3001}{2040}\left[(x+\frac{1}{2})^2+(y-\frac{1}{2})^2\right]}\right]norm - E(x,y,0),$$

for $(x,y) \in \Omega$. The constant *norm* denotes the normalization value, which guarantees that assumption (3.4) is satisfied.

The introduction of NPIs such as the use of masks, school closure, social distancing, was, until the introduction of vaccination, in late December of 2020, the only way to control disease spread by reducing contacts and its ability to infect. For our study, we focus on the inclusion of use of mask and social distancing, together with the lockdown implementation. The course of the first NPI's implemented in Portugal until June 2020 can be found in *Table* 5.2.

Date	**Description**
12^{th} March 2020	Announcement of schools closure
16^{th} March 2020	Closure of schools
18^{th} March 2020	State-of-Emergency Announcement
22^{th} March 2020	Beginning of lockdown
28^{th} April 2020	Announcement of lockdown phase-out
04^{th} May 2020	First wave of lockdown phase-out
18^{th} May 2020	Second wave of lockdown phase-out
01^{st} June 2020	Third wave of lockdown phase-out

Table 5.2: Chronology of implementation of Non-Pharmaceutical Interventions in Portugal in combat to COVID-19 pandemic from February to June 2020.

We assume that the NPIs affect the disease transmission intensity and for simplicity we assumed that it has the same affect in all the domain, hence it will correspond to a multiplicative factor affecting the transmission intensity function. We assumed that the closure of schools, lockdown implementation and overall compliance to mask usage reflected a reduction of 69% on the disease transmission intensity function which took effect on the 18^{th} of March, as estimated in [5]. Later, with the lifting of some NPI's, on the 30^{th} of April it was estimated that transmission intensity suffered an increase of 14% [5].

Hence, we set the disease transmission intensity function to be a piece-wise function defined as

$$\beta(x,y,t) = \beta_0(x,y)\delta(t), \quad (x,y) \in \Omega, \quad t > 0, \tag{5.1}$$

with

$$\delta(t) = \begin{cases} 1 & \text{if} \quad 0 \leq t < b_1 \\ 1 - 0.69 & \text{if} \quad b_1 \leq t < b_2 \\ 1 - 0.55 & \text{if} \quad t \geq b_2 \end{cases}, \quad t > 0, \tag{5.2}$$

where b_1 and b_2 denote the moment of mathematical implementation. For our first simulations we chose $b_1 = 37$ and $b_2 = 90$.

In what follows we assumed $\beta_0(x, y)$ to be constant and set $\beta_0(x, y) = \frac{2.2}{3.4}\frac{100}{\pi}$, so that by applying *Lemma 3.3.14* we expect $\mathscr{R}_0$ to be bigger than 2.2 at the beginning of the simulations [20].

Lastly, it is important to note that although a percentage of the infected individuals with COVID-19 do not develop symptoms, these are still able to infect others. For the sake of simplicity, in our model we aggregate the symptomatic and asymptomatic infected individuals in the same class. To be able to compare the result of our simulations to the number of cases notified, following [5], we have assumed that the proportion of asymptomatic infected individuals is constant over time and it represents 44.5% of all infected cases.

5.2 Results and Simulations

In this section we consider the Δ-SEIRS model with the adapted parameters described in the previous section and using the numerical method proposed in *Chapter 4* we obtain some numerical results that are illustrated in *Figures 5.1-5.5*.

First we study the impact of changes in the diffusion coefficient of exposed individuals, which determines the velocity of dispersal of the disease in the population. The illustrations progress from the non-spatial model, *i.e.*, model with population uniformly distributed in space and $d_E = 0$, to d_E equal to 0.0001, 0.001 and 0.01, respectively. In *Figure 5.1* we plot the total exposed and infected population for a non-spatial SEIRS model and for three different scenarios of the spatially non-homogeneous Δ-SEIRS model, taking those several choices of d_E.

For the non-homogeneous model simulations, the spatial distribution of infected individuals is illustrated in *Figure 5.2*. In *Figure 5.2* the first column of the circular graphics regards the distribution of infected individuals in the initial conditions, the second and third columns to the instants of higher values of daily total infected population and the last column represents the final spatial distribution of infected individuals.

For the remaining simulations we will fix $d_E = 0.001$.

Following the chronology of events in Portugal displayed in *Table 5.2*, we defined several scenarios for the implementation of NPI's. First, *Figure 5.3* illustrates the Δ-SEIRS model simulations for the course of the COVID-19 disease in Portugal, where the lockdown is implemented on the 18^{th} of March and the lockdown phase-out on the 10^{th} of May. *Figures 5.3(b)-5.3(e)* represent the spatial distribution of infectious cases.

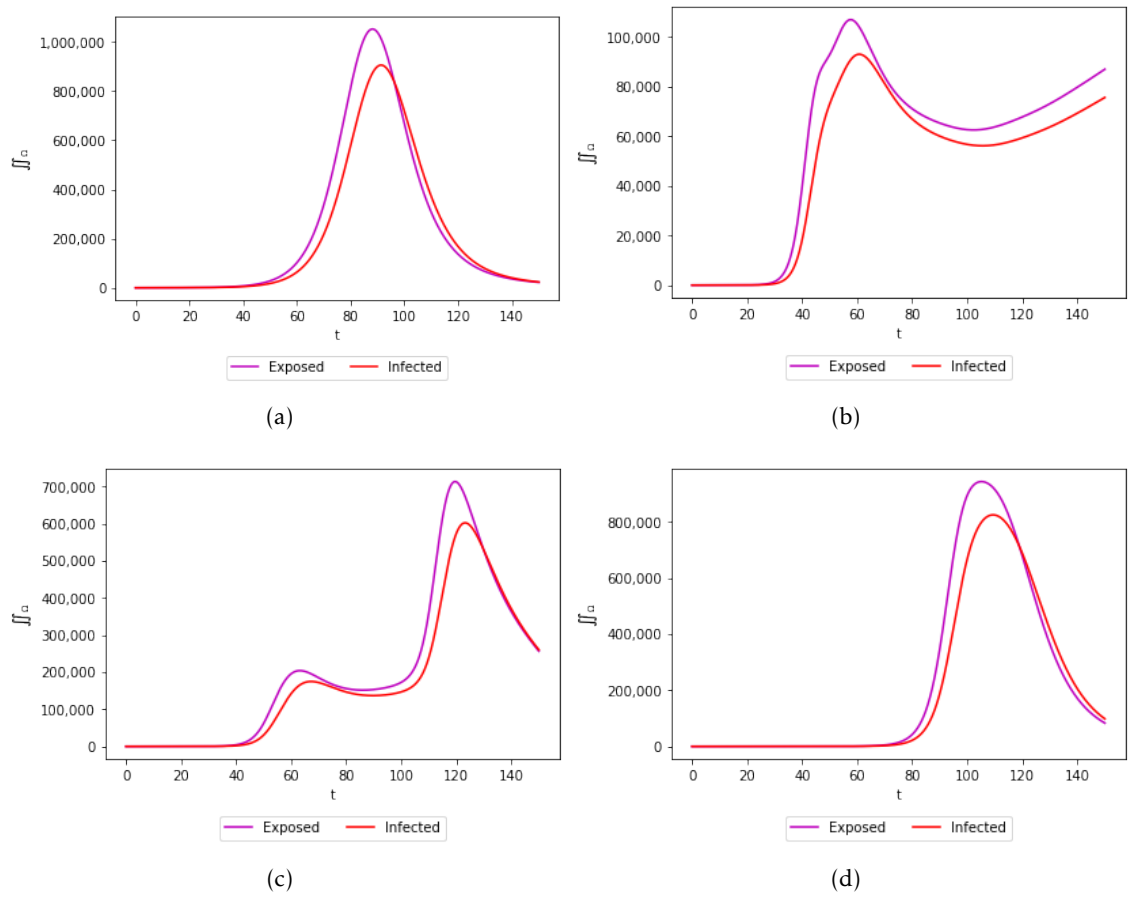

Figure 5.1: **Total population in Exposed and Infected compartments for:** (a) Non-spatial model. Spatially non-homogeneous model with: (b) $d_E = 0.0001$, (c) $d_E = 0.001$, (d) $d_E = 0.01$. Disease transmission intensity function is set as $\beta_0(x, y) = \frac{2.2}{3.4}\frac{100}{\pi}$.

Note that the time points for which the NPIs take effect were estimated using an age-structured model that has no spatial heterogeneity. We vary these time points to evaluate the impact on disease transmission. We first studied the impact of changing the lockdown implementation and next we proceeded to analyse the impact of changes in the lockdown phase-out dates. Our simulations correspond to changing the date of the first reduction in the disease transmission intensity to 8^{th} of March, 18^{th} of March and to the 26^{th} of March. In the second set of simulations we illustrated different lockdown phase-out scenarios, where the increase on $\beta(x, y)$ corresponds to the 1^{st} of April, 17^{th} of April and 10^{th} of May, assuming that the lockdown started on the 18^{th} of March for all scenarios. Hence these correspond to two week, one month and two months lockdowns, respectively. *Figures 5.4* and *5.5* depict these simulations where only the proportion of asymptomatic infected cases is shown and the grey vertical lines indicate the date of lockdown implementation or phase-out, respectively.

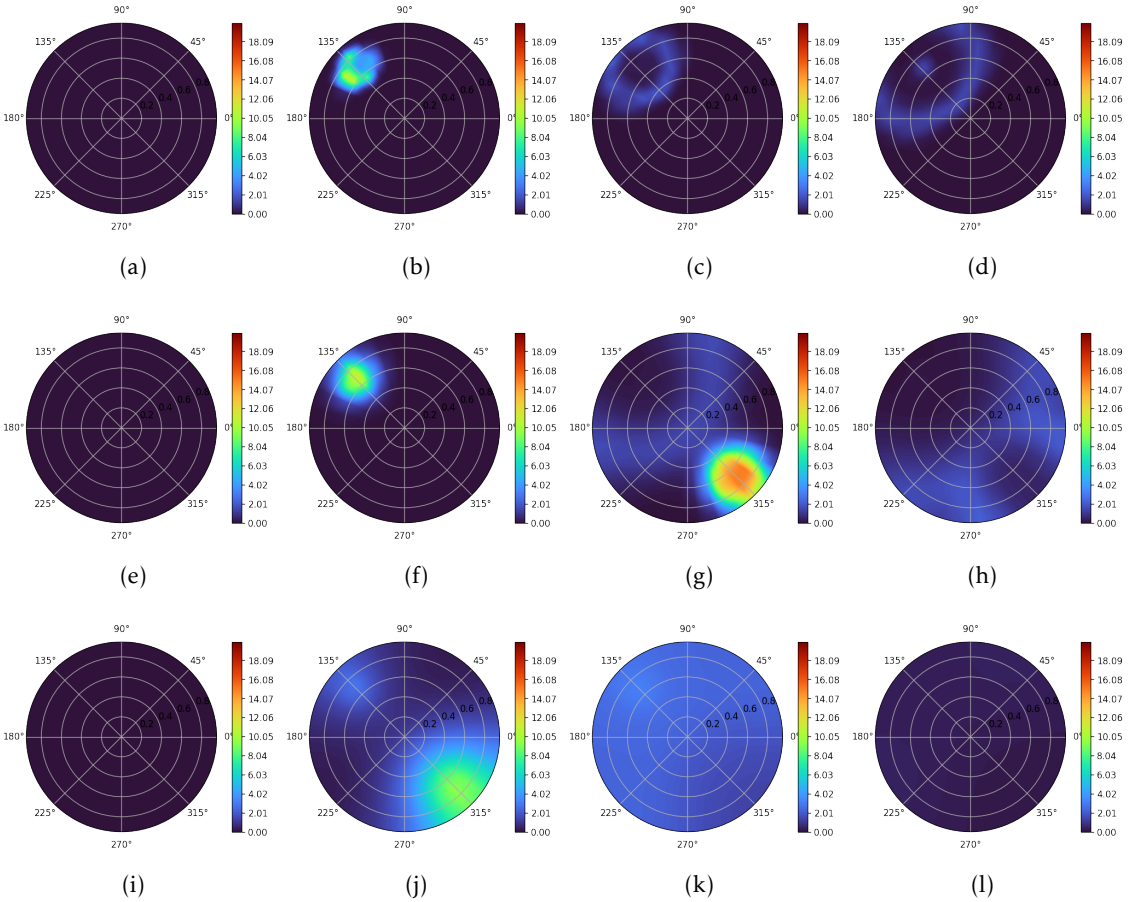

Figure 5.2: **Spatial distribution of Infected individuals for non-homogeneous model with:** $d_E = 0.0001$ at:(a) $t = 0$ (b) $t = 60$ (c) $t = 100$, (d) $t = 150$. $d_E = 0.001$ at: (e) $t = 0$, (f) $t = 60$, (g) $t = 120$, (h) $t = 150$. $d_E = 0.01$ at: (i) $t = 0$, (j) $t = 100$, (k) $t = 120$, (l) $t = 150$.

5.3 Discussion

We now briefly discuss the simulations illustrated from *Figure 5.1* to *5.5* and some implications of these results on disease control.

First we studied the difference between the non-spatial SEIRS model versus the spatially non-homogeneous Δ-SEIRS. In *Figure 5.1* we see that for the non-spatial model the peak is higher. Although it is not visible in *Figure 5.1(a)* because of the scale of the two dimensional graphic, the non-spatial model approximations show that the population would have reached the first 1000 cases as soon as $t = 28$, which corresponds to the 9^{th} of March.

Furthermore, we also inspect the impact of changing the value of the diffusion coefficient of the exposed individuals, d_E, which will determine the velocity of dissemination of the disease. Analysing the model simulations for the different values of d_E we see that we can have more than one peak with different heights. By further comparing *Figures 5.1(b)-5.1(d)* with their respective circular graphics referring to the spatial dynamics of infected

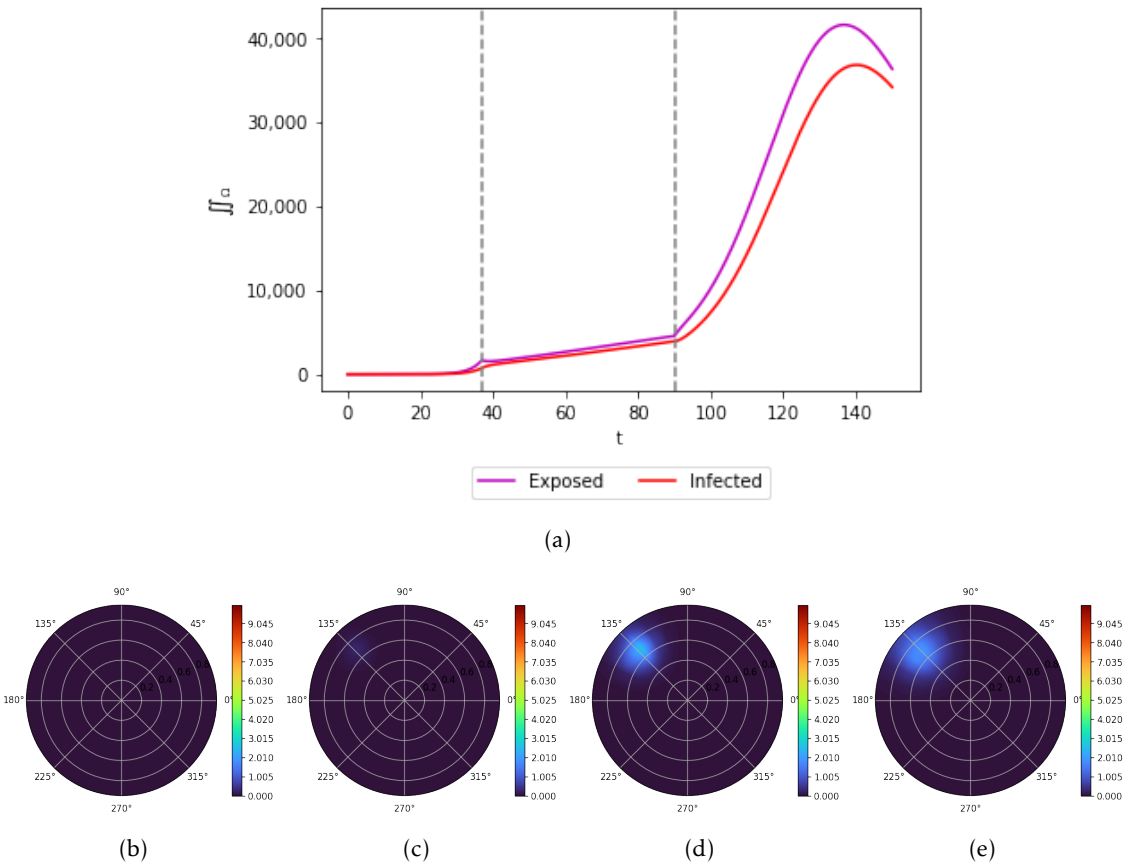

Figure 5.3: **Lockdown implementation and phase-out.** (a) Exposed and Infected. The disease transmission intensity function is decreased on the $18^{th} of March$ following lockdown measures and increases on the $10^{th} of May$ following the lockdown phase-out. Spatial distribution of Infected individuals for: (b) $t = 0$, (c) $t = 60$, (d) $t = 120$, (e) $t = 150$. Diffusion coefficient of exposed individuals set as $d_E = 0.001$.

individuals, we see that for the intermediate value of the diffusion coefficient $d_e = 0.001$ we have two epidemic waves, the first affecting mainly Oporto, where the initial exposed individuals were located, and then affecting Lisbon. We note that the second wave reaches a higher number of infected individuals, which is expected given that Lisbon is a more populated region. For lower the diffusion coefficient $d_e = 0.0001$ we only see, in this time frame, the first wave affecting the population located in the region of Oporto. Finally, for the higher diffusion coefficient $d_e = 0.01$ the two waves happen almost simultaneously.

By close inspection of *Figures 5.1(b)* and *5.1(d)* together with the circular graphics, we conclude that whereas for d_E set equal to 0.0001 the disease spreads at a much lower rate then what was reported in Portugal, for 0.01 the disease dissemination is quicker then what available data demonstrates.

We are then led to analyse the scenario illustrated in *Figure 5.1(c)*, which is of special interest. Analysing the instants in higher number of daily infected cases together with the respective circular graphics we see that the first increase in the total infected population

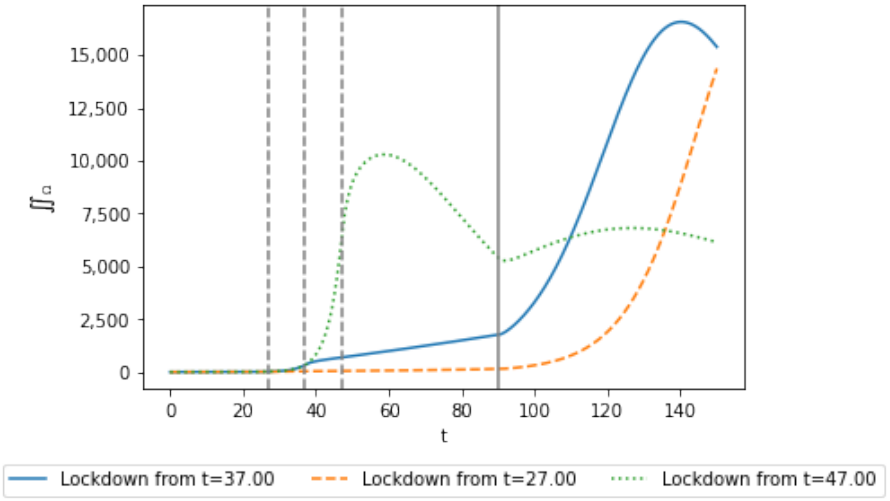

Figure 5.4: **Asymptomatic infected individuals for a spatially non-homogeneous model with implementation of lockdown on the 8^{th} of March, 18^{th} of March and 17^{th} of April, respectively.** Dashed grey lines refer to different lockdown implementations and continuous grey line to lockdown phase-out.

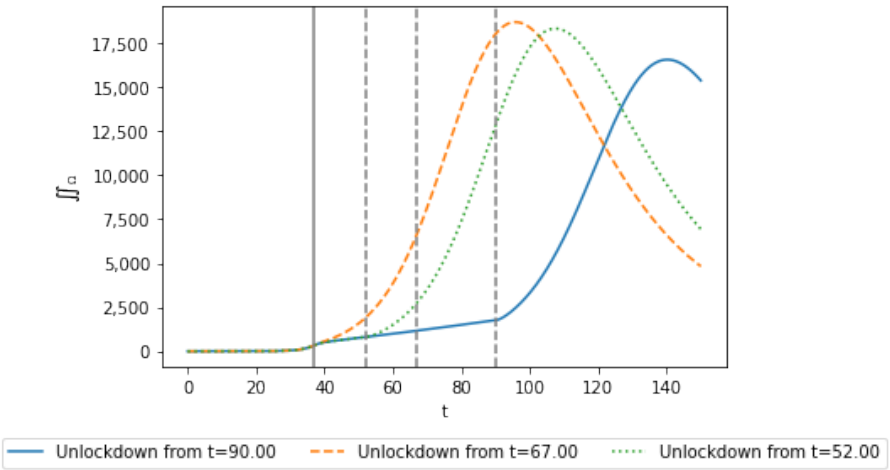

Figure 5.5: **Asymptomatic infected individuals for a spatially non-homogeneous model with phase-out of lockdown on the 1^{st} of April, 17^{th} of April and 10^{th} of May, respectively.** Continuous grey line refers to lockdown implementation and dashed grey lines to different lockdown phase-outs.

is due to the spread of the disease in the city of Oporto and the second in the city of Lisbon. Thus, for this choice of d_E, the spatial model illustrates that each city generates separate epidemics in the total population of infected individuals. Hence, this simulation illustrates the advantages that the inclusion of spatial dynamics adds to an epidemic model.

From the scenarios studied and taking into account the available data in reference to the spread of COVID-19 in Oporto and Lisbon between February and June 2020, we conclude that, from our simulations, the diffusion coefficient $d_E = 0.001$ represents the most suitable choice for modelling the implementation of mitigation measures.

Note that, *Figure 5.2* illustrates the model simulations for the worst case scenario, where no NPI's or treatment is implemented. Here it can be seen that, without the employment of any mitigation measures, the epidemic model estimates that the number of infected individuals (symptomatic and asymptomatic) would have reached almost 700000 infected individuals.

Finally, we introduce the implementation of some mitigation measures to understand if the model has the ability to correctly depict how COVID-19 disseminated in Portugal and the effect that the NPIs had in the spread of the disease. First we focused our simulations on the mathematical implementation of lockdown and lockdown phase-out according to the unfolding events in Portugal. This simulation is depicted in *Figure 5.3*, where it can be seen that the model projections estimate that the implementation of lockdown at 18^{th} of March reduced the daily total infectious population in 254490 infected individuals. Analysing the circular graphics with respect to the infected individuals spatial distribution in contrast to *Figures 5.2(e)-5.2(h)*, we see that the implementation of lockdown delayed the speed of propagation of COVID-19, only progressing the infected individuals from Oporto to the rest of the domain when the transmission intensity function is increased (lockdown phase-out).

In *Figure 5.4* and *5.5* several lockdown implementation and phase-out scenarios are investigated, respectively. Following the model simulations, it can be seen that if the introduction of NPI's and lockdown was introduced as soon as 6^{th} of March 2020 (only four days after the first confirmed case) the increase of infected individuals would have been delayed to a month later. Looking at the lockdown phase-out simulations we understand that, as it was expected, the longer the lockdown measures are implemented the longer the delay in the disease incidence is observed.

Although the Δ-SEIRS epidemic model simulations do not replicate with exactness the number of COVID-19 infected individuals confirmed in Portugal, from our analysis we conclude that this model is capable of replicating the dissemination of the disease. The difference from the number of infected cases simulated to those observed in Portugal from February to June 2020 may also be explained by some inaccuracy in the model fit strategy.

Nonetheless, from the results here presented, we conclude that mathematical modelling of infectious diseases is one of the most beneficial and useful tools to predict infectious diseases spread, giving policymakers useful data to assess which mitigation measures to implement.

6

Discussion and Future Work

In this work, we proposed a SEIRS reaction-diffusion population model and demonstrated the existence of a global solution. We then introduced the equilibrium problem where the equilibrium solutions, the disease-free equilibrium (DFE) and the endemic equilibrium (EE) were defined. The main focus of our study was the DFE solution where the existence of a DFE was proved for our Δ-SEIRS model and the steady states were studied. For this purpose, two separate epidemic problems were distinguished. The first considered all diffusion coefficients to be positive constants and the second explored the case where only the diffusion coefficient of the exposed individuals, d_E, was a non-zero constant. For the first case, we were able to show the uniqueness of a DFE, the basic reproduction number, $\mathscr{R}_0$, was characterized and estimated, and the threshold criterion was shown to hold. In the second problem, similar results were demonstrated, but since the number of positive diffusion coefficients departed from the previous problem, the arguments for characterizing the $\mathscr{R}_0$ of the model and the local asymptotic stability of the DFE's required different approaches. Furthermore, an explicit definition of basic reproduction number was established and asymptotic results, related to the d_E, of $\mathscr{R}_0$ were studied.

In order to obtain an approximate solution of the system of partial differential equations associated to the Δ-SEIRS model a numerical method, based on finite difference schemes, for the two dimensional case in a circular domain was used. To illustrate the theoretical results proved in *Chapter 3*, the proposed numerical method was applied to the Δ-SEIRS epidemic model for several choices of the parameters.

Finally, the epidemic model was considered to a small case study of a current infectious disease, COVID-19. The spread of coronavirus-19 in Portugal was simulated between the period of February 2020 and June 2020. Here, we presented the parameters choice and the model strategy. Different scenarios were illustrated, where the importance of including heterogeneous spatial population distribution was demonstrated from implementing a non-spatial and a spatial case with the chosen parameters. Moreover, the introduction of non-pharmaceutical interventions was studied. Here, we also concluded

that, although the model presents a simple adaptation of COVID-19 disease, the reaction-diffusion model is still able to correctly model the spread of the contagious disease.

We now point out that in [3] the authors proved the global asymptotic stability of the DFE and the existence of an endemic equilibrium. However, due to the non-locality of the density-dependent transmission factor and for the complexity of working with a system of four equations, we were unable to establish similar results. Such results will be left as future work.

In addition, for future work we intend to study the convergence properties of the numerical method presented in *Chapter 3*, to develop a numerical method to approximate the eigenvalues of the elliptic problems (3.30) and (3.49) and also to explore the introduction of local health enclosures and vaccination to the case study of the spread of COVID-19 in Portugal.

Bibliography

[1] W. Abid et al. "Review on Finite Difference Method for Reaction-Diffusion Equation Defined on a Circular Domain". In: *The interdisciplinary journal of Discontinuity, Nonlinearity and Complexity* 5.2 (2016), pp. 133–144. DOI: 10.5890/dnc.2016.06.003 (cit. on pp. 43, 44).

[2] L. J. S. Allen et al. "Asymptotic Profiles of the Steady States for an SIS Epidemic Patch Model". In: *SIAM Journal on Applied Mathematics* 67.5 (2007), pp. 1283–1309. DOI: 10.1137/060672522 (cit. on pp. 1, 2, 17).

[3] L. J. S. Allen et al. "Asymptotic profiles of the steady states for an SIS epidemic reaction-diffusion model". In: *Discrete Continuous Dynamical Systems - A* 21.1 (2008), pp. 1–20. DOI: 10.3934/dcds.2008.21.1 (cit. on pp. 1, 2, 40, 72).

[4] K. E. Atkinson. *An Introduction to Numerical Analysis*. Second. John Wiley y Sons., 1989. ISBN: 978-0471624899 (cit. on p. 49).

[5] C. Caetano et al. "Mathematical Modelling of the Impact of Non-Pharmacological Strategies to Control the COVID-19 Epidemic in Portugal". In: *Mathematics* 9.10 (2021), p. 1084. DOI: 10.3390/math9101084 (cit. on pp. 4, 61–64).

[6] K. Deng and Y. Wu. "Dynamics of a susceptible–infected–susceptible epidemic reaction–diffusion model". In: *Proceedings of the Royal Society of Edinburgh: Section A Mathematics* 146.5 (2016), pp. 929–946. DOI: 10.1017/s0308210515000864 (cit. on pp. 1, 2, 21).

[7] O. Diekmann, J. Heesterbeek, and J. Metz. "On the definition and the computation of the basic reproduction ratio $\mathscr{R}_0$ in models for infectious diseases in heterogeneous populations". In: *Journal of Mathematical Biology* 28.4 (1990) (cit. on pp. 1, 2, 6, 7, 13, 16).

[8] P. van den Driessche and J. Watmough. "Reproduction numbers and sub-threshold endemic equilibria for compartmental models of disease transmission". In: *Mathematical Biosciences* 180.(1-2) (2002), pp. 29–48 (cit. on pp. 1, 2, 8, 15).

[9] D. Henry. *Geometric theory of semilinear parabolic equations*. Vol. 840. Springer, 2006 (cit. on p. 12).

[10] P. Hess. "On the eigenvalue problem for weakly coupled elliptic systems". In: *Archive for Rational Mechanics and Analysis* 81.2 (1983), pp. 151–159. DOI: 10.1007/bf00250649 (cit. on p. 31).

[11] R. Horn and C. Johnson. *Matrix analysis*. Second. Cambridge: Cambridge Univ. Press, 2012. ISBN: 978-0-5215-4823-6 (cit. on p. 76).

[12] Y. Lou and T. Nagylaki. "Evolution of a semilinear parabolic system for migration and selection without dominance". In: *Journal of Differential Equations* 225.2 (2006), pp. 624–665. DOI: 10.1016/j.jde.2006.01.012 (cit. on p. 41).

[13] Y. Luo et al. "Analysis of a general multi-group reaction–diffusion epidemic model with nonlinear incidence and temporary acquired immunity". In: *Mathematics and Computers in Simulation* 182 (2021), pp. 428–455. DOI: 10.1016/j.matcom.2020.11.002 (cit. on p. 24).

[14] Y. Mammeri. "A reaction-diffusion system to better comprehend the unlockdown: Application of SEIR-type model with diffusion to the spatial spread of COVID-19 in France". In: *Computational and Mathematical Biophysics* 8.1 (2020), pp. 102–113. DOI: 10.1515/cmb-2020-0104 (cit. on pp. 4, 61).

[15] W. H. Organization. *Coronavirus disease (COVID-19)*. 2021. URL: https://www.who.int/health-topics/coronavirus#tab=tab_1 (visited on 11/08/2021) (cit. on p. 61).

[16] W. H. Organization. *COVID-19 natural immunity*. 2021. URL: https://www.who.int/publications/i/item/WHO-2019-nCoV-Sci_Brief-Natural_immunity-2021.1 (visited on 11/09/2021) (cit. on p. 62).

[17] PORDATA. *Densidade Populacional*. 2021. URL: https://www.pordata.pt/Municipios/Densidade+populacional-452 (visited on 07/31/2021) (cit. on p. 62).

[18] P. Song, Y. Lou, and Y. Xiao. "A spatial SEIRS reaction-diffusion model in heterogeneous environment". In: *Journal of Differential Equations* 267.9 (2019), pp. 5084–5114. DOI: 10.1016/j.jde.2019.05.022 (cit. on pp. 31, 39).

[19] H. R. Thieme. "Spectral Bound and Reproduction Number for Infinite-Dimensional Population Structure and Time Heterogeneity". In: *SIAM Journal on Applied Mathematics* 70.1 (2009), pp. 188–211. DOI: 10.1137/080732870 (cit. on p. 76).

[20] J. Viana et al. "Controlling the pandemic during the SARS-CoV-2 vaccination rollout". In: *Nature Communications* 12.1 (2021), p. 1084. DOI: 10.1038/s41467-021-23938-8 (cit. on pp. 4, 61, 62, 64).

[21] W. Wang and X. Zhao. "Basic Reproduction Numbers for Reaction-Diffusion Epidemic Models". In: *SIAM Journal on Applied Dynamical Systems* 11.4 (2012), pp. 1652–1673. DOI: 10.1137/120872942 (cit. on pp. 2, 7–11, 13–15, 26, 27, 36, 38).

A

Auxiliary Definitions and Results

Definition A.0.1 Spectrum

Let $A : \Omega \to \Omega$ be a bounded linear operator on a normed complex space X. The spectrum of A, $\sigma(A)$, is defined as the set of $\lambda \in \Omega$ such that the operator $A - \lambda I$ is not invertible.

Definition A.0.2 Spectral Radius

Let $\lambda_1, \ldots, \lambda_n$ be the eigenvalues of a $n \times n$ matrix, A. Then its spectral radius $\rho(A)$ is defined as

$$\rho(A) = \max\{|\lambda_1|, \ldots, |\lambda_n|\}.$$

Definition A.0.3 Spectral Bound

The spectral bound of a closed linear operator A is defined as

$$s(A) := \sup\{Re\ \lambda | \quad \lambda \in \sigma(A)\},$$

where $\sigma(A)$ denotes the spectrum of A.

Definition A.0.4 Quasi-positive Matrix

A square matrix, $A = [a_{ij}]$, is said to be quasi-positive if it is not the zero matrix and it's off-diagonal elements are non-negative, *i.e.*,

$$a_{i,j} \geq 0 \quad \forall i \neq j.$$

Definition A.0.5

For any given $n \times m$ matrix $A = [a_{ij}]$, define $|A| = [|a_{ij}|]$ and $ind(A) = [\mu_{ij}]$, in which

$$\mu_{ij} = \begin{cases} 1, & \text{if } a_{ij} \neq 0 \\ 0, & \text{if } a_{ij} = 0 \end{cases}.$$

The matrix $ind(A)$ is denoted as the indicator matrix of A.

Theorem A.0.6 [11]

Let A denote a $n \times n$ matrix and I define the $n \times n$ identity matrix. The following are equivalent

1. *A is irreducible;*
2. *$(I + |A|)^{n-1} > 0$;*
3. *$(I + ind(A))^{n-1} > 0$.*

Definition A.0.7 Principal Eigenvalue

Let L be an elliptic differential operator and Ω a bounded domain. The principal eigenvalue, $\lambda(L,\Omega)$, of the operator L in Ω is defined as

$$\lambda(L,\Omega) = \sup\left\{\mu \in \mathbb{R} : \ \exists \varphi \in \mathscr{C}(\overline{\Omega}) \text{ with } \varphi > 0 \text{ in } \Omega, \text{such that } (L+\mu)\varphi \leq 0 \text{ in } \Omega\right\}.$$

Theorem A.0.8 [19]

Let A be the generator of a $\mathscr{C}_0$-semigroup, S, on an ordered Banach space X with a normal and generating cone X^+. Then A is resolvent-positive if, and only if, S is a positive semigroup, i.e., $S(t)X^+ \subseteq X^+$ for all $t \geq 0$. If A is resolvent positive, then

$$(\lambda - A)^{-1}x = \lim_{b\to\infty} \int_0^b e^{\lambda t} S(t)x\,dt, \quad \lambda > s(A), \quad x \in X.$$

Theorem A.0.9 [19]

Let B be a resolvent-positive operator in X with $s(B) < 0$, and $A = C + B$ a positive perturbation of B. If A is resolvent-positive, then $s(A)$ has the same sign as $\rho(-CB^{-1}) - 1$.

Numerical Method Implementation

The numerical method studied in this work was implement using *Python*.

```
import numpy as np
import matplotlib.pyplot as plt
import math
import copy
from sympy import *

def beta(x,y):
    #return math.exp(-15*(x+1/2)**2-15*(y-1/2)**2)/1000
    return 2.5/2000

def alpha(x,y):
    return 1/10

def gamma(x,y):
    return 1/6

def epsilon(x,y):
    return 1/5

def maximum_list(lista,P,M):
    a = lista[0,0]
    for i in range(P):
        for j in range(M):
            a = max(a,lista[i,j])
    return a

def minimum_list(lista,P,M):
    a = lista[0,0]
```

```
    for i in range(P):
        for j in range(M):
            a = min(a,lista[i,j])
    return a

def met2d(
    r, a, b, c, d, P, M, t, T, ds, de, di, dr, n0
):
    hr=(2*r)/(2*P+1)
    hTh = (2*math.pi)/M

    ht= t/T

    iterR = [(i+1-1/2)*hr for i in range(P)]
    iterTh = [j*hTh for j in range(M)]
    iterT = [ht*i for i in range(T+1)]

    #Initial Conditions
    susc = np.zeros( (P,M) )
    expo = np.zeros( (P,M) )
    inf = np.zeros( (P,M) )
    rec = np.zeros( (P,M) )
    total_pop = np.zeros( (P,M) )

    inf[:,:] = 0
    rec[:,:] = 0
    for j in range(M):
        for i in range(P):
            expo[i,j]=5
            susc[i,j]=100/(math.pi)-5

    for i in range(P):
        for j in range(M):
            total_pop[i,j]=susc[i,j]+expo[i,j]+inf[i,j]+rec[i,j]
    #Auxiliar
    betalist = np.zeros( (P,M) )
    alphalist = np.zeros( (P,M) )
    gammalist = np.zeros( (P,M) )
    epsilonlist = np.zeros( (P,M) )

    for i in range(P):
```

```
    for j in range(M):
        betalist[i,j] = beta(iterR[i]*math.cos(iterTh[j]),
                        iterR[i]*math.sin(iterTh[j]))
        alphalist[i,j] = alpha(iterR[i]*math.cos(iterTh[j]),
                        iterR[i]*math.sin(iterTh[j]))
        gammalist[i,j] = gamma(iterR[i]*math.cos(iterTh[j]),
                        iterR[i]*math.sin(iterTh[j]))
        epsilonlist[i,j] = epsilon(iterR[i]*math.cos(iterTh[j]),
                        iterR[i]*math.sin(iterTh[j]))

alph = alphalist[0,0]
gama = gammalist[0,0]
epsil = epsilonlist[0,0]

#Calculo para R_0:
betagammalist = np.zeros( (P,M) )
for i in range(P):
    for j in range(M):
        betagammalist[i,j] = betalist[i,j]/gama
maximo_beta_gamma = maximum_list(100*betagammalist,P,M)

print('Maximo(beta(x)/gamma(x))= %.1f' %(maximo_beta_gamma))
if maximo_beta_gamma<1:
    print('R0<1')
else:
    print('Não temos R0<1')

#Main Matrix
delta = [1/(2*(i-0.5)) for i in range(1,P+1,1)]
sigma = [1/(((i-0.5)*hTh)**2) for i in range(1,P+1,1)]

dim = P*M
S = np.diagflat([sigma[i] for i in range(P)])
Q = np.diagflat([1-delta[i] for i in range(1,P)],-1)+np.diagflat([-2
    for i in range(P)])+np.diagflat([1+delta[i] for i in range(P-1)], 1)
Q[P-1,P-1] = -1+delta[P-1]

J = np.zeros( (M,M) )
J[1,0] = 1
J[M-1,0] = 1
J[0,M-1] = 1
```

```
J[M-2,M-1] = 1
for i in range(1,M-1):
    J[i-1,i]=1
    J[i+1,i]=1

L1 = np.kron(np.eye(M,dtype=int),Q-2*S)
L2 = np.kron(J,S)
L = L1+L2

ct = -ht/(hr**2)
As=np.identity(dim)+ds*ct*L
Ae=np.identity(dim)+de*ct*L
Ai=np.identity(dim)+di*ct*L
Ar=np.identity(dim)+dr*ct*L
A0 = np.zeros( (dim,dim) )
A = np.block([[As, A0, A0, A0],[A0, Ae, A0, A0],[A0, A0, Ai, A0],
        [A0, A0, A0, Ar]])

aux_s = np.diagflat([-ht*alph for i in range(dim)])
aux_e = np.diagflat([ht*epsil for i in range(dim)])
aux_i1 = np.diagflat([-ht*epsil for i in range(dim)])
aux_i2 = np.diagflat([ht*gama for i in range(dim)])
aux_r1 = np.diagflat([-ht*gama for i in range(dim)])
aux_r2 = np.diagflat([ht*alph for i in range(dim)])

A0 = np.zeros( (dim,dim) )
Fs = np.block([[A0, A0, A0, aux_s],[A0, A0, A0, A0],[A0, A0, A0, A0],
        [A0, A0, A0, A0]])
Fe = np.block([[A0, A0, A0, A0],[A0, aux_e, A0, A0],[A0, A0, A0, A0],
        [A0, A0, A0, A0]])
Fi = np.block([[A0, A0, A0, A0],[A0, A0, A0, A0],[A0, aux_i1, aux_i2, A0],
        [A0, A0, A0, A0]])
Fr = np.block([[A0, A0, A0, A0],[A0, A0, A0, A0],[A0, A0, A0, A0],
        [A0, A0, aux_r1, aux_r2]])

AA = A+(Fs+Fe+Fi+Fr)
#Auxialiar Matrices for Circular Graphics
susc_aux_graf = np.zeros((P,M+1))
expo_aux_graf = np.zeros((P,M+1))
inf_aux_graf = np.zeros((P,M+1))
rec_aux_graf = np.zeros((P,M+1))
```

```
total_pop_aux_graf = np.zeros((P,M+1))
for i in range(P):
  susc_aux_graf[i,M]=susc[i,0]
  expo_aux_graf[i,M]=expo[i,0]
  inf_aux_graf[i,M]=inf[i,0]
  rec_aux_graf[i,M]=rec[i,0]
  total_pop_aux_graf[i,M] = total_pop[i,0]
for j in range(M):
  for i in range(P):
    susc_aux_graf[i,j] = susc[i,j]
    expo_aux_graf[i,j] = expo[i,j]
    inf_aux_graf[i,j] = inf[i,j]
    rec_aux_graf[i,j] = rec[i,j]
    total_pop_aux_graf[i,j] = total_pop[i,j]

new_susc1 = copy.deepcopy(susc_aux_graf)
susc_record = []
susc_record.append(new_susc1)

new_expo1 = copy.deepcopy(expo_aux_graf)
expo_record = []
expo_record.append(new_expo1)

new_inf1 = copy.deepcopy(inf_aux_graf)
inf_record = []
inf_record.append(new_inf1)

new_rec1 = copy.deepcopy(rec_aux_graf)
rec_record = []
rec_record.append(new_rec1)

new_total_pop1 = copy.deepcopy(total_pop_aux_graf)
total_pop_record = []
total_pop_record.append(new_total_pop1)

soma_pop_lista = np.zeros( (T+1) )
soma_s = np.zeros( (T+1) )
soma_e = np.zeros( (T+1) )
soma_i = np.zeros( (T+1) )
soma_r = np.zeros( (T+1) )
zeros = np.zeros( (P,M) )
```

```
soma_pop_lista[0] = soma_pop(susc, expo, inf, rec, hr, hTh, P, M, iterR)
soma_s[0] = soma_pop(susc, zeros, zeros, zeros, hr, hTh, P, M, iterR)
soma_e[0] = soma_pop(zeros, expo, zeros, zeros, hr, hTh, P, M, iterR)
soma_i[0] = soma_pop(zeros, zeros, inf, zeros, hr, hTh, P, M, iterR)
soma_r[0] = soma_pop(zeros, zeros, zeros, rec, hr, hTh, P, M, iterR)

B = np.zeros( (4*P*M) )

#Local R0 calculation
r0 = np.zeros( (P,M+1) )
for i in range(P):
    for j in range(M):
        r0[i,j]=(betalist[i,j]/gama)*(susc[i,j]/(total_pop[i,j]))
    r0[i,M]=r0[i,0]

new_r0 = copy.deepcopy(r0)
r0_record = []
r0_record.append(new_r0)

#Iteration
for ti in range(1,T+1):
    for j in range(M):
        for i in range(P):
            B[j*P+i] = (susc[i,j]-ht*betalist[i,j]*susc[i,j]*inf[i,j])
            B[M*P+j*P+i] = (expo[i,j]+ht*(betalist[i,j]*susc[i,j]*inf[i,j]))
            B[2*M*P+j*P+i] = (inf[i,j])
            B[3*M*P+j*P+i] = (rec[i,j])

    seirs = np.linalg.solve(AA,B)

    for j in range(M):
        for i in range(P):
            susc[i,j] = seirs[j*P+i]
            expo[i,j] = seirs[M*P+j*P+i]
            inf[i,j] = seirs[2*M*P+j*P+i]
            rec[i,j] = seirs[3*M*P+j*P+i]
    for i in range(P):
        for j in range(M):
            total_pop[i,j]=susc[i,j]+expo[i,j]+inf[i,j]+rec[i,j]
```

```
        for i in range(P):
            susc_aux_graf[i,M]=susc[i,0]
            expo_aux_graf[i,M]=expo[i,0]
            inf_aux_graf[i,M]=inf[i,0]
            rec_aux_graf[i,M]=rec[i,0]
            total_pop_aux_graf[i,M] = total_pop[i,0]
        for j in range(M):
            for i in range(P):
                susc_aux_graf[i,j] = susc[i,j]
                expo_aux_graf[i,j] = expo[i,j]
                inf_aux_graf[i,j] = inf[i,j]
                rec_aux_graf[i,j] = rec[i,j]
                total_pop_aux_graf[i,j] = total_pop[i,j]
        for i in range(P):
            for j in range(M):
                r0[i,j]=(betalist[i,j]/gama)*(susc[i,j]/total_pop[i,j])
            r0[i,M]=r0[i,0]

        new_susc = copy.deepcopy(susc_aux_graf)
        new_expo = copy.deepcopy(expo_aux_graf)
        new_inf = copy.deepcopy(inf_aux_graf)
        new_rec = copy.deepcopy(rec_aux_graf)
        new_total_pop = copy.deepcopy(total_pop_aux_graf)
        new_r0 = copy.deepcopy(r0)

        susc_record.append(new_susc)
        expo_record.append(new_expo)
        inf_record.append(new_inf)
        rec_record.append(new_rec)
        total_pop_record.append(new_total_pop)
        r0_record.append(new_r0)

        soma_pop_lista[ti] = soma_pop(susc, expo, inf, rec, hr, hTh, P, M, iterR)
        soma_s[ti] = soma_pop(susc, zeros, zeros, zeros, hr, hTh, P, M, iterR)
        soma_e[ti] = soma_pop(zeros, expo, zeros, zeros, hr, hTh, P, M, iterR)
        soma_i[ti] = soma_pop(zeros, zeros, inf, zeros, hr, hTh, P, M, iterR)
        soma_r[ti] = soma_pop(zeros, zeros, zeros, rec, hr, hTh, P, M, iterR)

    return soma_pop_lista, soma_s, soma_e, soma_i, soma_r, total_pop_record,
            susc_record, expo_record, inf_record, rec_record, r0_record
```